Ph.D. Thesis
博士論文

Quantitative Analysis of Economy and Environmental Adaptability of Tokamak Fusion Power Reactors

（トカマク型核融合動力炉の経済性及び
環境適合性に関する定量的評価研究）

by

Koji Tokimatsu
時松宏治

The University of Tokyo,
School of Engineering,
Department of Electrical Engineering
東京大学大学院　　工学系研究科　電気工学専攻

Research Supervisor: Professor Makoto Katsurai
指導教官：桂井誠　　教授

December 19, 1997
1997 年 12 月 19 日

Ph.D. Thesis
博士論文

Quantitative Analysis of Economy and Environmental Adaptability of Tokamak Fusion Power Reactors

（トカマク型核融合動力炉の経済性及び
環境適合性に関する定量的評価研究）

by

Koji Tokimatsu
時松宏治

The University of Tokyo,
School of Engineering,
Department of Electrical Engineering
東京大学大学院　　工学系研究科　電気工学専攻

Research Supervisor: Professor Makoto Katsurai
指導教官：桂井誠　　教授

December 19, 1997
1997 年 12 月 19 日

Acknowledgements

This study began with my own idea, and many professors and Drs then expressed much interest. Without the many comments and discussions, this thesis could never be completed. Among these professors and Drs, the author would like to especially acknowledge to Professor Makoto Katsurai (Department of Electrical Engineering, the University of Tokyo) who allowed me to engage this research topic and has taken care of me and given me all the possible educational opportunities.

The author would like to express his great thanks to Professor Kenji Yamaji (Department of Electrical Engineering, the University of Tokyo), who gave me his continuing guidance and encouragement and without whom this thesis could never been carried out. The author expresses his great thanks to an Emeritus Professor Yoichi Kaya (Department of Electrical Engineering, the University of Tokyo), who gave the author inspiration and the chance to engage this research topic.

The author would like to sincerely thank to Dr. Kunihiko Okano (Komae Laboratory of the Central Research Institute of Electric Power Industry), who gave me numerous helpful comments and discussions. Without him this thesis could not have been completed. The author would also like to express his sincere thanks to Professor Nobuyuki Inoue and Associate Professor Yuichi Ogawa (Department of Quantum Engineering and Systems Science, the University of Tokyo), who provided the author with basic knowledge regarding the "conventional" aspect ratio tokamak rector design. Especially Associate Professor Yuichi Ogawa especially was always available to the author with helpful comments and discussion.

The author would like to express his special thanks to Dr. Ronald L.Miller (Department of Applied Mechanics and Engineering Sciences and Fusion Energy Research Program, The University of California, San Diego), who provided me with a lot of research papers and cost analysis accumulations from the ARIES study. The author is also grateful to Dr.Miller for providing ARIES-ST reactor properties.

The author would like to express his thanks to Mr. Hondo Hiroki (Socio-economic Research Center of the Central Research Institute of Electric Power Industry), who lectured regarding methodology and provides a lot of data for Life Cycle Assessment. Without his collaboration, Part IV of this thesis could not have been completed. The author also expresses his thanks to Professor Hisashi Ishitani and Associate Professor Ryuji Matsuhashi, who provided the author with many reports regarding Life Cycle Assessment and resource assessment.

The author would like to express his thanks to Drs. Yasushi Seki, Satoshi Nishio, and Mitsuru Kikuchi (Japan Atomic Energy Research Institute), specialists who gave me many references, calculation codes, and comments. Special thanks are given to Drs. Yasushi Seki and Takashi Tabara (JAERI on leave from Sumitomo Atomic Energy Industries, Ltd.,) who gave the author induced radioactivity decay data for SSTR.

The author would like to acknowledge Drs. Yujiro Ikeda (JAERI), Koichi Maki (Hitachi Co., Ltd.,), and Mr. Keiichiro Shibata (Hitachi Co.) for giving the author a lot of data and information regarding induced radioactivity for various structural materials and the ITER. The author also would like to acknowledge Professor Shunsuke Kondo and Associate Professor Shinya Nagasaki (Department of Quantum Engineering and Systems Science, the University of Tokyo), who provides me much information regarding radioactive waste data.

The author is also deeply indebted to members of meetings at the CRIEPI or IDLT, Professor Tadasu Takuma (Kyoto University), Associate Professor Akiyoshi Hatayama (Keio University), Mr. Tomoaki Yoshida, Dr. Yoshiyuki Asaoka, Mr. Toshiya Nanahara (CRIEPI), Mr. Hideto Miyachika (SRC, Co., Ltd.,), Dr. Haruki Murakami (Toshiba R&D center), Dr. Takashi Yamamoto (NIFS), and Mr.Ryoji Hiwatari (Department of Quantum Engineering and Systems Science, the University of Tokyo).

The author is also deeply indebted to Mr. Yasushi Kozaki (Osaka University) as a pioneer in reactor evaluation studies in Japan, Professor F.Najmabadi, Drs. T.K.Mau, M.S.Tillack (UCSD) for their useful comments and discussion, Professor. Osamu Mitarai (Kyushu Tokai University) for giving the author reactor design papers, and Mr. Koji Nagano (CRIEPI) and Professor Shunsuke Mori (Science University of Tokyo) who gave me information about energy systems analysis.

In addition to all the above professors and Drs, the author has been helped by the following persons. I would like to express my acknowledgements to Associate Professor Yasushi Ono, Mr. Toshihumi Itagaki (Department of Electrical Engineering, the University of Tokyo), Drs. Ayumu Morita, Paul H.Aoyagi (Hitachi Co.), Chen Qing, Mrs. Yoshio Yamagishi, Ko Yamaguchi, Takayoshi Akao, and D.B.Kovarev (Department of Electrical Engineering, the University of Tokyo), Mr.Masahito Takahashi (CRIEPI), professor Yoichi Okabe and his laboratory members, who gave me a lot of care, comments and discussions.

I am also grateful to the following members of Katsurai-Ono laboratory, Yamaji and his related laboratory; Mrs Takayuki Okazaki, Masayoshi Ohi, Mitsuo Toyoda, Keigo Akimoto, Nozomu Hayashi, Michiaki Inomoto, Shin' ichiro Sakai, Junichi Fujino, Daigo Hirano, Ryo Ono, Yoshinobu Ueda, Hajime Yasuda, Takeo Imanaka, Takayuki Takeshita, Tomohumi Matsuyama, Norihito Yanagita, Shin'ya Takeuchi, Tatsuro Morino. Special thanks to Mrs Inomoto, Sakai, Ueda, and Yasuda who took good care of the computers and undergraduates, and Matsuyama, Yanagita, Takeuchi, Morino, and Tsuruta who helped me with a lot of copies and figures.

I would like to express thanks to the secretaries of the Department of Electrical Engineering; Saori Yatsufuji, Mayumi Masuda, Yoriko Watabiki, and Shuko Tanaka, and office workers Mrs. Abe, Miss Miyagawa, Mr. Iwasawa, Mr. Yonemura.

Finally, I wish to express my sincere thanks to my parents and my entire family, and all my friends who always encourage and accompany me.

Table of Contents

Abstracts

We are now facing global warming problems that may be caused by greenhouse gases (GHG). Moreover, global warming problems are deeply connected with sustainable development. To avoid these crises, numerous countermeasures are being taken, e.g., researches and development (R&D) for new technologies, energy and economy policy studies, and critiques of lifestyle/civilization/philosophy. Fusion energy is expected to be an advanced energy technology. Moreover, from the beginning of fusion research, fusion researchers have asserted that fusion energy is a source of "dream energy", i.e., clean, safe, and eternal. Based upon this assertion, the early realization of fusion reactors is expected because fusion energy will be able to resolve issues of both energy security and global warming. Despite the potential of fusion reactors, there has been much suspicion regarding their feasibility. Some believe that R&D for fusion reactors should be stopped because there is no practical hope of creating a working fusion reactor, even if large amounts of money are spent on fusion R&D.

Based upon this background, the main object of this Ph.D thesis is to discuss the possibilities for tokamak-type fusion reactors, which have made the most progress among all the fusion types. In particular, it is important to explore and discuss the following points -- (1) the present R&D status of tokamak-type nuclear fusion research, (2) reactor comparing studies based upon present scientific knowledge, and (3) the present economic feasibility and environmental compatibility of the tokamak-type reactor.

In Part I, fusion reaction and plasma confinement methods now being investigated and discussed, and the principles of tokamak fusion reactors are described. Based upon those explanations, readers can obtain basic knowledge of the physics and mechanisms of tokamak fusion reactors.

In Part II, a simple review of tokamak physics experimental studies, power reactor design studies, and fusion reactor assessment studies is provided. In this review, the following three points are presented. (1) The results of plasma physics experiments which have been conducted since the 1980s make possible to predict the self-ignition condition. DT fueled experiments have been investigated since 1991. The ITER (International Thermonuclear Experimental Reactor) has been designed to aim 1000 sec DT fusion buring in a controlled way. The reversed shear mode and spherical tokamak demonstrated their excellent physics properties. (2) Significant progress has been made in the evaluation of the physics of power reactor design. Especially progress in plasma physics makes reactor studies realistic. (3) Reactor evaluation studies are now in progress based upon the most recent advances in reactor studies as well as physics.

In Part III, the impact of design parameters on the Cost of Electricity (COE) is studied through a parameter survey in order to minimize the COE. Tokamak fusion reactors are discussed in light of "conventional" aspect ratio tokamaks using water cooling technology that are practical use in fission power plants. Three kinds of operating modes are considered; First Stability (FS), Second Stability (SS), and Reversed Shear (RS). The COE is calculated by a coupled physics/engineering/cost computer system code. Deuterium-Tritium type, 1000MW(e) at electric bus bar, steady-state tokamak reactors with aspect ratio A from 3 to 4.5 are assumed. Several criteria are used for the parameter survey; for example, 1) thermal to electricity conversion efficiency is assumed to be 34.5% by use of water as a coolant 2) the average neutron wall load must not exceed 5 MW/m^2 with plasma major radius $R_p > 5$ m. 3) a 2 MeV Neutral Beam Injector is applied. It is found that the RS operating mode most minimizes the COE among the three operating modes by reducing the cost of current drive and coils/structures. The cost-minimized RS reactor can attain high f_{bs}, high β_N and low q_{95} at the same time, which results in short R_p = 5.1 m, low B_{max} = 13.0 Tesla of maximum magnetic toloidal field (TF) of TF coils, and low A = 3.0. It can be concluded that this cost-minimized RS reactor is the most cost-minimized within the framework of this study. This cost-minimized RS reactor has *two advantages:* one is that the B_{max} = 13 Tesla TF coil can be made *by use of ITER coil technology,* and the other is that *the same cooling technology of the ITER (water cooling)* can be used.

In Part IV, economy, energy gain, carbon dioxide (CO_2) emission (Life Cycle Assessment: LCA) by weight as well as the volume of tokamak fusion reactor components, and waste disposal of tokamak fusion power reactors are evaluated in this study compared with 1) reactor types, 2) structural materials, and 3) other present Japanese energy sources. We reveal quantitatively fusion power reactor properties that the costs of fusion power reactors are high, fusion reactors also produce high energy gain while causing relatively small environmental impact. The reactors treated in this study are (1) a conventional physics performance ITER-like reactor based upon the ITER, (2) a RS reactor using the reversed shear safety-factor/plasma current profile, and (3) a ST (spherical torus) reactor based upon the ARIES (Advanced Reactor Innovative Engineering Study)-ST. The construction cost and cost of electricity (COE) are evaluated based upon the ITER cost calculation to avoid future cost uncertainty. Input energy and CO_2 emission from these reactors are calculated basically by multiplying the weight of the fusion reactor components and materials with the datum of energy intensities and/or CO_2 intensities, which are updated as much as possible to suit those reactors. Waste disposal volume is calculated in consideration of neutron wall load and neutron fluence. Following results were obtained. (1) The construction cost of the ST reactor is minimized and the COE of the RS reactor is minimized as well as that of the ST reactor. *These fusion reactors beyond range of the cost of other present Japanese energy sources.* (2) CO_2 emission from the ITER-like reactor is less than that from PV (photo voltaics). The RS reactor as well as the ST reactor can reduce the input energy and the CO_2 emission to half of that of the ITER-like reactor. *The energy gain and*

CO_2 emission intensity of these fusion reactors are as excellent as those of fission reactors and hydro-electric generation. (3) *Silicon carbide (SiC) used as the structural material of inner vessel components is best for energy gain and CO_2 emission reduction.* However the construction cost and the COE of the material is the highest. (4) *The waste disposal volume from fusion reactors at deccmmission is smaller by two orders than those from fission reactors.* From the stand point of fusion research and development (R&D), we assert that (1) RS reactors or ST reactors should be developed, (2) cost reduction must be done by any means, and (3) low activation and low cost, low energy consumption materials should be developed. At the same time, it must be asserted from the stand point of energy supply development that tokamak fusion reactor R&D should be continued because they provide the possibility of excellent energy gain with low CO_2 emission, and also of performing at a no bad economic level as well as creating low levels of waste volume.

Part V includes a summary and discussions as well as conclusions regarding R&D for tokamak fusion reactors. ***It can be asserted that it is worthwhile to proceed with tokamak fusion R&D*** because (1) physics performance, engineering, and material improvements, as well as cost reduction can be expected, (2) the advanced RS reactor and the ST reactor can have excellent environmental compatibility. However, it cannot be asserted that fusion R&D must proceed actively because this study does not analyze the positive conditions for proceeding with fusion R&D. Therefore, prudent decisions must be made when huge amounts of money are required. *It should be admitted that tokamak fusion reactors can contribute to global environmental warming because of the small CO_2 emission intensity.* Although this study quantitatively demonstrates that fusion energy is clean, it cannot be said that "safe and eternal" by this study. Other papers should be referred to regarding to the safety aspects of fusion. It is uncertain as to whether fusion reactors are "eternal", hence they can contribute to the "sustainable development problem" because the resource availability problem is left for future study. Fusion research should focus on the contribution of fusion energy to the "sustainable development problem".

Part I

Introduction

1. Fusion energy as an eternal energy source

1.1 Fusion energy relative to the global environment and sustainable development problems

We are now facing global warming problems that may be caused by greenhouse gases (GHG). The mechanism by which global warming occurs have still not been clarified, and we do not yet what the extent of the problem will be. It is believed, however, that severe damage will occur as a result of this global warming. Accordingly international negotiations have begun to address the issue, as with COP3 at Kyoto, December 1997. It is said that in our country 90 % of all GHG are emitted as a result of energy consumption [MITI]. Because energy consumption is an inevitable consequence of an active economy, global warming is inextricably connected with both energy consumption and the state of the economy.

Moreover, global warming problems are deeply connected with sustainable development. There are many definitions of "sustainable development" [D.W.Pearce]. Here, however, the phrase "sustainable development" is not so strictly defined as in the Ref. [D.W.Pearce] – Here we use it to mean the achievement of a state somewhat above the unsustainable development" state of our present lifestyle, which could lead to potential catastrophe. It is not difficult to imagine the way in which this catastrophic state could occur and what might happen. A disastrous state could be caused by global warming, running out of energy resource, food exhaustion, or economic disruption. We therefore must do as much as possible to resolve these easily imagined.

To avoid these crises, numerous countermeasures are being taken, e.g., researches and development (R&D) for new technologies, energy and economy policy studies, and critiques of lifestyle/civilization/philosophy. Based on the above, a simulation model approach has been developed concerning energy supply techniques, the economy, and climate in worldwide, over long time span [T.Murota, T.Morita&Y.Matsuoka, S.Mori]. The "Limits of the Growth" [D.H.Meadows] is the most prominent example of this early stage of this research field. Several simulation models have recently been developed in Japan. For example, the DNE21 model [K.Yamaji&Y.Fujii] can evaluate various energy-supply technologies by minimizing the energy-supply cost. The MARIA model [S.Mori] can maximize the present value of economic utility derived from energy technologies, land use, food supply, and global warming damage. Finally, the AIM model [T.Morita&Y.Matsuoka] can scrutinize the economy, GHG, climate change, and economic damage.

In the reconstruction of the "Geo Resuscitation Plan" [MITI] advocated by the MITI (Ministry of International Trade and Industry), the calculation results using the DNE21 model are shown in the cases of carbon dioxide (CO_2) concentrations for (1) business as usual (BAU), (2) technological development and transfer normal case, and (3) technological development and transfer accelerated case. The CO_2 emission, reduction, and disposal for the "Geo Resuscitation" plan for case (3) is shown in Figure I-1, and the network energy-supply content for the three cases is shown in Figure I-2. Based upon these results, Ref. [MITI] has concluded that the following several policies must be put in place to suppress CO_2

concentration's below 550 ppm in the year 2100.

1) The present energy conservation technologies must be carefully implemented in the short term, and advanced energy conservation technologies must be developed for the long term
2) R&D for renewable energy sources such as Photo Voltaics (PV) or R&D for a cost-down of clean energy such as fission reactors should be carried out.
3) Advanced energy techniques such as fusion energy should be developed and put into use.
4) Advanced environmental techniques for CO_2 fixation should be further promoted.
5) CO_2 recovery and stock technology should be developed.
6) Newly developed energy and environmental techniques should be promoted worldwide.

In this "Geo Resuscitation Plan", fusion energy is expected to be an advanced energy technology. Moreover, from the beginning of fusion research, fusion researchers have asserted that fusion energy is a source of "dream energy", i.e., clean, safe, and eternal. Based upon this assertion, the early realization of fusion reactors is expected [T.Sekimoto] because fusion energy will be able to resolve issues of both energy security and global warming. Despite the potential of fusion reactors, there has been much suspicion regarding their feasibility. Some believe that R&D for fusion reactors should be stopped because there is no practical hope of creating a working fusion reactor, even if large amounts of money are spent on fusion R&D [A.Tsuchida, H.Morinaga].

It appears that these various arguments are made because fusion reactors are not fully understood. Therefore, an evaluation study of fusion energy should be carried out to respond to these high expectations and the suspicious. Such evaluative studies have not yet been made in the Japanese fusion community. As a result, only the lack of possibilities for fusion energy, especially evaluated by Japanese researchers, made the introduction of the ITER (International Thermonuclear Fusion Reactor) in Japan difficult.

1.2 Structure of this thesis

Based upon this background, the main object of this Ph.D thesis is to discuss the possibilities for tokamak-type fusion reactors, which have made the most progress among all the fusion types. In particular, it is important to explore and discuss the following points -- (1) the present R&D status of tokamak-type nuclear fusion research, (2) reactor comparing studies based upon present scientific knowledge, and (3) the present economic feasibility and environmental adaptability of the tokamak-type reactor. For this purpose, following structure is made.

In Part I, fusion reaction and plasma confinement methods now being investigated and discussed, and the principles of tokamak fusion reactors are described. Based upon those explanations, readers can obtain basic knowledge of the physics and mechanisms of tokamak fusion reactors.

In Part II, a simple review of tokamak physics experimental studies, power reactor design studies, and fusion reactor assessment studies are provided. In this review, the following three points are presented.

(1) The results of plasma physics experiments which have been conducted since the 1980s make possible to predict the self-ignition condition. (2) Significant progress has been made in the evaluation of the physics of power reactor design. (3) Reactor evaluation studies are now in progress based upon the most recent advances in physics.

In Part III, fusion reactors are discussed in light of "conventional" aspect ratio tokamaks using water cooling technology that are practical use in fission power plants. These reactors are optimized in terms of the cost of electricity (COE). Based on this optimization, the impact of design parameters on both the COE and reactor operation modes is discussed. The water cooling reactor with a conventional aspect ratio was chosen because these reactors have been made the most progress and may be able to be put into use the soonest. Three types of reactors are described in Part I. The COE is minimized by the use of sensitivity analysis via the coupled physics/engineering/cost tokamak systems code. Through this study, it is explained how the reactor parameters should be chosen and which reactor types are economically superior.

In Part IV, evaluation studies are carried out in terms of cost based upon the ITER cost estimation, energy analysis, and CO_2 emissions (Life Cycle Assessment: LCA) by weight as well as the volume of tokamak fusion reactor components, and radioactive waste disposal. The power reactors treated in this study are an ITER-like reactor which is scaled up from the ITER, the cost-minimized reactor derived in Part III, and the conceptual study of the spherical torus (ST) reactor which is out of range in Part III. The possibilities for these tokamak fusion reactors are quantitatively evaluated in these terms, comparing reactor types, structural materials, and other current energy sources.

Part V includes a summary and discussions as well as conclusions regarding R&D for tokamak fusion reactors.

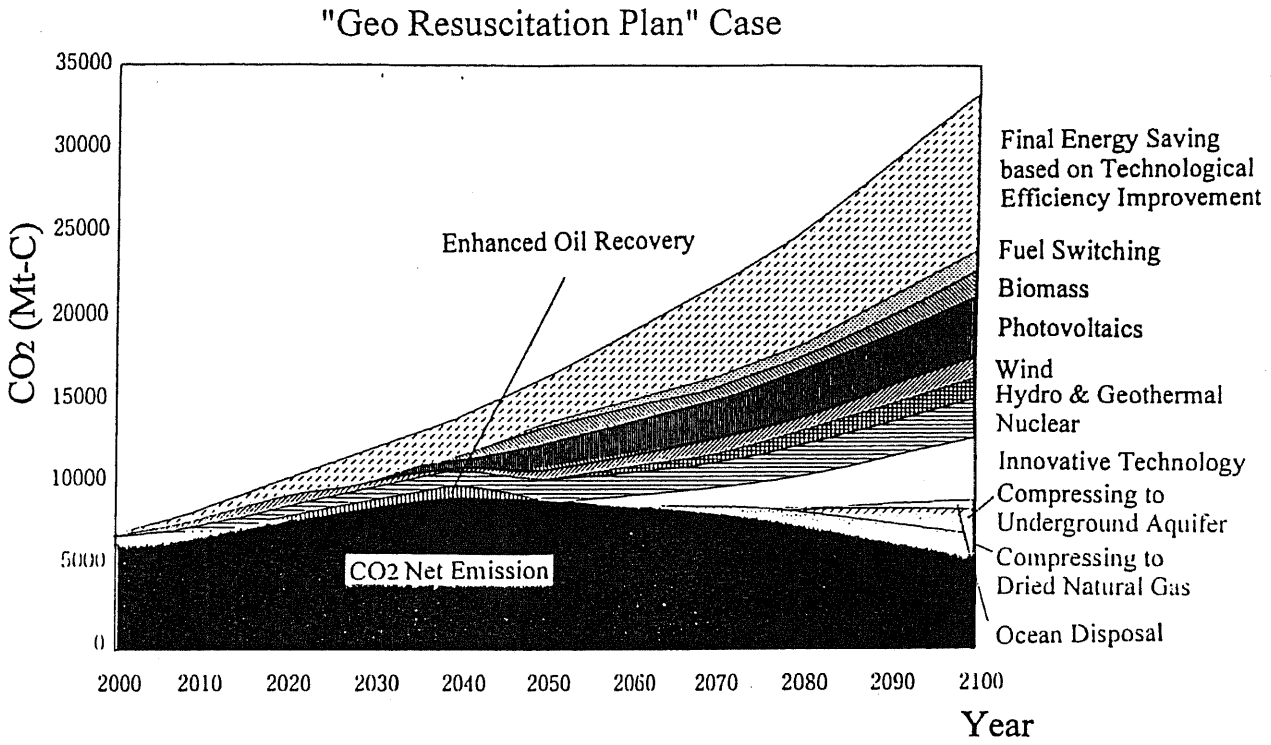

Figure I-1 *CO_2 emission, reduction and fixation in the case of "Geo Resuscitation Plan" (Ref. [MITI]). This graph is calculated by the DNE 21 model (Ref. [K.Yamaji&Y.Fujii]) as it can solve to minimize total energy supply cost. Fusion is expected to contribute for CO_2 reduction as one of "innovative" technologies.*

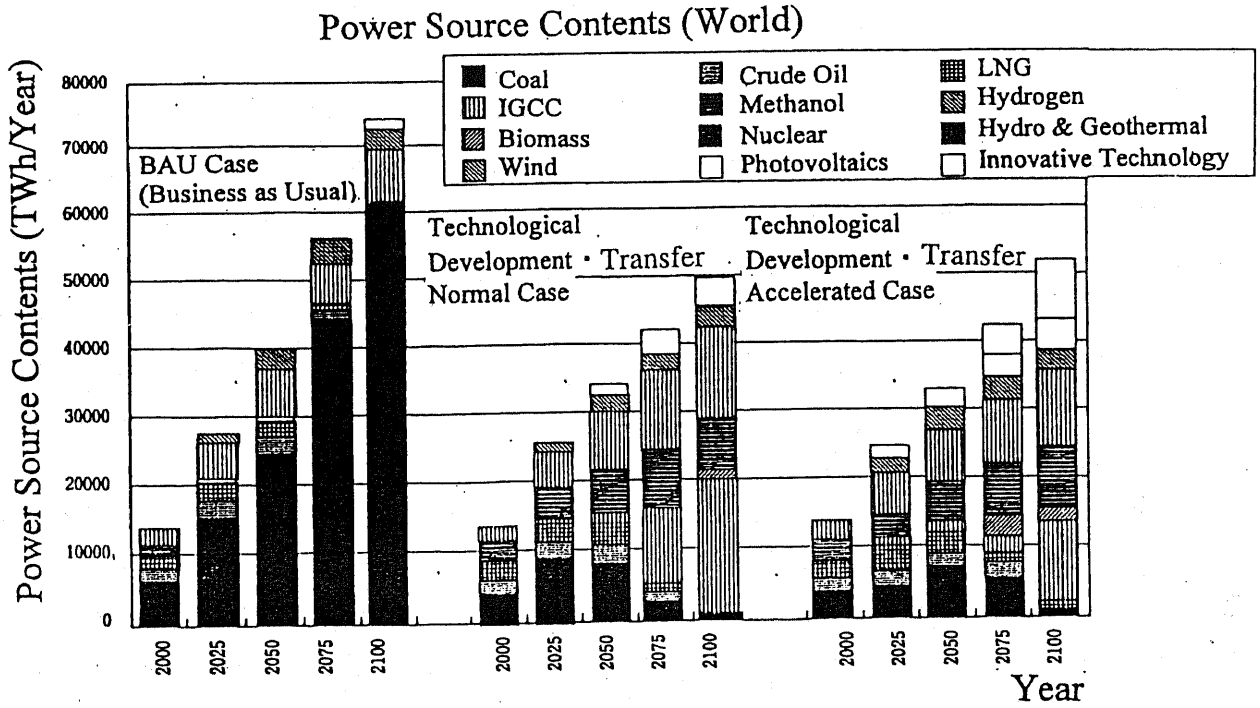

Figure I-2 *Contribution of every energy supply for each cases (Ref. [MITI]).The "innovative" energy technologies includes fusion energy in "Technological Development / Transfer Accelerated" case*

2. Fusion reaction and confinement methods

2.1 Fusion reaction

Fusion reaction can be carried out with plasma, which can be obtained by heating gases. Plasma is neither a solid, liquid, or gas, but is instead considered to be a fourth physical state. There are various kinds of plasmas which can be found in the sun, weak plasma used in fluorescent light, process plasmas for thin films, and fusion plasmas for obtaining electricity. In the fusion plasmas, the following three fusion reactions are candidates for fusion reactors [T.Sekiguchi, K.Miyamoto, T.Uchida].

(DT reaction) $D + T \rightarrow {}^4He$ (3.52 MeV) + n (14.06 MeV)

(DD reaction) $D + D \rightarrow T$ (1.01 MeV) + p (3.03 MeV)

(DD reaction) $D + D \rightarrow {}^3He$ (0.82 MeV) + n (2.45 MeV)

(D ^{3}He reaction) $D + {}^3He \rightarrow {}^4He$ (3.67 MeV) + p (14.67 MeV)

The DT reaction is considered to be the easiest to carry out and is the main route for fusion R&D because it is the easiest to make among these three, i.e., the cross section is the largest. The DD and D ^{3}He reactions are considered to be "advanced fusion reactions" because their cross sections are smaller than those of DT reaction by one order. The fuel for the DD reaction is deuterium, which can be collected from sea water. Therefore, the DD reaction is attractive in terms of energy security because it has no fuel resource restriction. The D^{3}He reaction is attractive because neutron emission from the reaction is almost negligible and clean. These advanced reactions have been investigated [A.A.Harms, D.L.Jassby. H.Momota]. Cold fusion, which has been sensational in Japan, has not been recently investigated.

2.2 Magnetic confinement methods

Plasmas must be confined within a defined space to make a fusion reaction. One method which utilizes magnetic fields is called magnetic confinement fusion (MCF), another method utilizing lasers is called inertial confinement fusion (ICF). Recently, MCF research has been investigated with confinement method such as tokamak, helical, mirror, RFP (Reversed Field Pinch), FRC (Field Reversed Configuration), and spheromak plasmas. All the last three are categorized as CTs (compact torus). The relation among these plasmas is shown in Figure I-3.

All these confinement methods have been studied in Japan. Tokamak has been investigated by the JAERI (Japan Atomic Energy Research Institute), helical by the NIFS (National Institute for Fusion Science), mirror by the University of Tsukuba and the Electrotechnical Laboratory, compact torus by the universities such as University of Tokyo, Nihon University, Osaka University, and Himeji Institute of Technology, and laser by the ILE (Institute of Laser Engineering). Figure I-4 shows the physics attainment in terms of fusion triple product for the confinement methods. The fusion triple product is an indicator of which can reach "break-even condition" and "self-ignition condition". The figure which displays the triple product in terms of plasma temperature is called Lawson's figure.

The $Q = 1$ line indicates the break-even condition, in which the input power is equal to the output power obtained by the fusion reaction. The $Q = \infty$ line means the self-ignition condition in which ^{4}He particles (alpha particles) generated by the fusion reaction heat the plasmas themselves, which results in a sustainment of the fusion reaction. The tokamak has been developed further than the other methods.

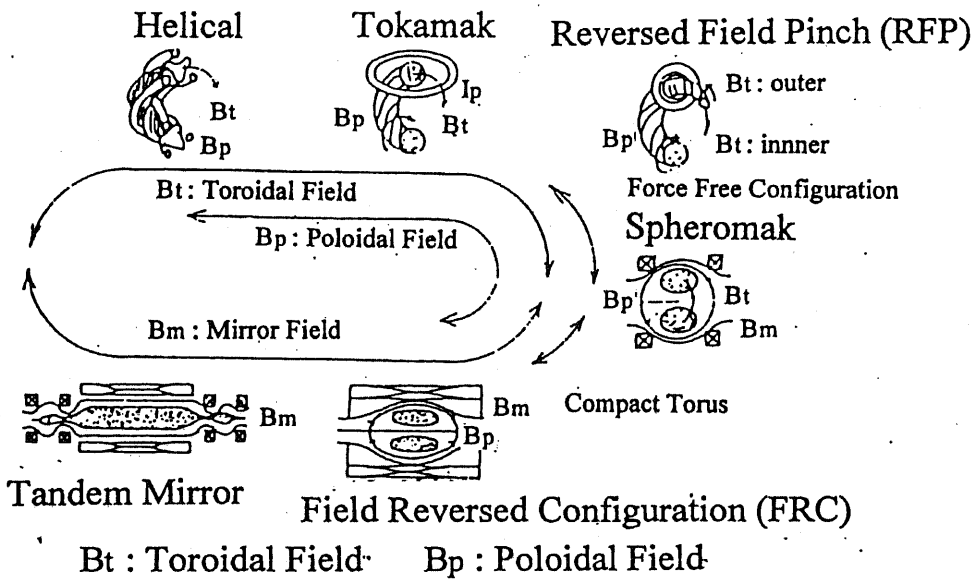

Figure I-3 Relation of magnetic confinement methods

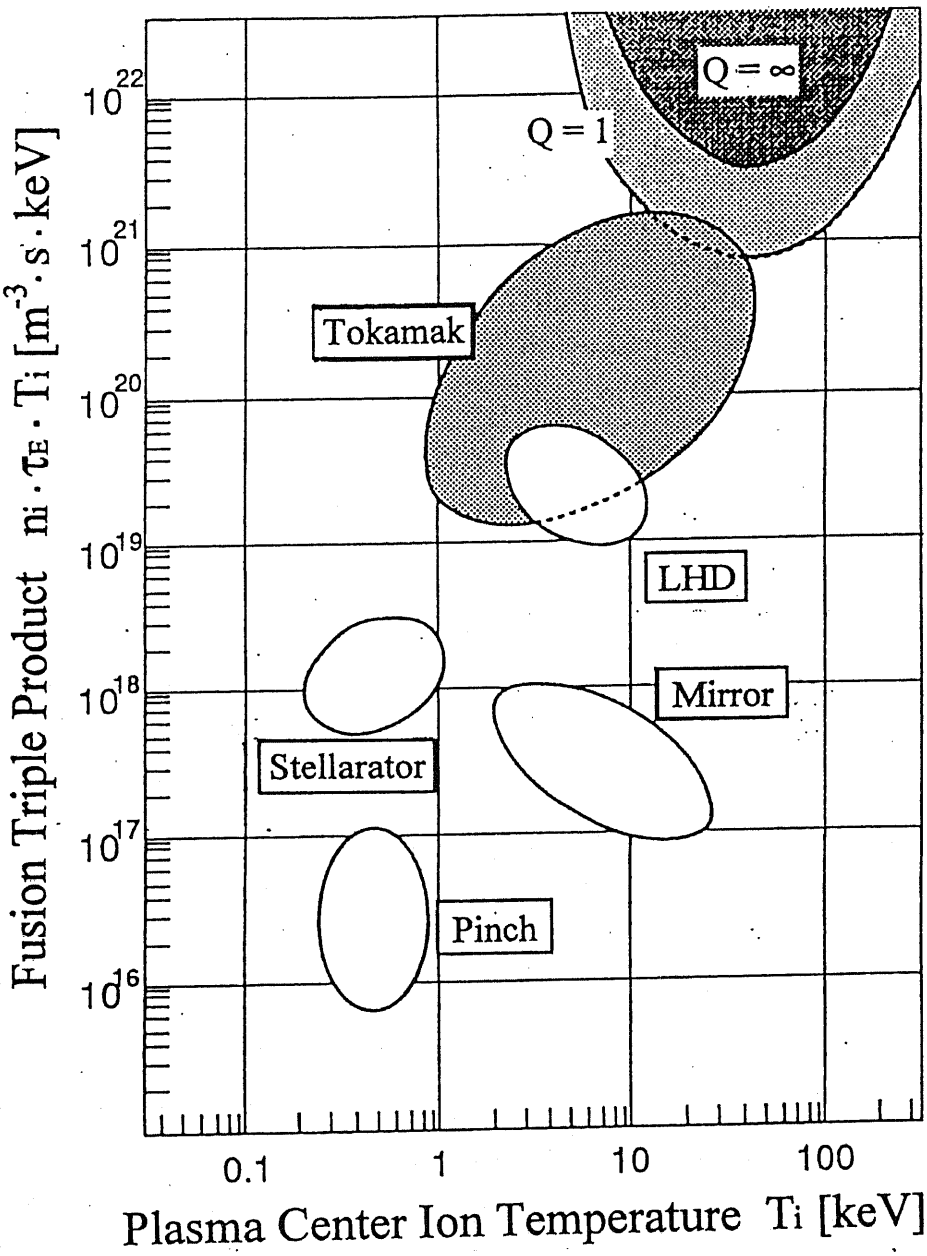

Figure I-4 Lauson's figure for displaying fusion triple product. Q = 1 indicates break even condition where the input energy for a reactor is the same as that output energy generated by fusion reaction. Q = ∞ indicates self ignition condition where plasmas are heated by alpha particles generated by fusion reaction.

3. Mechanism of tokamak fusion power reactors

3.1 Confinement method

The Tokamak fusion power reactor confines plasmas within a donut shape magnetic field. Its principle is shown in Figure I-5, and its plasma cross section is shown in Figure I-6. The distance from the torus center to the plasma center, which is denoted by R_p in Fig.I-6 is the plasma major radius. The distance from the plasma center to the plasma middle surface expressed by a_p is the plasma minor radius. The ratio of the plasma height to the plasma minor radius (b/a) is elongation κ, and d/a is triangularity δ

The large circle of the donut in Fig. I-5 is called toroidal, and the small circle is called poloidal. The plasma current I_p is made as a secondary coil of the transformer coil by a current change in the primary coil. This plasma current creates a poloidal magnetic field. A toroidal magnetic field is generated by toroidal field coils (TFcoils). The maximum toroidal field on the TF coils is called $B_{\max}$, and the toroidal magnetic field on the plasma axis is called B_0. The plasma can be confined by helical-shaped magnetic fields superimposed on poloidal magnetic fields and toroidal magnetic fields. The plasmas are confined by this torus-shaped helical magnetic field. The surface of the magnetic field is called a magnetic surface.

Some magnetic fields make a closed line. The numbers to rotate toroidal direction within one poloidal direction is called safety factor q, which is important to indicate plasma stability. If this safety factor is a rational number, the plasma will be unstable because resonance is easily caused by a magneto hydro wave under these conditions. The safety factor is continuously changes from the plasma center to the surface. A safety factor at the plasma center of q_0, and at 95% from the plasma center to the surface of q_{95} are usually used. Figure I-7 indicates the magnetic field in the case where $q = 2$.

The pitch angle is gradually changes because the safety factor continuously changes from the surface to the next outside surface. This change is called magnetic shear, whose conceptual figure is indicated in Figure I-8. Plasmas have their own plasma pressure, which is confined by magnetic pressure generated by magnetic fields. If the plasma pressure is greater than the magnetic pressure, an instability, which is called pressure driven instability occurs. In tokamak plasmas, several kinds of these instabilities occur, instabilities which are in general called MHD (Magneto Hydro Dynamics) instability. The magnetic shear is effective in suppressing these MHD instabilities. The D-shape plasma cross section serves the same purpose to suppress these MHD instabilities.

Plasma pressure is confined by magnetic pressure in cases of MCF. The indicator which can show the effectiveness of this confinement is called the beta value (β value), which is calculated as $\beta = \frac{\langle \kappa(n_e T_e + n_i T_i) \rangle}{B^2/2\mu_0}$. Here, κ is the Boltzmann constant, n_e, T_e is the plasma electron density and

temperature, n_i, T_i is the plasma ion density and temperature, B is the magnetic field, and μ_0 is the permeability. When the beta value is high, plasmas can be confined by a low magnetic field, and in turn, the volume of the TF coils as well as their cost can be decreased. Therefore, the beta value is also an economic indicator.

The beta value is restricted by MHD instability. The attainable beta value is expressed by Troyon scaling as $\beta = \beta_N \frac{I_p}{a_p B_0}$. Here the proportional constant is called the Troyon coefficient, which can indicate improvement in the beta value. This Troyon scaling is empirically derived through beta limits experiments, which are described in Part II. The β_N value is experimentally determined to be approximately 3 to 4, and 6 at a maximum. The confined high temperature plasma particles and the energy confined by the magnetic fields outside of the plasma, and they are exhausted through a plasma facing component called a divertor. In the case of the DT reaction, the thermal ^{4}He particles generated by fusion reactions should be confined; however, cooled ^{4}He particles (called He ash) which have already heated the other plasmas must be exhausted from the plasmas. The concentration percentage of this He ash is called the Helium concentration, which is usually set at about 10 to 15 % in reactor studies.

Energy is also lost by heat conduction or radiation from the plasmas. In order not to cool the plasmas, i.e., to keep plasmas to hot in order to sustain fusion reactions, the plasma must be heated. This is called additional heating. The value obtained by dividing thermal energy W [Joule] of the plasmas by plasma power P [Watt] turns to value of time [second]. This time $\tau_E = W/P$ is called the energy confinement time. This energy confinement time is an important physical value for the fusion triple product which indicates break-even or self-ignition condition.

As explained in Part II, achieving a long energy confinement time and a scaling formula to this time is extremely important. The energy confinement time scaling is empirically derived from various plasma parameters. Recently the energy confinement scaling had been summed as the ITER89P scaling derived from the ITER-EDA (Engineering Design Activity) or ITER93H scaling.

$$\tau_E^{ITER89P} = 0.048 I_p^{0.85} R_p^{1.2} a_p^{0.3} \kappa^{0.5} n_{20}^{-0.1} B^{0.2} M^{0.5} P^{-0.5}$$

M denotes the plasma average mass weight, which is 2.5 in the DT reaction.

The energy confinement time, which is longer than that predicted by ITER89P scaling can be experimentally obtained with the operating mode called the H-mode. The enhancement improvement factor, which is calculated by dividing the energy confinement time by the time predicted by a standard scaling such as ITER89P, is called the H-factor. The H-factor calculated by ITER89P when experimentally obtained is usually 2 to 3, and 4 at maximum.

3.2 Mechanism of the tokamak power reactors

Figure I-9 shows the poloidal cross section of a tokamak reactor, and Figure I-10 shows a conceptual figure of a tokamak fusion power plant. The Electricity-generating mechanism for tokamak fusion power reactors is follows: (1) heat from the fusion reaction is absorbed by a blanket, (2) the heat is transferred by cooling materials such as water or helium, (3) electricity can be obtained from heat by rotating generators as well as turbines through heat exchangers. The method for obtaining electricity from heat is the same as that of fission power plants or coal-fired power plants. The fusion power plant shown in Figure I-10 can roughly be divided into five parts, the fusion reactor inner components, auxiliary heating devices (current drive), heat transportation (heat trans), fusion reactor building components (except fusion reactor; reactor building), and the balance of plant.

Plasmas are at the center of the fusion reactor as shown in Fig. I-9. The first wall, blanket, divertor, shielding, vacuum vessel, and TF coils or PF (poloidal field) coils are located surrounding the plasmas from the inside of the reactor. To create fusion reactions, the inside of the vacuum vessel must be high vacuum (about 10^{-8} Torr) in order for plasmas to be obtained. The first wall protects the inner components of the vacuum vessel from damage by particles or heat from the plasmas. The particles from the plasmas are exhausted through divertor through the use of vacuum pumps.

The blanket serves to absorb, and multiply neutrons, and in breeding tritium; i.e., the kinetic energy of the neutrons is converted to thermal energy, multiplying the neutrons, and breeding tritium which is used for fusion reactions. The bred tritium is recovered from the blanket, and re-injected into the plasmas. Neutrons are shielded by the shield.

Fig.I-10 illustrates several components of a fusion power plant. Plasma ignitions, the sustainment of fusion reactions, and plasma current distribution are carried out by heating devices such as NBIs (Neutral Beam Injector) or RFs (Radio Frequency). A heat transportation system (Heat Trans) includes primary/secondary heat transportation systems and heat tanks. Fusion reactor building components (reactor building) include vacuum pumps, a coil power supply, and cryostat equipment. The balance of plant includes turbines, generators, fuel treatment, diagnostics and controls, gas distributions, electricity/mechanical equipment, and so on (please see Table III-7 as an example).

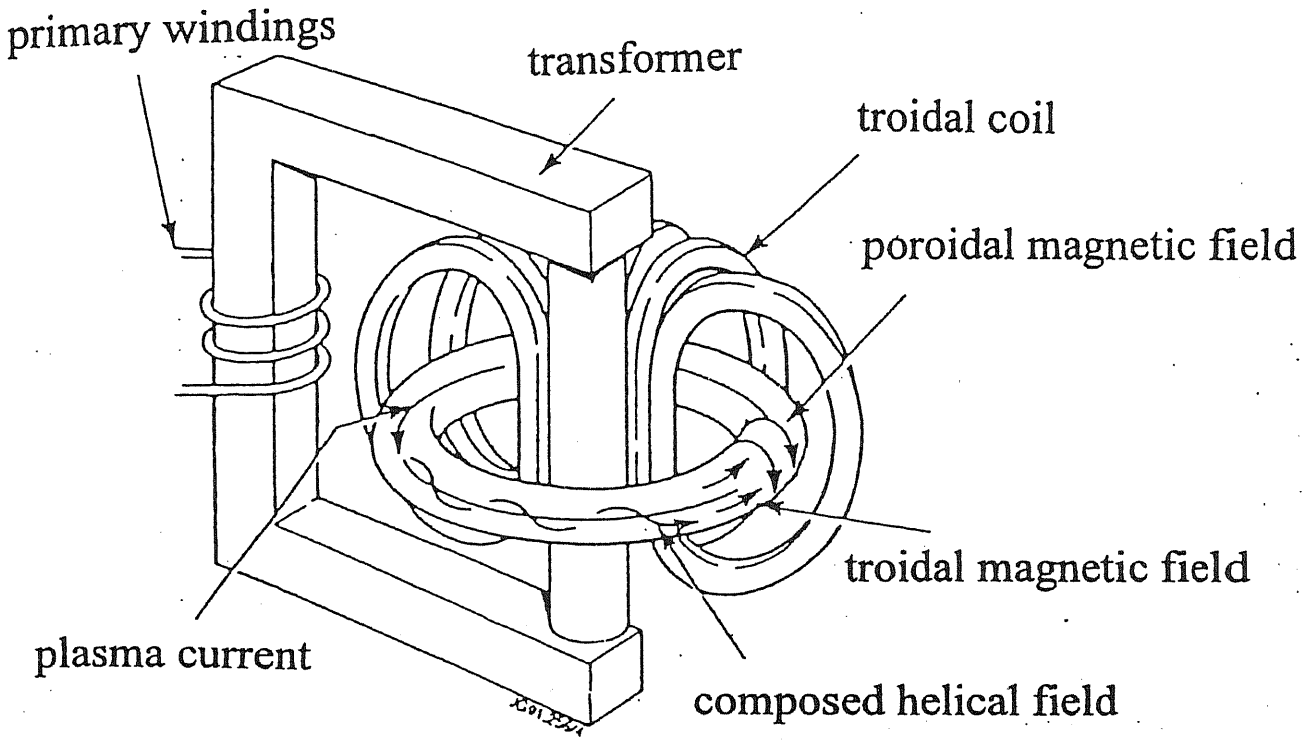

Figure I-5 Principle of Tokamak confinement method. Plasmas are confined by helical magnetic fields. One is toroidal magnetic field generated by toroidal coils, the other is poloidal magnetic field generated by plasma current.

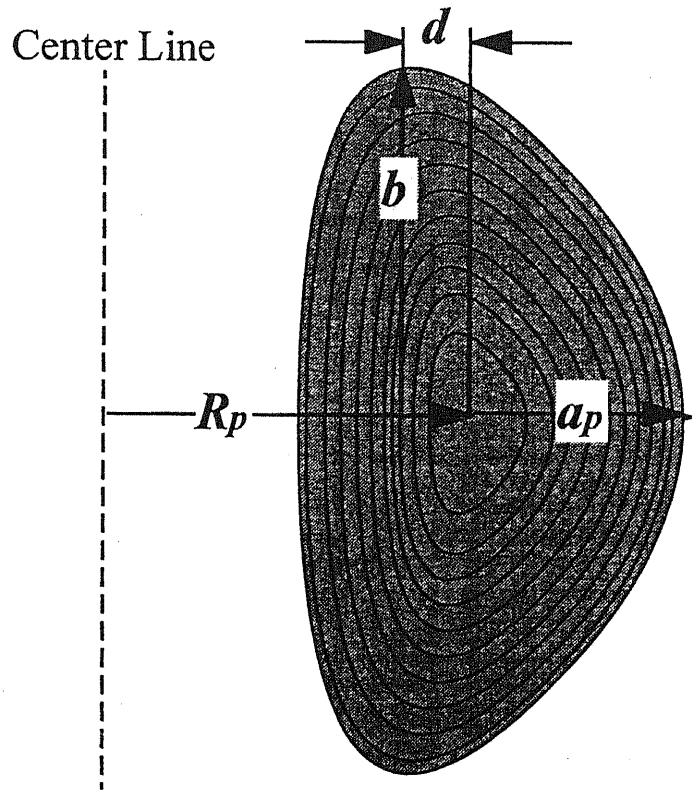

Figure I-6 Cross section of tokamak plasmas. R_p, a_p, R/a, b/a, and d/a means plasma major radius, minor radius, aspect ratio, elongation, and triangularity, respectively.

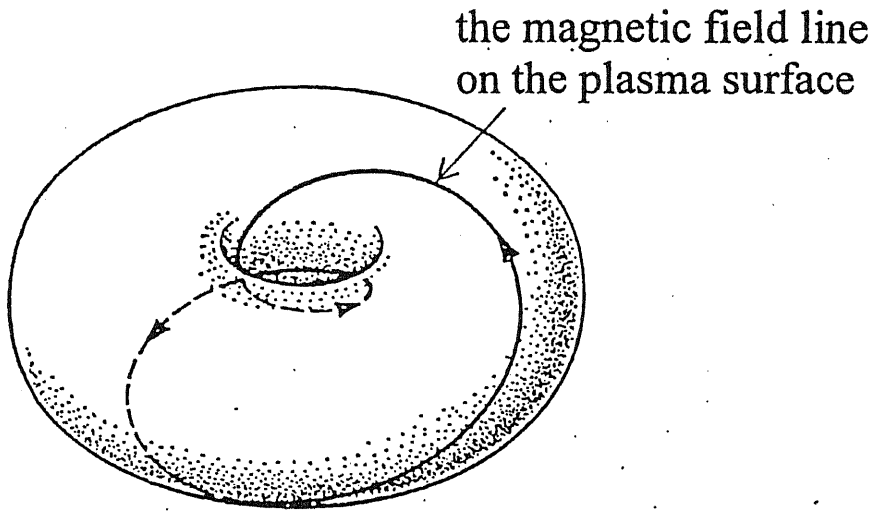

Figure I-7 Magnetic field for safety factor = 2. A magnetic field rotates two times for toroidal direction per one time for poloidal direction.

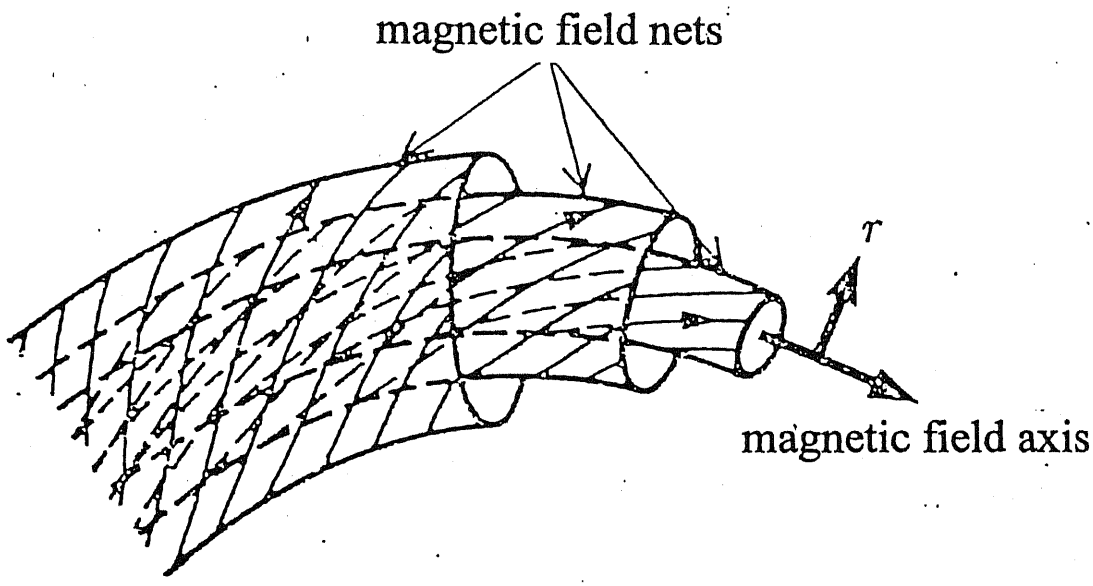

Figure I-8 Conceptual figure of magnetic shear. Safety factor is increased as outer magnetic field nets.

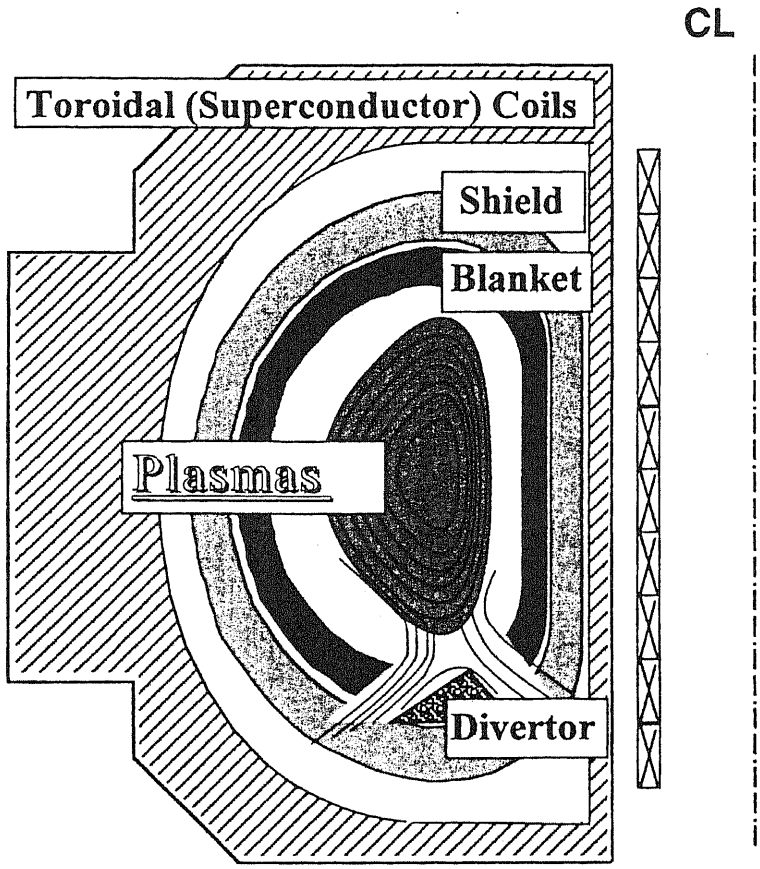

Figure I-9 Poloidal cross section of tokamak reactor.

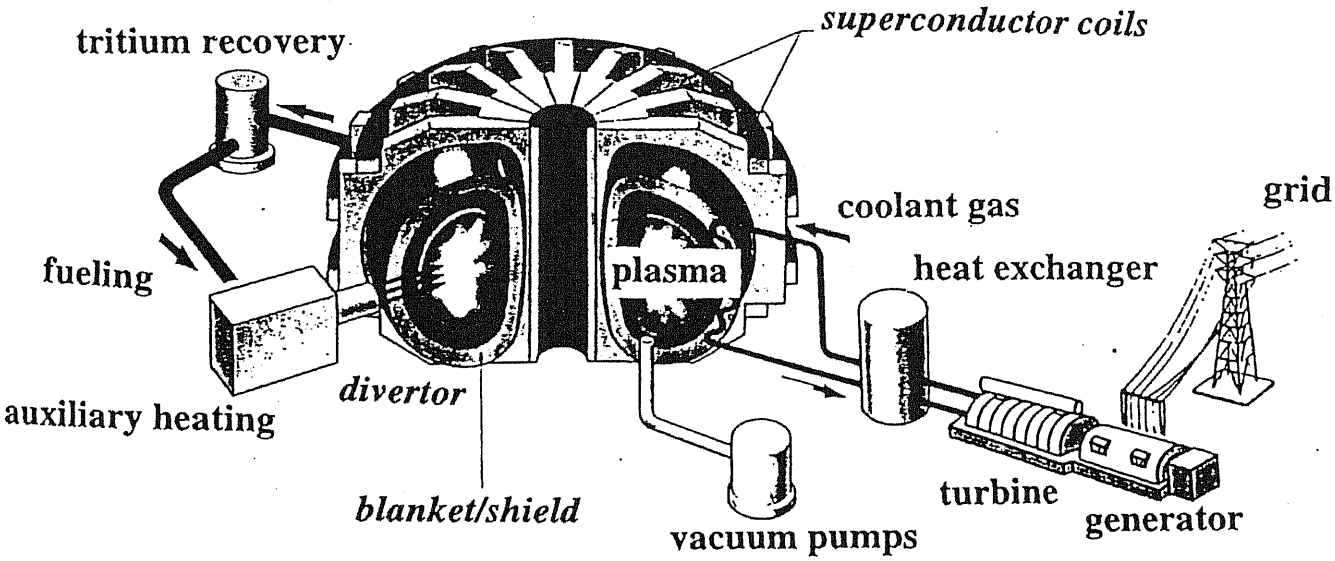

Figure I-10 Conceptual figure of a tokamak fusion power reactor.

Part II

Review of Plasma experiments, Reactor designs, and Evaluation studies of Tokamak fusion reactors

1. Progress of physics experiments for "conventional[1]" aspect ratio tokamaks

1.1 Till auxiliary heating experiments in the 80s

Tokamak physics experiments have been carried out in order to achieve high temperatures, high density, and a long confinement time for self-ignition and to improve the plasma confinement efficiency. Plasma experiments first obtained high temperatures, high density, and a long confinement time. Then the tokamak type confinement method took the spotlight when T-3 device achieved 1 keV plasmas in 1965, which was epoch-making at that time [K.Miyamoto96].

After the T-3 attainment, several tokamak devices were constructed, by which the plasma confinement time and temperature greatly improved [Y.Ogawa94]. At that time, the heating method for plasmas was ohmic heating by an inductive current induced by Ohmic Heating (OH) coils. Plasma confinement time was expressed by neo-Alcator scaling, which take into account the plasma density, the plasma minor radius, and the safety factor [D.R.Cohn] (eq. II-1). Therefore, break-even condition can be attained by high plasma density, reactor enlargement, and high plasma temperatures in according to neo-Alcator scaling.

Additional heating experiments using heating devices begun in 1980 [S.Tanaka]. The experiments were designed to raise the plasma temperature, or to replace the inductive plasma current with a non-inductive current by use of an NBI (Neutral Beam Injector) or LHW (Lower Hybrid Wave). These experiments were success; e.g., 10 keV plasmas were achieved, and a partial or whole plasma current was achieved using additional heating devices.

Based on these additional heating experiments, beta limits experiments have also been carried out. The purpose of attainment to attain high beta is to obtain cost-effective fusion reactors. Several beta limit experiments were presented at the IAEA international conference in Brussels, 1980. The JFT-2 and ISX-B devices attained a 3.2 % beta value by 1.2 MW heating power, and a 2.5 % beta value by 2.5 MW heating power, respectively.

It has been observed, however, that beta limits, MHD instabilities, and energy confinement time were degraded [S.M.Kaye85a]. Experimental results by NBI and ICRF (Ion Cyclotron Radio Frequency) were indicated no identifiable scaling by neo-Alcator scaling. In addition, when the confinement time was shorten to 1/2 or 1/3 that of those values for the ohmic heating regime, the PDX device found a "fishbone" instability using high beta experiments, as reported at the IAEA international conference in Baltimore, 1982.

Experiments in 1989s proceeded in two different directions; i.e., high beta experiments concerning beta limits and MHD instability caused by high beta, and confinement improvement experiments to overcome plasma confinement degradation. It was revealed through high beta experiments

[1] In this part, "conventional aspect ratio" is assumed from 2 to 5, compared with low aspect ratio

that MHD limit scaling (Troyon scaling) can predict attainable beta values and density limit scaling (Greenwald-limit), which are indicators of attainable plasma density. Several kinds of confinement improvement modes were found through confinement improvement experiments. The confinement improvement mode can lead to an 80 % bootstrap current, which is spontaneous current created by pressure gradient of plasmas. This improved mode leads to reversed shear experiments and break-even condition. Figure II-1 displays the evolution of these plasma experiments.

1.2 High beta experiments

Several MHD instabilities, such as kink, ballooning, sawtooth oscillation, fishbone, and disruption, were found through the high beta experiments. The goals of the beta limit experiments were (1) to overcome these instabilities, (2) to derive a formula to predict the attainable beta value, and (3) to improve the beta limit.

Troyon scaling was derived from a simulation study to predict the stability limit for pressure driven kink instability. This scaling formula was expressed as $\beta = \beta_N \frac{I_p}{a_p B_0}$, where β_N is a constant. This scaling was experimentally confirmed, and the β_N value was limited to approximately 2.8 to 3.5 (Figure II-2), through devices such as the D-III [R.D.Stambaugh], PDX [K.McGuire], ASDEX [O.Gruber], or DIII-D [E.J.Strait].

In the high beta experiments, plasma cross section shape modification experiments were carried out. Plasma cross section was devised in a variety of shapes, including bean shape, D shape, spherical (see chapter 3), a large elongation, and a high aspect ratio. The D-III [R.D.Stambaugh 85] and PBX [M.Okabayashi] devices were used for the experiments of the D shaped and bean shaped cross section, respectively. The PBX experimental results indicated that a bean shape could attain a higher beta value than the D shape at the same plasma current (Figure II-3).

Moreover, high beta experiments were performed with the intent attaining a "second stability" with a much higher beta value than the "first stability" region. Plasmas can reach another level of stability, which is called second stability, after first stability becomes unstable. High poloidal beta experiments by LHW at the Versator II device in 1989 [S.C.Luckhardt], $q_0 = 6 \pm 2.5$、$\varepsilon\beta_p = 1.3$, suggested that the discharge could attain a second stability region. The PBX-M device, which is strongly modifies the bean shape of the PBX device, came close to achieving a approached to second stability region [N.Sauthoff], but in the end this was not accomplished. PBX-M device has not attained a second stability region.

The experiment to attain a second stability region was performed by reversed shear experiments [E.A.Lazarus91] as discussed in section 1.5. Ref. [E.A.Lazarus91] attained toroidal beta β_t 11 %, central beta $\beta(0)$ 44 %, where the plasma center was able to reach a second stability region.

1.3 Plasma confinement improvement experiments

Plasma confinement improvement experiments was begun when the ASDEX device was found to have no degradation discharge with a divertor configuration [F.Wagner82]. The new discharge mode for the ASDEX was called "H-mode" and the previous degraded discharge mode was called "L-mode" [F.Wagner84]. Several confinement improvement discharge modes were found from the ASDEX H-mode. The prominent modes are the H-mode, an ELMy H-mode with the ASDEX device, and the supershot-mode with the TFTR device [R.J.Hawryluk87].

The differences among these modes can be characterized as the differences in the plasma density and the temperature profile. For the H-mode, the plasma temperature and density are offset at the plasma edge (r/a > 0.9) by the confinement barrier and then increase to the plasma center as with the L-mode profile (Figure II-4). The electron/density profile of supershot-mode indicate peaked profile in the plasma center.

Characteristics of the H-mode of the ASDEX based on the 1982 shot are (1) an increment of electron density/ temperature as well as poloidal beta at the L/H transition where the discharge mode changes from the L-mode to the H-mode, and (2) a reduction in H_α radiation and hard x ray radiation (Figure II-4). This L/H transition can occur with some threshold (e.g., 1.9 MW for ASDEX case). The energy confinement time improved to 40-55 ms which was 2 times of that of the L-mode and as long as the confinement time for the ohmic heating region.

The TFTR supershot-shot mode can be attained by directly injecting particles with NBI to the target ohmic region using low density plasmas. Before the injection, particle recycling from the vacuum vessel must be reduced as much as possible by a strong cleaning discharge. The supershot-mode was improved to the supershot-mode with H-mode [C.E.Bush]. This improved mode could still progress to high β_p-mode.

These energy confinement improvement experiments improve the energy confinement scaling. The prominent L-mode scalings are neo-Alcator scaling, Kaye-Goldston scaling, and ITER89P scaling; that for the H-mode is ITER93 ELMy H-mode.

neo-Alcator	$\tau_E^{NA} = 0.07\bar{n}_{20}R^2aq^*$ (eq. II-1)	[D.R.Cohn]
Kaye-Goldston	$\tau_E^{KG} = 0.055I_p^{1.24}R^{1.65}a^{-0.49}\kappa^{0.28}\bar{n}_{20}^{0.26}B^{-0.09}(M/1.5)^{0.5}P^{-0.58}$	[S.M.Kaye85b]
ITER89P	$\tau_E^{ITER89P} = 0.048I_p^{0.85}R^{1.2}a^{0.3}\kappa^{0.5}\bar{n}_{20}^{0.1}B^{0.2}M^{0.5}P^{-0.5}$	[ITER-PGL]
ITER93ELMyH-mode	$\tau_E^{ITER93-ELMyH} = 0.031I_p^{1.06}B^{0.32}P^{-0.67}M^{0.41}R^{1.79}n_e^{0.17}\varepsilon^{-0.11}\kappa^{0.6}$	[K.Thomsen]

1.4 High poloidal beta experiments and high bootstrap current fraction experiments

Bootstrap current, the existence of which was predicted theoretically in 1971 [R.J.Bickerton], is a spontaneous current which occurs when the pressure gradient is large enough. The bootstrap current fraction f_{bs} is roughly proportional to poloidal beta β_p. It can be considered that a steady state operation is easy in a large f_{bs} because high f_{bs} can reduce injection power into plasmas.

The TFTR device experiment of the supershot-mode [R.J.Hawryluk87] along with the high poloidal beta experiment (β_p is 2.2 at maximum) provided the first experimental evidence for the existence of the bootstrap current. The JET device attained a 0.85 MA bootstrap current for 3 MA total current in 1988 [JET89a], a bootstrap current of 0.7 MA for a 2 MA total current was obtained in 1989 [C.D.Callis]. The JT-60U device obtained 80 % of bootstrap current fraction for high poloidal beta experiments [S.Ishida91]. Through these experiments, the existence of the bootstrap current was confirmed. At this time, a steady state operated power reactor using a high bootstrap current fraction was proposed [M.Kikuchi].

The JT-60U operating mode is called the high β_p-mode [S.Ishida92a]. The JT-60U devised a high β_p H-mode, which coincides with confinement improvements of the plasma center by high β_p-mode with an edge plasma by H-mode [S.Ishida92b]. In this mode, the confinement improvement factor (H-factor by ITER89P scaling) reached 2.5 to 3.6, and also attained $n_i(0)\cdot\tau_E\cdot T_i(0) = 1.1\times10^{20}\mathrm{m}^{-3}\cdot\mathrm{s}\cdot$ keV (world record) [M.Mori]. The DIII-D device achieved a VH-mode [G.L.Jackson], where the H-factor ~ 3.6 and β_N ~ 3.6. Ref. [T.C.Simonen] demonstrates four excellent discharges obtained by DIII-D (Figure II-6).

1.5 Reversed shear experiments

The Reversed shear profile is characterized by the following safety factor profile illustrated in Figure II-7; there is a high safety factor at the plasma center, which decreases to a minimum safety factor value $q_{\min}$ from the plasma center to the plasma surface, and the increases again. This reversed shear profile has evolved from the PEP(Pellet Enhance Performance)-mode of the JET device or high β_p-mode. The preliminary reversed shear experiments, however, were not focused on. In Ref. [S.Ishida92a] it was reported that the hollow current profile (i.e. reversed shear profile) was naturally obtained when the bootstrap current fraction was up to 70 % to 80 % in the high β_p experiments. The PEP-mode has been primarily discussed for JET device [JET89b, P.Smeulders]. The Ref. [M.Hugon] first reported that confinement was improved by a reversed shear profile in the JET device. The reversed shear profile was not paid attention to, however, for the DIII-D device [E.A.Lazarus91]. At these times, detailed safety factors were not directly measured; the safety factor profile was obtained by calculation. The numbers of

the reversed shear experiments increased when a detailed safety factor profile was obtained by use of MSE (Motional Stark Effect) [F.M.Levinton89].

After these experiments, the excellent performance of the reversed shear, including a high bootstrap current fraction f_{bs} close to unity as well as a high Troyon coefficient β_N close to 5 by the conductor shell near the plasma surface, was demonstrated by several simulation studies [C.Kessel, J.Manickam, A.D.Turnbull]. Based upon these simulation studies, it was shown that a reversed shear profile can lead to cost-effective power reactors [R.J.Goldston].

Recently reversed shear has been investigated in DIII-D, TFTR, and JT-60U by MSE measurements. Experiments with DIII-D described in Ref. [E.J.Strait95] resulted in the observation of high ion temperature (20 keV) and high toroidal rotation speed (500 km/s), and a second stability region was achieved for ideal MHD ballooning mode. The attained H-factor and β_N values were H-factor = 3 and β_N = 4 [E.J.Strait95], H-factor = 2.5 and β_N = 2.24 [B.W.Rice], respectively. An f_{bs} of 75 %was attained by Ref. [B.W.Rice].

The TFTR device [F.M.Levinton] could attain a peaked plasma electron profile reaching 1.2×10^{20}, as well as a peaked electron/ion temperature. This experiment also indicated the great improvements in the particle diffusion coefficient D_e and thermal diffusion coefficient χ_i. Results from the JT-60U device showed a plasma electron temperature profile that was drastically changed at the transport barrier and the occurrence of an electron thermal transport barrier [T.Fujita]. Break-even conditions were reached in the JT-60U device with the use of a reversed shear profile. The reversed shear experiments are currently proposed for the ITER [D.Boucher].

Based on the above, it is clear that the reversed shear profile demonstrate excellent physics performance. There are, however, two problems. The first is that the steady operation has not been achieved with the reversed shear profile. Recently reversed shear profile has been transiently obtained with a high speedy current ramp-up. An inductive current penetrates from the plasma surface to the center as inductive electric fields penetrate from the plasma surface into the plasma center. When the plasma current ramp-up is made much faster than the magnetic field diffusion time, the edge plasma density increases faster than that of the plasma center, resulting in a hollow current profile. Therefore, the current density of the plasma center will be increased. Moreover, if the hollow current profile can be sustained by additional heating, beta collapse occurs at β_N = 1.8～2. Nevertheless, several quasi steady state discharges have been obtained using the ELMy H-mode [Y.Kamada, E.A.Lazarus96, Y.Koide]. The second problem is impurities in addition to fuel are confined by the transport barrier, which results in a dilution of fuel. These problems must be resolved in the reversed shear profile.

1.6 Deuterium-Tritium (DT) experiments

The first DT experiment was performed by the JET PTE (Preliminary Tritium Experiment) [JET92]. The objects of the JET-PTE experiments were to generate (1) more than 1 MW of energy by a controlled fusion reaction, (2) to test the adequacy of the transport code for predicting particles generated by the DT reaction, and (3) to develop methods for tritium handling, removal, and stock.

Total neutron emission rate was 6.0×10^{17} (neutrons/s); and the total neutron emission was 7.2×10^{17} (neutrons) by the high power phase for a 2 sec discharge at 11 % tritium concentration. The fusion reaction multiplication ratio Q_{DT} was approximately 0.15 at 1.7 MW peak. The TRANSP code was used to check neutron emission and neutron emission fractions between thermal-thermal, beam-thermal, and beam-beam.

50 % tritium concentration DT experiment had begun by the TFTR device in 1993. The following results obtained from 1993 through Sep. 1995 [M.G.Bell, R.J.Hawryluk95]. A fusion power of 10.7 MW by the supershot-mode with 39.5 MW, and 6.7 MW by high β_p discharge by current lump down were obtained. The DT reaction continued for approximately 1 sec, and the Q_{DT} reached 0.27 at maximum. The fusion power density had a peaked profile, with the supershot-mode reaching 2.8 MW/m^3, which is higher than that of the ITER. The plasma ion temperature reached 44 keV by the supershot-mode and 30 keV by the high β_p-mode. The fusion triple product $n_i(0)\cdot\tau_E\cdot T_i(0)$ were 5.5 and 3.7, respectively. The H-factor were 2.4 and 3.2 for β_N 2.0 and 3.0, respectively.

In DT experiments, not only these parameters but also, (1) Tritium transport, recycling, handling, and safety, (2) alpha particle transport, and (3) ICRF heating/current drive. These issues descrived in Refs. [M.G.Bell, R.J.Hawryluk95, T.Nishitani&R.Shimada]

1.7 International Thermonuclear Experimental Reactor (ITER)

The ITER collaboration plan was said to have begun with a U.S.- former U.S.S.R. presidents meeting in 1985. The ITER-CDA (Conceptual Design Activity) was carried out by the U.S., EU, U.S.S.R, and Japan for three years starting 1988. The ITER-EDA (Engineering Design Activity) had succeeded the ITER-CDA, which will end in 1998. Some reports [ITER-EDA, ITER-IDR, ITER-DDR] have been published during this EDA. Here, the physics issues were based upon the Detailed Design Report (ITER-DDR). The objectives of the ITER can be summarized as (1) self-ignition condition must be continued for 1000 sec, with a heat flux of approximately 1 MW/m^2, and (2) to obtain tritium handling experiences. The cross section of the ITER and reactor design parameters are shown in Figure II-8.

The operation sequence of the ITER is shown in Figure II-9. The TFTR could successfully achieve 10 MW fusion power for 1 second, while the ITER must sustain 1.5 GW fusion power for 1000 seconds. Moreover, the fusion power of the TFTR is controlled by additional heating, while the fusion power of the ITER must be sustained by alpha particles generated by a fusion reaction. Therefore the goals

for the ITER are much more difficult than those of the TFTR.

The ELMy H-mode is assumed for ITER plasma discharge with sawtooth oscillation, to hold plasmas for a long time by dissipating heat from the plasma edge with the addition of impurities such as Ne or Ar. Plasma parameters are determined by scaling or extrapolation based upon past experimental data. The energy confinement time is set for 6 sec for the ITER. This confinement time scaling is derived from the ITER93H scaling [K.Thomsen],which is shown in Figure II-10. The energy confinement time of the ITER corresponds to H-factor = 2.6 by ITER89P scaling [R.Aymar]. The Troyon co-efficient is 2.4. Therefore, the plasma parameters of the ITER are conservative.

It should be considered, however, that the control of current profile of the ITER is worse than that of other recent experimental devices, because the ITER is not designed to control current profile so well than that of other experimental devices. Moreover, the Troyon co-efficiency decreases as the safety factor decreases. It has been pointed out that the ITER operating point is not always within the operation region in terms of MHD stability because β_N / q_a = 0.7~0.9 is the upper limit, while the value of β_N / q_a is 0.8. Moreover, it may be possible for sawtooth oscillation to occur within a large part of the plasma center, which results in a failure of the self-ignition condition or a transition to fusion power, as well as a sudden heat flow to the divertors [Y.Ogawa96].

As explained in section 1.1.3, heat power above a threshold must be injected to achieve an L/H transition. Two empirical scalings have been proposed for this L/H transition. One is $P_{th} = 0.044 n_e BS$ proposed by [F.W.Perkins], and the other is $P_{th} = 0.45(0.6 n_e R^2)^{\alpha} n^{0.75} BR^2$ (-0.26 < α < 0.25), proposed by [T.Takizuka], where P_{th} is the threshold input power, and S is the plasma surface square. The former formula estimates P_{th} = 300 MW, which is a supposed overestimation, and the the latter estimates 40~50 < P_{th} < 130~210 MW. Uncertainties must be overcome by experimental studies.

The ITER density exceeds 15 % of the Greenwald-limit [M.Greenwald]. Confinement degradation or disruption are observed close to the Greenwald-limit, and understanding and improvement of the density limit is therefore an important issue. However, a discharge whose density is more than 2 times that of the Greenwald-limit when using a pellet injection to the plasma center. Hence a more rational understanding is required.

In short the ITER is designed based upon recent physics experimental data by use of a scaling formula. There are, however, still many remaining physical uncertainties. Therefore, plasma experimental researches as well as engineering R&D must proceed to resolve these problems.

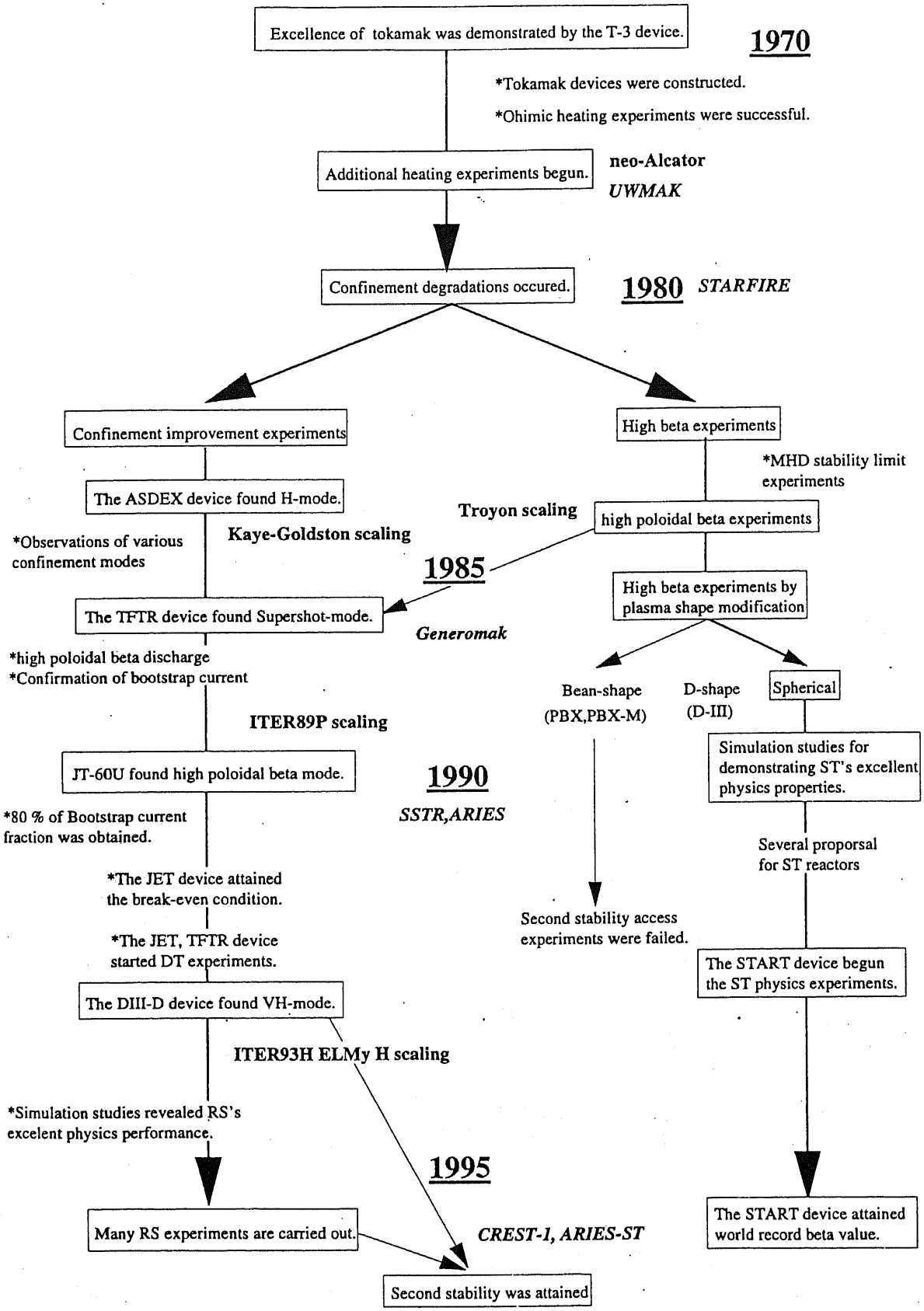

Figure II-1 Progress of physics experiments, scaling, and reactor studies

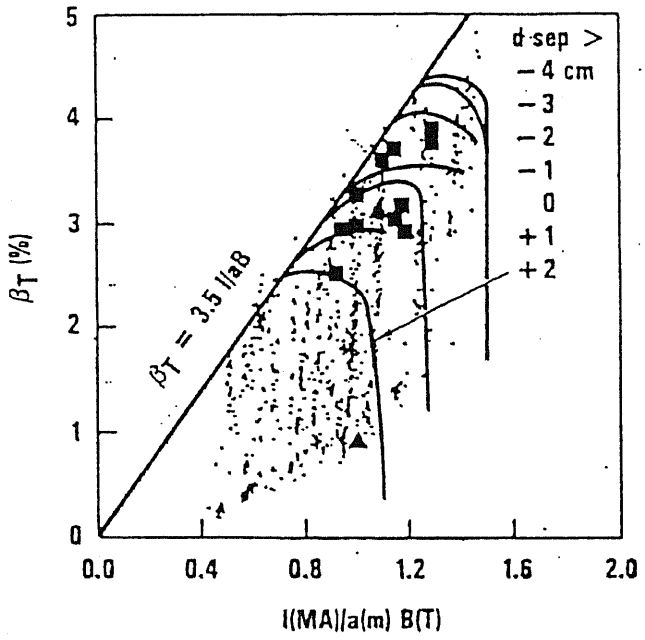

Figure II-2 Beta limit expressed by Toroyon scaling (Ref.[R.D.Stambaugh85]). This figure indicates β_N was restricted to 3.5.

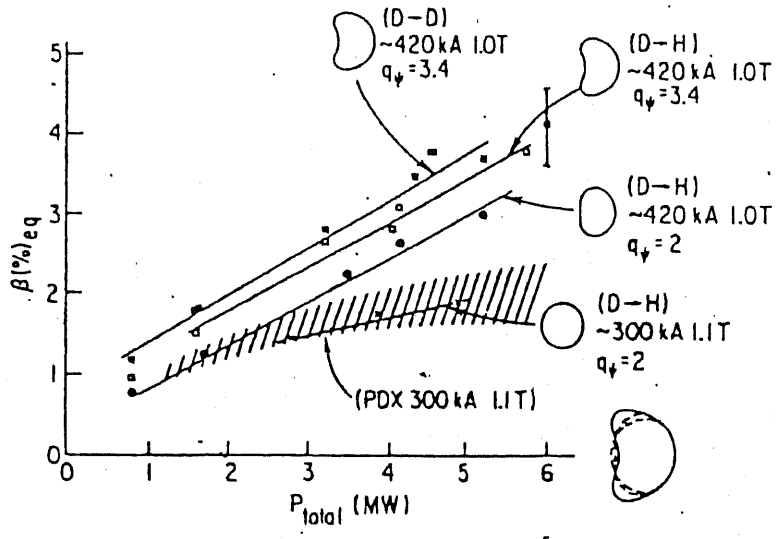

Figure II-3 High beta experiments by plasma cross section modifications (Ref. [M.Okabayashi]). This figure indicates that beta raises by modifying plasma cross section from circle, dee, and bean.

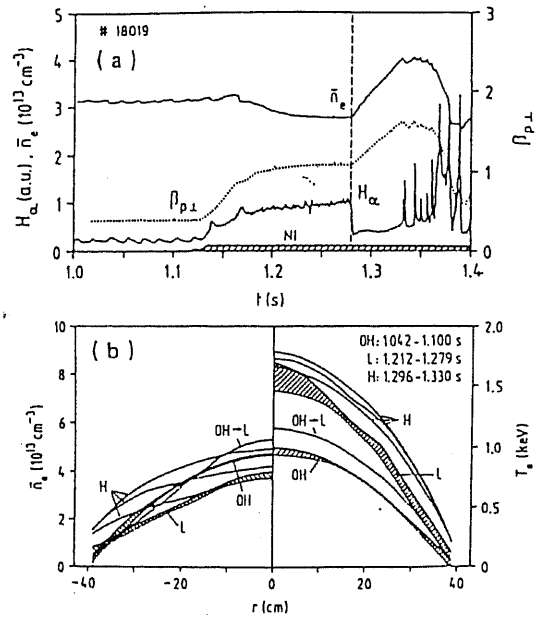

Figure II-4 H_α *electron temperature, and density profile by ASDEX H-mode (Ref.[ASEDX]). The right half side of the broken line in Figure (a) corresponds H-mode. Temperature raising can be seen from OH, OH→L, L, to H in Figure (b).*

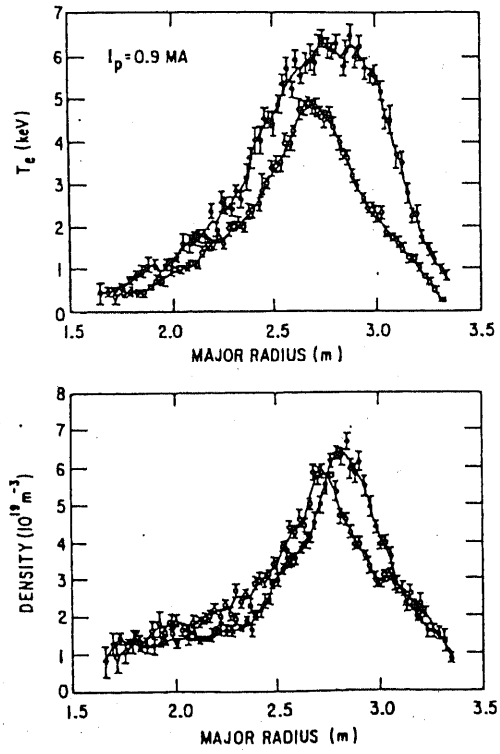

Figure II-5 Electron temperature and density profile of supershot-mode by the TFTR device (Ref. [R.J.Hawryluk87]). Black circles correspond to supershot-mode, white circles correspond to other discharges. Especially electron temperature is seen to raise by the supershot-mode.

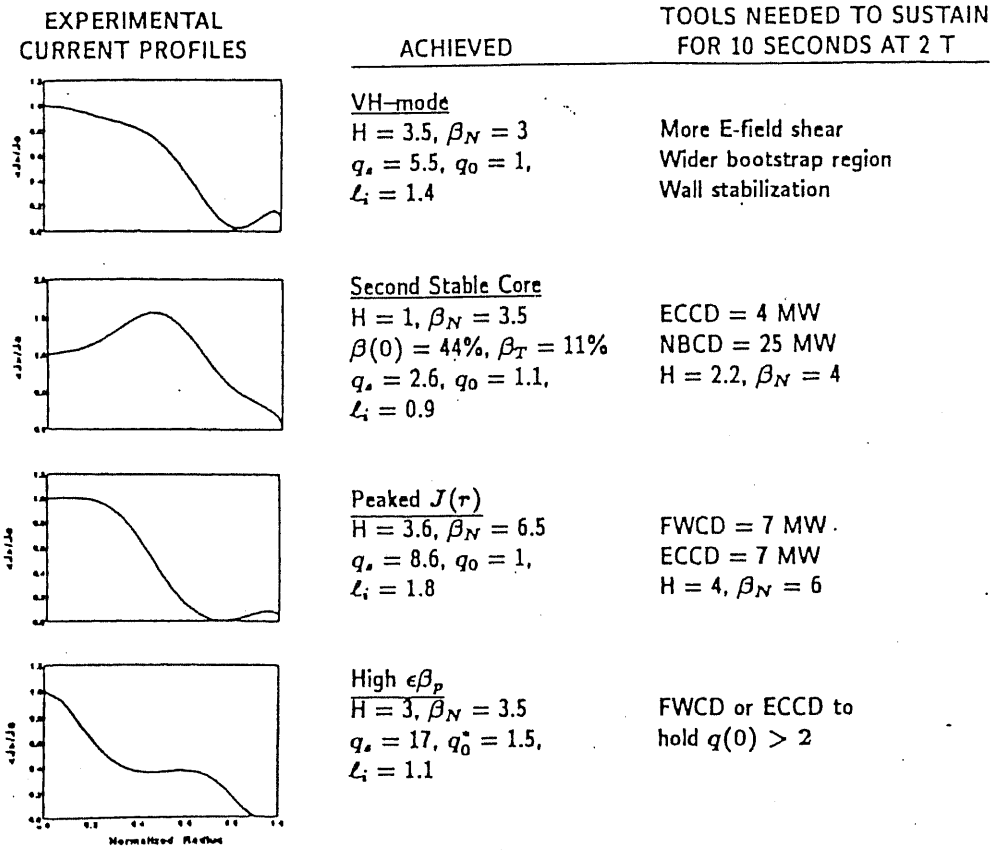

Figure II-6 VH-mode by the DIII-D device (Ref.[T.C.Simonen]). The most excellent discharge is the Peaked J(r) discharge. The second stable core discharge shows "hollow" current profile, which is regarded as "reversed shear" operation mode.

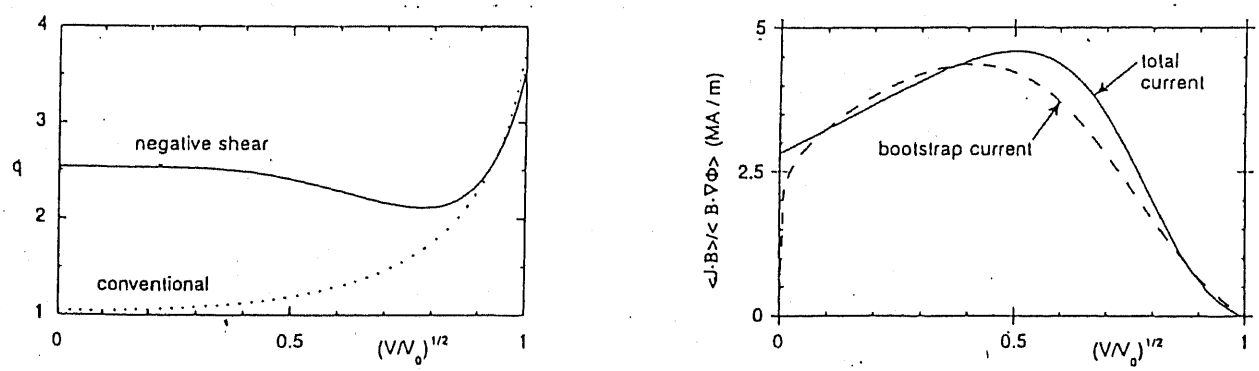

Figure II-7 Reversed shear profile compared with conventional profile (Ref. [C.Kessel]). Simulation studies by Refs. [C.Kessel, J.Manickam, A.D.Turnbull] displayed excellence physics performance obtained by reversed shear profile.

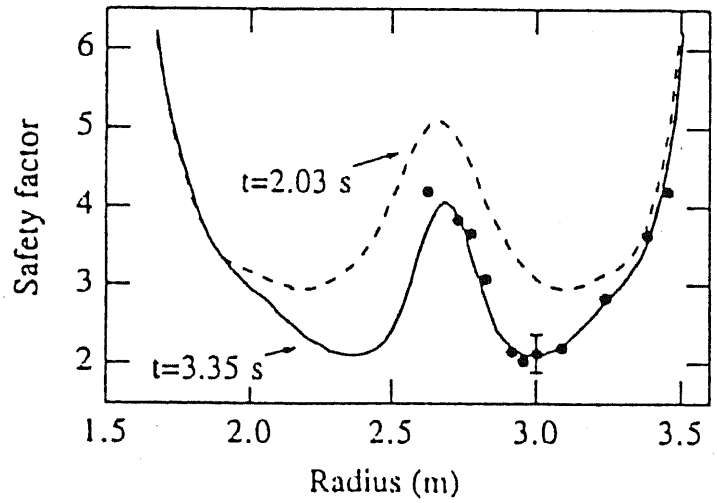

Figure II-8 Safety factor profile measured by MSE (Ref.[F.M.Levinton95]). By development of MSE, reversed shear experiments with detailed safety factor measurement were started to carry out.

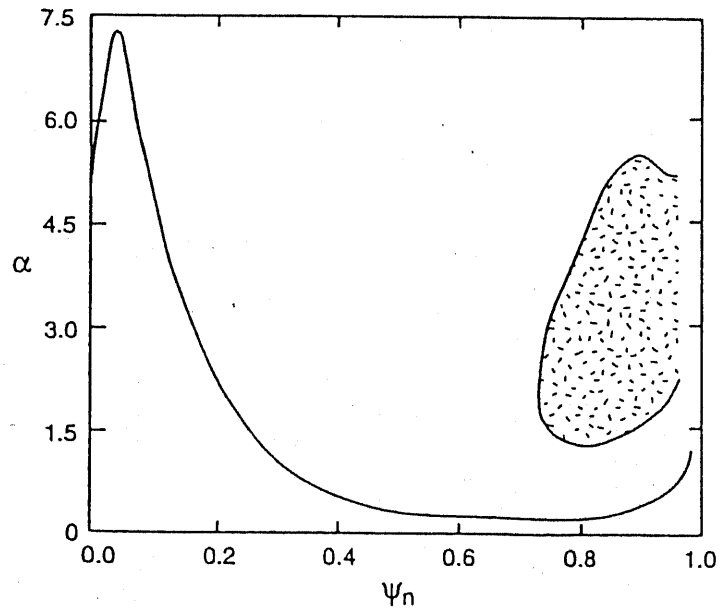

Figure II-9 Pressure gradient comparative to plasma minor radius. This figure indicates the second stable region could be accessed at plasma core (from ψn (= normalized minor radius) 0.0 to 0.4) by reversed shear profile.

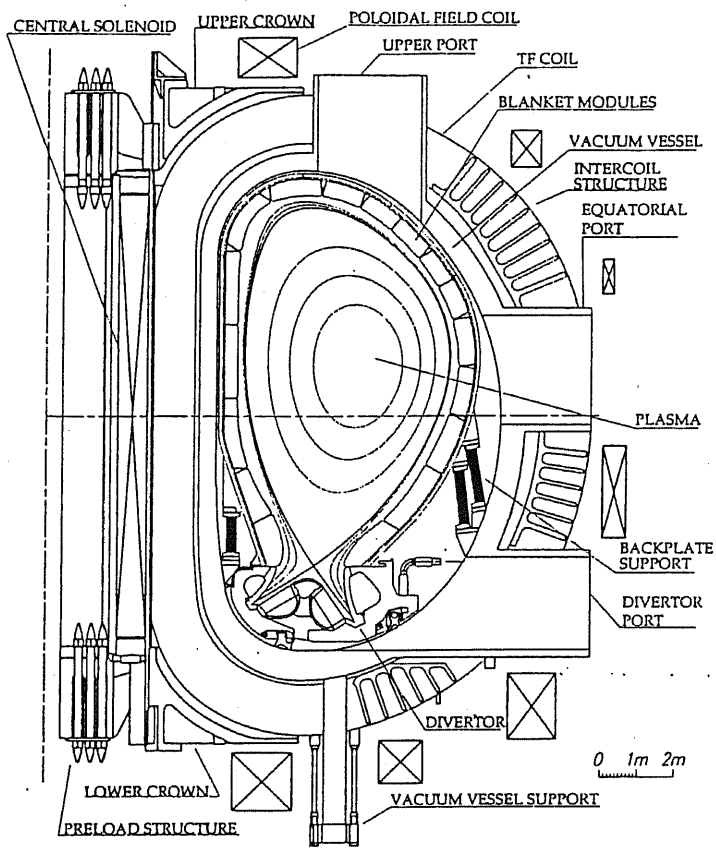

Parameters	Nominal	Low density	Range[2]
Major radius, R (m)	8.14	←	7.75-8.5
Minoe radius, a (m)	2.80	←	2.4-2.8
Elongation, κ_{95}	1.60	←	1.6-2.0
Triangularity, δ_{95}	0.24	←	0.2-0.3
Toroidal field, B (T)	5.7	←	4-5.7
Current, I_p (MA)	21	←	12-24
Safety Factor, q_{95}	3.0	←	2.6-5.2
Fusion power, P_{fus} (MW)	1500	1200	$\leq$ 1500
Burn duration (s)	1300	1400	500-10000
Auxiliary power, P_{aux} (MW)	0	0	$<$100
Volume-average beta, $\langle\beta\rangle$ (%)[1]	2.9	2.7	*
β_N [=$\langle B\rangle$ (%) a (m) B (T)/I (MA)]	2.2	2.0	$\leq$2.5-3.5
Electron density, $\langle n\rangle$ ($10^{20}m^{-3}$)	1.0	0.85	0.2-2
Average temperature, $\langle T\rangle$ (keV)	12	13	3-30
Plasma thermal energy W_{th} (GJ)	1.0	0.95	$\leq$1.2
Plasma magnetic energy W_m (GJ)[3]	1.1	1.1	$\leq$1.2
Energy confinement time, $\tau_{E_{trans}}$(s)	5.8	6.5	*
Impurity factions (n_Z/n_e) (%): Be	2	2	*
He	9	9	*
Ar	0.16	0.15	*
Effective-Z, Z_{eff}	1.8	1.8	*
Radiation from plasma core, P_{core} (MW)	110	100	60-120
Radiation from plsama mantle, P_{edge} (MW)	40	30	20-150
Radiation from SOL/divertor, P_{div} (MW)	100	60	50-200
Power to divertor target plates P_{div} (MW)	50	50	$\leq$100

[1]The notation $\langle\ \rangle$ denotes the volume average of the respective quantity.
[2]Including possible operation with reverse-shear or other optimized plasma configurations.
[3]Internal magnetic energy including 10% for ex-seoaratrix magnetic energy.
*At present, predictions are subject to large uncertainties.

Figure II-10 Cross section of the ITER and its design parameters

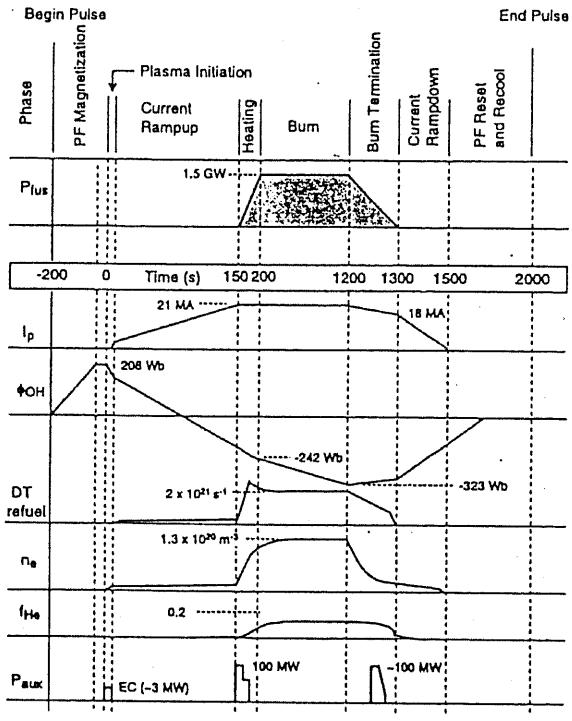

Figure II-11 Discharge sequence of the ITER. This figure indicates that the ITER aims 1.5 GW DT burning for 1000 seconds.

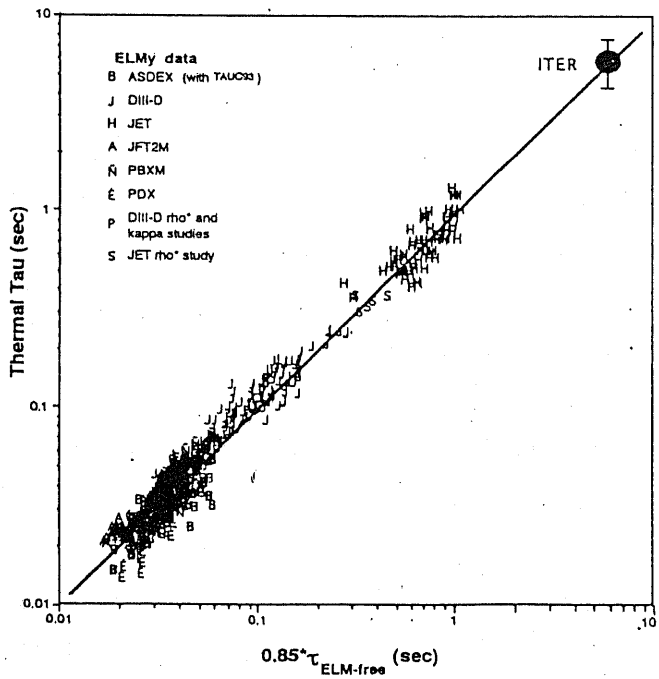

Figure II-12 Prediction of the ITER confinement time predicted by the ITER93 ELMy H-mode discharge. The scattered points are referred from present experimental devices.

2. Design and evaluation studies for "conventional" aspect ratio tokamak demo/power reactors

2.1 Reactor and evaluation studies before 1980

Many tokamak fusion power reactor design studies were carried out before 1980. For example, power reactors such as the Culhum-Mark I in 1972 and UWMAK-I in 1973 were studied. The first international workshop on reactor design (IAEA-TCMI: Technical Committee Meeting) was held in 1974 and the second IAEA-TCMII in 1978 [IAEA-TCMI,II]. From 1974 to 76, UWMAK-II&III by the university of Wisconsin [UWMAK-II&III], reactor design by JAERI [K.Sako 74,76], Culhum-MarkII by Culhum laboratory [Culhum-MKII], were studied. The cross section and design parameters of the UWMAK-II are displayed in Figure II-11.

UWMAK-II has a 5 GW fusion power, a 1.7 GW electric output, a 13 m plasma major radius, a 2.6 aspect ratio, and 1.5 hour pulse duration time. The time duration of the UWMAK-II is shorter than that of the present reactor, although UWMAK-II belongs to the present large reactor. The fusion power density of the UWMAK-II is estimated to be less than 0.78 [MW/m^3], which is as low as a present demonstration reactor (IDLT-DEMO [IDLT-DEMO]). Therefore, low fusion power density leads to a large reactor size as well as a large plasma volume. Moreover, the plasma electron density is very high ($6\times10^{20}[m^{-3}]$), which results in a plasma current of 14.9 MA, 38 times of the Greenwald limit. It can be considered that the high plasma density is due to the application of the neo-Alcator scaling. The energy confinement time is 4 sec, which is appropriate in terms of present physics knowledge.

The NbTi superconductor, constant tension, and D-shaped TF coils were applied, with a maximum toroidal field of 8.3 Tesla. $LiAlO_2$ was applied for the tritium breeder, Be for the neutron multiplier, SS316 for structural materials, and He for coolant. All materials except for SS316 and NbTi are similar to or the same as those applied for present reactor design. A low neutron wall load (1.16 [MW/m^2]), which may result in low fusion power density, enables the UWMAK-II to apply SS316.

UWMAK-III was made compact (e.g. plasma major radius 8.1 m) by increasing total beta up to 9 %, and the neutron wall load up to 2.5 [MW/m^2]. Troyon co-efficient becomes 6.2 as the plasma major radius becomes 2.7 m, the plasma current becomes 15.8 MA, and the toroidal field on the plasma axis becomes 4.05 Tesla. Moreover, the bootstrap current fraction increases almost 100 % as the poloidal beta becomes 2.2 and the aspect ratio becomes 3. The total beta, the Troyon co-efficient, and the bootstrap current fraction are not less than the present maximum value obtained by simulation studies. It can be considered that the reactor design at that time was carried out with a lack of physics knowledge as compared to recent physics knowledge, when we consider that 3 % of total beta was obtained by JFT-2M, ISX-B, T-11 in 1982 and bootstrap current was first observed in 1986 by TFTR.

Evaluation studies were made at that time. In Ref. [UWMAK-III], the cost of the UWMAK-III was estimated to be as 1154 ($/kW), 60 (mill/kWh) by 1975 US$. The unit construction cost was twice that

of the present ARIES-RS [ARIES-RS], the COE (Cost of Electricity) was almost the same. Ref. [UWMAK-III] also pointed out that the cost of fusion was almost the same as that of other energy sources (e.g. MHD generating plant) that would be used after 1990. On the contrary, Ref. [IAEA-TCMII] described that the unit construction cost increased from the order of hundreds of dollars in 1974 to thousands of dollars in 1978, and that therefore the cost of fusion will not be lower than that of fission unless the penalty cost for the environmental impact of the fission is made much larger. Moreover, the timing for introduction of fusion energy to other energy systems will be the late 20th century or the beginning of the 21st century, and the time when fusion energy can provide 10 % of the total energy supply will be sometime after at the beginning of the 21st century.

2.2 Reactor and evaluation studies in the 1980s

In 1979, several power reactors were designed; e.g., NUWAK which succeeds UXMAK-I,II,III, Culhum-IIC from Culhum-MKII, STARFIRE by ANL (Argonne National Laboratory), SPTR-P by JAERI [IAEA-TCMIII]. Figure II-12 displays the STARFIRE and its reactor design parameters. These reactors are as simple as present power reactors such as the SSTR [SSTR] or the CREST [K.Okano 97a-c], however the plasma current and safety factors are small. The Troyon co-efficient is quite high, e.g., 6.2 for NUWMAK and 7.46 for STARFIRE. It can be considered that the physics knowledge for ballooning instability was not still very advanced since Ref. [IAEA-TCMIII] mentioned that those reactor parameters are based upon the MHD ballooning stability limit. The most important issue was that the cost evaluation study was carried out by STARFIRE work. The Pacific Northwest Laboratory especially developed cost evaluation guidelines [PNL78,79] under U.S. Department of Energy. The COE at that time were still cheaper than the present estimation; the COE of the NUWMAK is 35 (mill/kWh), and the STARFIRE 40 (mill/kWh). However, with the development of these guidelines, economic evaluation studies became more prevalent in the U.S. than other countries.

In 1985-6, J.Sheffield et al. in ORNL (Oak Ridge National Laboratory) developed the Generomak model [Generomak] for evaluating overall magnetic confinement fusion reactors based upon past experimental or power reactors. This model can study parameter dependence of fusion reactors, not only tokamaks but also other magnetic confinement fusion reactors. Its physics models are not useful, although, its economic model can be used even still. For example, scaling methodology is now used for ASC (ARIES systems code) [ASC] or for this study. This methodology had already been developed in 1975 by J.Sheffield [J.Sheffild].

1987-8, the ESECOM study was made by the LLNL (Lawrence Livermore National Laboratory) group concerning the environment, safety, and economy of tokamak reactors. This study was presented in Ref. [R.A.Krakowski], comparing five kinds of tokamak reactors; i.e., a base case, a second stability reactor, a reactor with high toroidal field coils, a spherical torus, and a PCSR-E designed by EU. The difference from the Generomak model was that the scalings were have upgraded, included the Troyon scaling, Kaye-Goldston scaling, and the current drive efficiency, all were assumed to be appropriate.

In EU, an evaluation study proceeded from the NET (Next European Torus) to Ref. [W.R.Pears85] in 1985 and Ref. [W.R.pears86a] in 1986. In 1988-9, the EEF (Environmental, Safety-Related and Economic Potential of Fusion Power)-study was performed, whose results are summarized in the Main Report [Main Report]. In this study, the SCAN-S code [W.R.Pears86b] for cost evaluation was used, which was modified from SCAN (System for Cost Analysis of NET), which, in turn, was developed from the tokamak systems code SUPER-coil code [K.Borrass] for design of NET. The SCAN-2 code is more complicated than the Generomak model. In the European study, following points were different from those of the U.S. (1) SCAN-2 is a FOAK (First of a kind) reactor. (2) Plant availability and discount rate are different among the first, second, and after third year. (3) cost data is referred from NET, past reactor design, PNL data of U.S., and fission experiences.

In Japan, the fusion community considered fusion studies to be plasma science. Evaluation studies, therefore, have been frequently carried out. The CRIEPI (Central Research Institute for Electric Power Industry) studied the Fusion-Fission Hybrid reactor [CRIEPI-T12]. JAERI did not investigate cost issue through SPTR, however, the TORSAC (Tokamak Reactor System Analysis Code) code was developed in 1987 to evaluate the relative COE of the INTOR through an FER (Fusion Experimental Reactor) study. This code has not been used recently because of the systems code's complexity.

2.3 Reactor and evaluation studies in earlier 1990s

In 1990s, the available physics knowledge is assumed to have been compiled in the ITER Physics Guide Lines [ITER-PGL] including the MHD stability limit, confinement time scaling, density limit, and current drive efficiency. Engineering knowledge has also advanced for major reactor components such as superconductor techniques, NBI, blanket, shield, and structural materials.

Based upon the physics/engineering knowledge, SSTR (Steady State Tokamak Reactor) [SSTR] and ARIES (Advanced Reactor Innovative and Evaluation Study)-I [ARIES-I] were independently proposed at the same time. These reactors are very similar in the following points. (1) High bootstrap current fraction (~75 %) by high aspect ratio (A = 4), high safety factor, and high β_p are applied. (2) low fusion power density resulting from a high safety factor was compensated by the use of a high magnetic field on the TF coil (e.g., 16 Tesla).

Figure II-13 shows the SSTR. Low activation materials (HT-9) are applied for SSTR as structural materials, and water is used as a coolant. TiAl and He with SiC particles are applied for SSTR-2 to raise the electricity [SSTR-2]. In the ARIES study, advanced reactor technologies, such as the use of 20 Tesla superconductor coil, Vanadium alloy, and SiC for structural materials and He for coolant, were applied. ARIES-I uses 19.8 Tesla superconductor coils and SiC structural materials. ARIES-II is second stability operation by DT reaction using Vanadium alloy. ARIES-III is D^3He fueled second stability operation using HT-9. ARIES-IV is a DT fueled second stability using SiC [ASC]. A PULSAR study for pulsed operated reactor was also performed [PULSAR].

JAERI studies the DREAM (DRastically EAsy Maintenance) reactor [DREAM]. The objective

of this reactor is set to be to attain high availability by making maintenance easy. Therefore physics performance is set to be conservative ; e.g., a Troyon co-efficient of less than 3, a safety factor of more than 3, and an H-factor of less than 2. In contrast, the aspect ratio is increased to 8 and the plasma major radius is increased to 16 m both to make the maintenance easy and to obtain a high bootstrap current fraction. Moreover, to compensate for the low physics performance, the maximum toroidal field is increased to 20 Tesla, which results in a fusion power density of 5.5 GW and electric power at bus bar 2 GW. SiC is used as the structural materials for an increment of efficiency for replacement work and safety.

In contrast to these reactors, a conceptual design study for the early realization of tokamak fusion reactors based upon present physics/engineering knowledge was carried out by a group at the University of Tokyo. The proposed reactor series are called IDLT (Inductively Driven Long pulse Tokamak) reactors, whose pulse duration is as long as 6 hours only using OH coils for plasma burning. IDLT-DEMO can generate 0.2 GW electricity for 4.5 hours a demonstration reactor using the same physics/engineering of the ITER-EDA. The IDLT-commercial reactor [T.Yamamoto] is designed based upon conservative physics (e.g., H-factor = 1.8, Troyon co-efficient 2.7, bootstrap current fraction 46 %), and the fusion power is increased to 3 GW pulse interval time as short as 10 min in order to play a role as a commercial reactor. The IDLT-advanced reactor is a compact reactor whose plasma major radius is decreased to 7.5 m by increasing physics the performance with an H-factor of 2.6, a bootstrap current fraction of 63 %, and a Troyon co-efficient of 4.4.

Evaluation study has been carried out through an ARIES-study and SSTR. The ARIES-study will be succeeded by the Starlite-study, which is currently being carried out, and is explained in chapter 4. In Japan, there has been a recent trend of evaluating fusion economy. JAERI evaluated the cost of SSTR to be about 720 Billion yen, 16 yen/kWh [SSTR-JAERImemo]. The Institute for Future Technology evaluated the SSTR to be approximately 930 Billion yen [IFT]. The largest difference between these are (1) the utility cost and interest during construction (total 92 Billion yen), (2) varieties of components (e.g., primary cooling system, machinery, other equipment; 66 Billion yen). These two values are two times of the cost difference between reactor components (about 55 Billion yen). Therefore the estimation for reactor components is a high accurate evaluation, although other costs tends to have large uncertainties.

2.4 Evaluation studies except economy

2.4.1 Energy analysis

Energy analysis is for analysis of energy consumption in producing goods or services. Ref. [Y.Kaya] provides the first energy analysis document. In Ref. [Y.Kaya] not only energy production but also industry, agriculture, transportation, fabrications, and consuming goods are widely evaluated. In assessment for power plants, the input energy to power plant for the construction and operation of power reactors is compared with the output energy from the power plant, and energy gain is evaluated for the power plant. The most prominent paper was the work of Ref. [P.F.Chapman] for claiming fission power reactor's energy gain.

Two energy analysis studies have been made for fusion reactors in Japan [Y.Kozaki, Y.Shimazu86,88]. Ref. [Y.Kozaki] is the first Japanese energy analysis treating the fusion power reactors UWMAK-II and III. The energy intensities for various materials are derived from the I/O method and PCA (Process Chain Analysis). The results indicated that energy gain is 34.5. Refs. [Y.Shimazu86,88] compared the energy gain for various fusion power reactors (Table II-1). It is, however, pointed out that energy gain decreases by one order when Li is collected from sea water, since a great amount of energy is consumed in that process.

Ref. [R.Bunde, D.Pfirsch] studied energy analysis abroad. The largest difference in these references is the energy required for fuel and disposal treatment and the decision as to whether the electricity generated by the fusion reactor itself should be used for this energy. No energy analysis has been made of recent power reactors. It is therefore necessary to evaluate the energy gain in recent reactors from revised energy intensity data to suit the present I/O matrix.

2.4.2 Safety and radioactive waste

The safety aspects of fusion reactors have been investigated. Ref. [IAEA-TCMII] has pointed out that the tritium inventory reaches 5 ~ 10 kg per 1 GW reactors. Ref. [M.S.Kazimi] has reviewed the safety aspects of fusion reactors based on the following points. (1) Emission and exposure of neutrons, compared with ^{131}I emission and its inventory, (2) induced radioactive level cooling as well as radioactive waste volume and weight, (3) disruption by loss of cooling accidents, (4) chemical reaction owing to Lithium. The conclusions were that fusion reactors are inherently safer than fission reactors, and that safety can be assured, although not completely. An additional risk-benefit analysis is necessary.

The ESECOM-study [ESECOM] evaluated safety, and environment impact. The evaluated reactors were not STARFIRE, but 10 kinds of tokamak, RFP (Reversed Field Pinch), and Fusion-Fission reactors. The radioactive waste volume for fusion ranges from 480 to 3100 m^3, and 5 of 10 reactors exceed 1000 m^3, compared with fission reactor's value (540 m^3). The DDI (Deep Disposal Index) to indicate deep disposal burial showed that DDI of fission reactors is higher by two orders than that of fusion reactors. The ESECOM-study concludes that radioactive waste from fusion reactor may be adaptable to a shallow disposal burial. Recently the same kinds of evaluation studies based upon ARIES-I or several demonstrator reactors have been reported in Ref. [W.M.Stacey]. Professor W.M.Stacey evaluated the radioactive waste volume to be from 500 ~ 2300 m^3.

In EU, the EEF-study in 1988 and the SEAFP (Safety and Environmental Assessment of Fusion Power)-study in 1995 engaged in safety and environmentally oriented reactor studies. The Fusion power of the SEAFP is at a 3 GW level, whose and the reactor design is based upon the ITER physics/engineering, using advanced materials for structural materials and/or for a high temperature tritium breeding blanket. Model 1 uses a Vanadium alloy, Lithium ceramics for the tritium breeder, and Helium for coolant. Model 2 uses reduced activation martensitic steel, Lithium Lead, and water cooling. The tritium inventory was reduced as much as possible; to 2 kg with 50 μ Sv/y.

Ref. [SEAFP] has studied various concerns relative to fusion reactors; e.g., plain accidents, earthquakes, waste disposal, proliferation, chemical hazards, resource availability. The SEAFP concludes that (1) there is no risk of uncontrolled runaway, (2) accidental probability is less than 10-7, (3) although radioactive waste volume is as much as that of fission reactors, it does not include such a long-lived nuclide as radioactive waste from fission, (4) no proliferation materials exist, and (5) there are no resource constraints. The Safety analysis was skipped, although readers can refer to references such as [T.Uda].

Table II-1 Energy gain results in Refs. [Y.Shimazu88], which mentioned that the energy gain of the fusion reactors are decreased by one order if the Li_2O is collected from seawater.

Reactor name	Type	Energy Gain
STARFIRE	Tokamak	20.5
SPTR	Tokamak	17.1
NUWMAK	Tokamak	26.8
WITAMIR-1	Mirror	20.7
SOLASE	Laser	22.0
CASETTE	Compact Tokamak	15.2
WILDCAT	DD Tokamak	5.90
PWR	Fission	18.2
Hydro powered		14.3
Geothermal		6.60
Wind		4.30

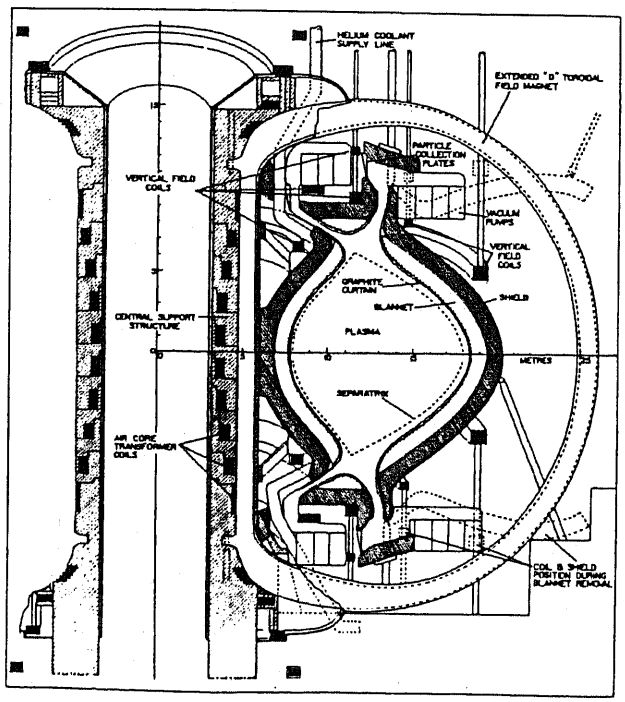

Plasma Radius	5m	Average Ion Temperature	15.2 keV
Major Radius	13m	Average Electron Temperature	13.5 keV
Aspect Ratio	2.6	Confinement Time	4 sec
First Wall Radius	5.5m	Average Ion Density	$6.46 \times 10^{13} cm^{-3}$
Chamber Wall Area (actual)	$3300 m^2$	Average Alpha Density	$0.09 \times 10^{13} cm^{-3}$
Plasma Current	14.9MA	Average Electron Density	$6.64 \times 10^{13} cm^{-3}$
Poloidal Beta	2.3	Fractional Burnup	2.75%
Stability Factor, q(a)	2.2	Power to Divertor (in Particles)	716 MW
Toroidal Field (on axis)	35.7kG	Radiation Wall Loading (Max.)	$3.42 w/cm^2$
Anomolous Resistivity Factor	3	Neutron Wall Loading (Max.)	$1.16 MW/m^2$

Figure II-13 Cross section of UWMAK-II and its design parameters

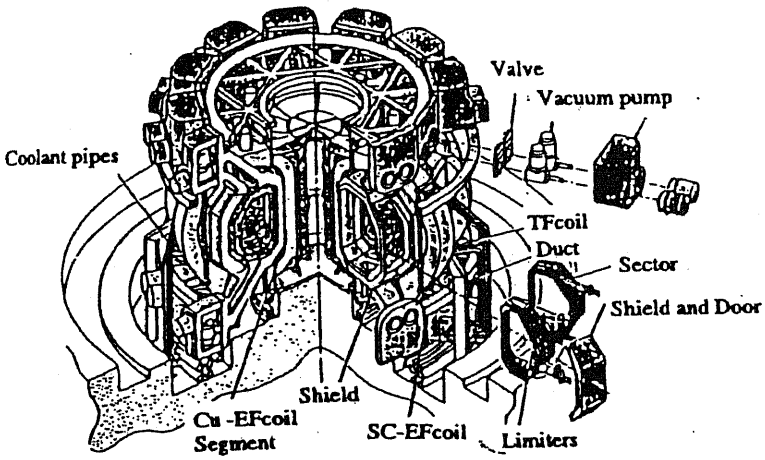

	STARFIRE
electric output power	1200
thermal power	4000
plasma major radius (m)	7.0
plasma minor radius (m)	1.94
plasma elongation	1.6
plasma current (MA)	10.1
average toroidal beta	6.7
safety factor (q_a)	5.1
Magnetic field on axis (T)	5.8
neutron wall load (MW / m^2)	3.6
First wall material / coolant	SUS/H_2O
Tritium breeder	$LiAlO_2$
Blanket material / coolant	SUS/H_2O
Maximum heat at material / coolant	450/320

Figure II-14 Bird's eye view of the STARFIRE power plant and its reactor design parameters

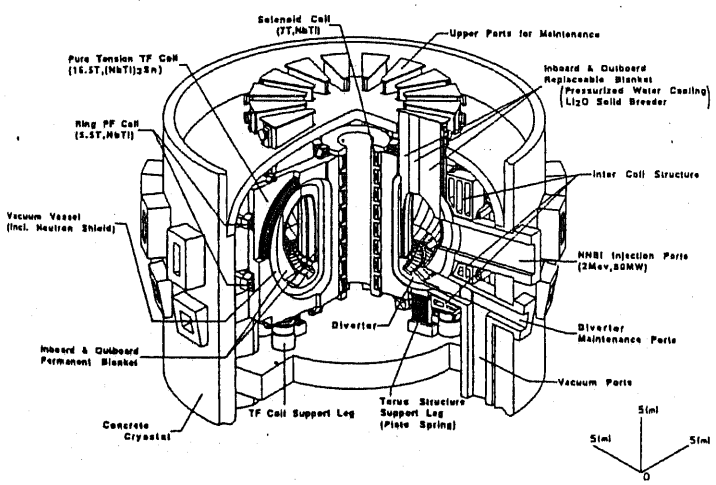

Plasma Current	(I_p)	12MA
Bootstrap Current	(I_{boot})	9MA
Beam Driven Current	(I_{bd})	3MA
Toroidal Field	(B_t)	9.0T
Maximum Field	(B_{tmax})	16.5T
Major Radius	(R_p)	7.0m
Minor Radius	(a_p)	1.7m
Elongation	(κ)	1.85
Safety Factor	(q_{95})	4.5
Toroidal Beta	($<\beta_t>$)	2.7%
Poloidal Beta	(β_p)	2.0
Average Temperature	($<T>$)	17keV
Average Density	($<n_e>$)	$1.4 \times 10^{20} m^{-3}$
Effective charge	(Z_{eff})	1.5
He concentration	(f_{He})	5%
Fusion Output	(P_f)	3GW
Energy Gain	(Q)	50
Total Thermal Output	(P_{th})	3710MW
Max.n Wall Load	(P_n^{max})	5MW/m^2
Net Electric Power	(P_e^{net})	1000MWe

Figure II-15 Bird's eye view of the SSTR reactor and its design parameters.

3. Progress of Low-Aspect-Ratio Tokamaks

3.1 Simulation study and reactor study

Ref. [K.Yamazaki] describes that the Low-Aspect-Ratio tokamak concept was proposed as ST (Spherical Torus) by Y.K.-M. Peng in the early 1980s in order to attain high beta through modification of the plasma cross section. Although other modifications of plasma cross section failed to demonstrate high physics performance, only ST can successfully indicate its excellent physics performance and is expected as a new feature. ST has a mixed property of both tokamaks and CTs (Compact Torus; e.g., RFP, FRC, Spheromak). CTs are also another means of attaining high beta. Therefore, it should be stressed that ST has the same origin in its attempt to achieve high beta, and it is derived from the "conventional" aspect tokamaks and CTs. Moreover, ST has a lot of attractive physics phenomena as it combines characteristics of both tokamaks and CTs.

The first published ST paper was Ref. [Y.K.-M. Peng85]. In this study, the conceptual ST reactor was analyzed by use of Troyon scaling, plasma start up by LHW, Mirnov or neo-Alcator scaling, a Murakami density limit, and so on. The reactor's properties are as followings: the toroidal field coil is made by a high-strength copper conductor of 2~3 Tesla, a plasma major radius of 1~1.6 m, and fusion power of 60 MW. This reactor is a very cost-effective reactor with a direct construction cost of 340 M$, and a total construction cost of 560 M$. The ST physics characteristics, revealed by an MHD equilibrium calculation, are explained in Ref. [Y.K.-M.Peng86]. This paper explained that the ST physics properties, i.e., high toroidal beta (> 0.2), low poloidal beta (< 0.3), natural elongation, high plasma current, high Troyon coefficient, and strong paramagnetism (Figure II-14).

In the 1990s, an ST rector study has been carried out based upon ITER physics. In Ref. [Y.K.-M.Peng90], the divertor heat load and CP (Center Post) radiation, which are considered to be problems in regard to the realization of the ST reactor because of the compactness of ST reactors. Divertor heat load is decreased to 3 MW/m^2 by use of a gas divertor as well as a long rectangular divertor heat channel. CP was designed to withstand a 5 MW/m^2 neutron wall load by use of forced flow water cooling, since a shield cannot be attached to CP due to the lack of space (Figure II-15). There are some power plant class reactor designs by M.Peng which can be found, such as a 1.6 GW fusion output power in the second stability region (Ref. [Y.K.-M.Peng90]), or 2.6 GW (Ref. [Y.K.-M.Peng95]); however, several kinds of VNS (Volume Neutron Source) or pilot plants (Refs. [Y.K.-M.Peng92,95,96]) can be found.

Other reactor studies can be found in addition to those of M.Peng. For example, power plants of 0.4 ~ 1.2 GWe by T.C.Hender [T.C.Hender], a pilot plant and power plant whose reactor size is close to DIII-D device by R.D.Stambaugh in General Atomics [R.D.Stambaugh96], ARIES-ST [ARIES-ST] optimized from ARIES-LAR [C.G.Bathke95] of 1 GWe by the Starlite team. Reactors by T.C.Hender are compact, having a 1.6 ~ 2.3 m plasma major radius by increasing the neutron wall load to 6 ~10 MW/m^2. Reactors by R.D.Stambaugh have an 8 MW/m^2 neutron wall load, a 90 % bootstrap current fraction, and a 2.5 elongation.

Both ARIES-LAR and ARIES-ST must have a 30 cm shield to meet Class C disposal requirements. The aspect ratio of the ARIES-LAR is 1.25, by which heat dissipation on the TF coils is up to 1.5 GW. This heat loss makes the fusion power large, which results in a 5 m plasma major radius due to a low (3.1 MW/m^2) neutron wall load. The ARIES-ST has been optimized in terms of compactness (a plasma major radius of less than 3 m) by increasing the aspect ratio up to 1.6 as well as decreasing the TF coil dissipation to 0.6 GW, and increasing the neutron wall load up to 7 MW/m^2. Ref. [A.J.Wootton] compared with these ST reactors and pointed out that ST reactors are not advantageous unless (1) high current drive efficiency as well as low safety factor are attained at the same time, and (2) a high H-factor, elongation, and neutron wall load are attained at the same time.

3.2 Experimental studies

The initial ST physics experiment was carried out by spherical torus devices, such as the HSE device [HSE] in 1987, the ROTAMAK device [ROTAMAK] in 1991, and the SPHEX [SPHEX] devices. Tokamak-like plasmas were generated by a toroidal magnetic field being superimposed onto spheromak plasmas by inserting a current-carrying center conductor in the HSE device and the SPHEX device. By this superimposing, the stability of the HSE plasmas had been improved. It was reported that with the ROTAMAK device a tokamak-like configuration was obtained which was high beta and had stable plasmas. It was reported that with the SPHEX device, an increment of electron temperature/density as well as toroidal current was observed, and that the plasma sustainment mechanism is the same as that of spheromaks. These plasmas are common in "cold plasmas" whose plasma center temperature is less than 30 eV.

The ST experimental studies using high temperature plasmas had begun in 1991 with the START (Small Tight Aspect Ratio Tokamak) device (see Figure II-16) [START92]. Its plasma properties are as follows; a plasma major radius of 0.32 m, an aspect ratio of 1.25, an elongation of 1.8 (at maximum 4 without feedback coils), a plasma electron temperature of 150 ~ 500 eV, a plasma current 180 ~ 250 kA, and a central toroidal field of 0.4 Tesla. Experiments in Ohmic heating were carried out before 1996, and the results are compiled in Ref. [A.Sykes94, START94]. The energy confinement time was 0.5 ~ 2.5 ms, which was two times that of confinement time predicted by neo-Alcator scaling, and was closer to that of Rebut-Lallia scaling. The electron density limit was consistent to the Greenwald-limit. The safety factor could be decreased to as low as q_{95} = 4.0, $q_{cyl} = 5a_p B_0 / R_p I_p$ = 1.25 at A = 1.35, respectively. No disruption occurred, however, IRE (Internal Reconnection Events) were observed.

In 1996, the START device had started with 40 keV, 0.5 MW NBI heating experiments [START96]. In 1997, $\beta_{total} > 30\%$, $\beta(0) \sim 50\%$, $\beta_N \sim 4$ were obtained [START97]. $\beta_{total} > 30\%$, $\beta(0) \sim 50\%$ are world records. It was revealed by an ideal stability analysis for high beta discharge that the high n ballooning mode and low n pressure driven internal mode were close to their limits. All the high beta discharges were terminated, causing IREs with no external modes. Therefore, high beta discharges by

the START device can be considered to be limited by internal low n modes. Murakami parameter $n_e R_p / B_0$ of 1.6 [10^{20}/m^{2}T] was attained, which was increased from 1.4 in 1996 and was twice that in the ohmic region. q_{95} decreased to 2.3 at an aspect ratio of less than 1.4, which is close to the MHD limit. The energy confinement time was close to ITER96L scaling than ITER97H scaling. The NBI power is scheduled to be up to 1 MW and pellet injection has also been proposed.

There are many other ST experiments derived from CT studies such as those using HSE or SPHEX devices. For example, there was HHFW (High Harmonic Fast Wave) using the CDX-U device, a helicity injection study using by HIT devices, and a tilt instability study using the TS-3 device [A.Morita].

3.3 Next step experimental devices

Several MA (Mega Ampere) class plasma current experimental devices have been designed and are now under construction in the U.S. (the NSTX device), in England (the MAST device), and in Russia (the GLOBUS-M device) which follows the START device.

NSTX

The NSTX (National Spherical Tokamak Experiment) device has been designed in collaboration with the PPPL (Princeton Plasma Physics Laboratory), ORNL, the University of Washington, and the University of Colombia. The NSTX is scheduled to ignite its first plasma in April 1999. Figure II-17 shows the NSTX design. The goal of the NSTX device is to obtain advanced physics to lead an ST VNS or power plant. There are two design parameters. The first is that a plasma major radius of 0.86 m, aspect ratio A = 1.25, elongation $\kappa = 2.2$, plasma current I_p = 1 MA, surface safety factor q_a = 12, beta 30 ~ 45 %, bootstrap current fraction f_{bs} 40 ~ 80 %, and discharge duration 5 sec. The second set of parameter is A = 1.4, $\kappa = 3$, I_p = 1 MA, q_a = 12, $\beta \leqq 45$, $f_{bs} \leqq 99\%$. The planned heating measures are to use CHI (Coaxial Helicity Injection), HHFW, NBI, and ECH. ECH is used for pre ionization, helicity injection for plasma start-up, 6 MW HHFW for plasma surface current control, and HHFW and NBI for heating and current drive. Conductor shells are used to stabilize high beta plasmas.

MAST

The MAST (Mega Ampere Spherical Torus) device has been designed primarily by the Culhum laboratory in England. The aim of this device is to reveal ST physics properties of the ASDEX and the DIII-D device class. The device hall will be completed in January 1997; the device pit is scheduled to be completed in August 1998, and initial plasma at the end of 1998. The plasma parameters are R_p = 0.7 m, A = 1.4, $\kappa = 1.8$, $I_p \leqq 2$ MA, $B_0 \leqq 0.63$ Tesla. Heating devices are 5 MW, 80 keV NBI and 1.5 MW, 60 GHz ECRH. Both a natural divertor configuration and a double null configuration are possible. The following experiments are planned; a disruption free, longer energy time confinement than predicted from

the energy confinement time, parameter scaling on SOL, high bootstrap current fraction discharge, and NBI current drive.

GLOBUS-M

The GLOBUS-M device is now being constructed by the A.F.Ioffe Physicio-Technical Institute at St.Petersbug in Russia. 80 % of the GLOBUS-M has already been constructed, and it will ignite its first plasma in the latter half of 1998. The plasma parameters are R_p = 0.36 m, A = 1.5, κ = 2.2, $I_p \leqq$ 0.5 MA, $B_0 \leqq$ 0.6 Tesla, plasma density 10^{20} [m^{-3}], quasi stationary discharge duration 0.2 sec. The parameters of the GLOBUS-M are set somewhat between those START device and NSTX/MAST devices. The following three objectives are set:

(1) Ohmic region plasmas in the conditions of particle flow and high heat flux to the vacuum chamber

(2) Plasma physics study depending on plasma shape which is different from those of the START and the MAST devices

(3) Additional heating or RF study by use of ICRF or HHFW to attain high beta plasmas. Three current drive techniques are planned; 40 MHz, 2 ~ 4 MW, 50 ~ 100 msec ICRF, 2.45 GHz, 1 MW, 50 ~ 100 msec LHCD, 30 ~ 50 MHz, 1 ~ 4 MW HHFW.

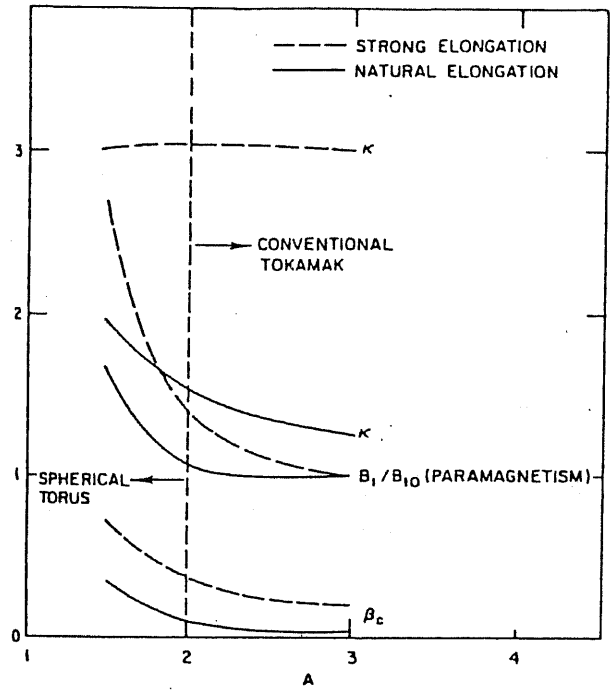

Figure II-16 ST physics analysis by M.Peng (Ref.[Y.K.-M. Peng]). This figure indicates beta value indicated by vertical axis can be increased as decreasing aspect ratio.

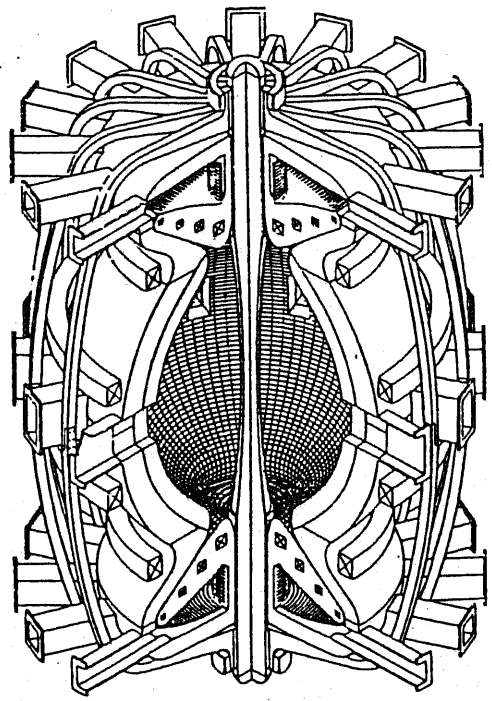

Figure II-17 ST pilot plant view by M.Peng (Ref.[Y.K.-M. Peng90]). This ST plant is designed so that the CP (Center Post) can be removed for easy maintenance.

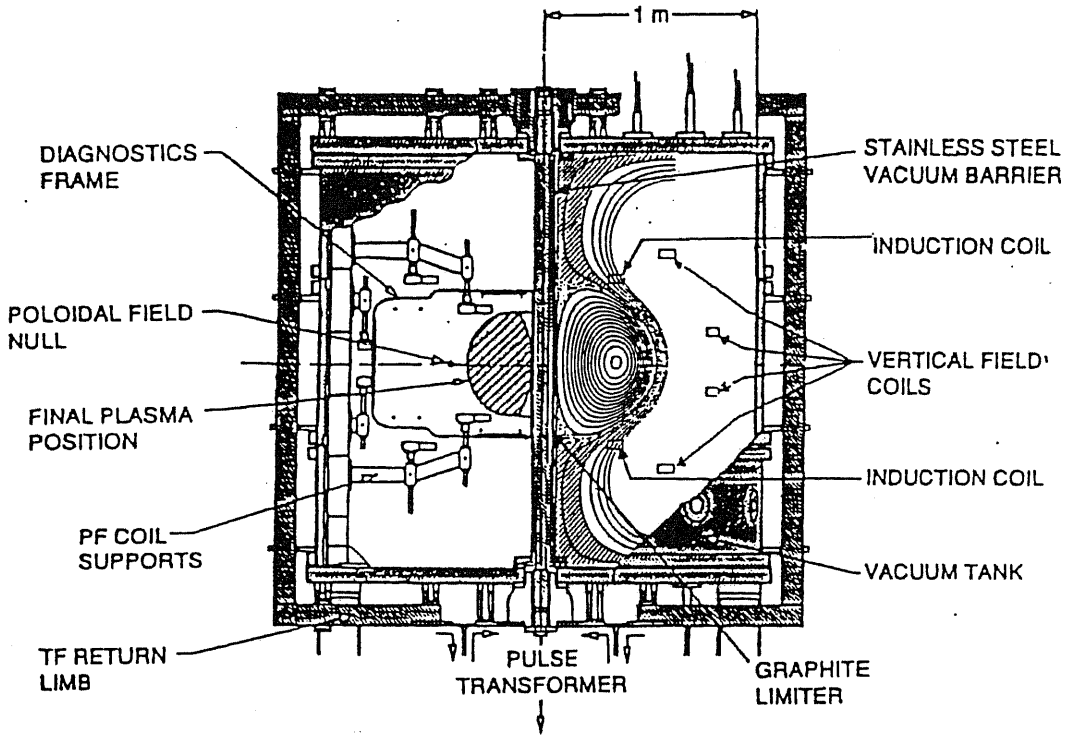

Figure II-18 The cross sectional view of the START device (Ref. [START94]). The START device could obtain excellence physics performance such as $\beta_{total} > 30\%$, $\beta(0) \sim 50\%$ (Ref. [START97]).

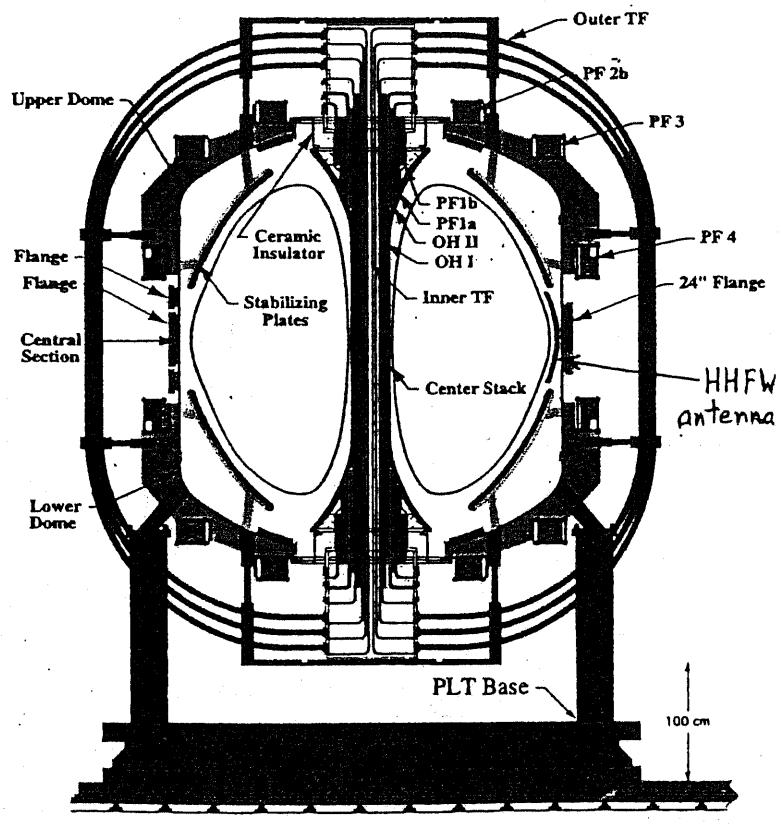

Figure II-19 The design figure of NSTX device.

4. Recent reactor design and evaluation study

Reactor designs have appeared which are based upon advanced physics performance such as RS (reversed shear) or ST (Spherical Torus). The ARIES team has designed ARIES-RS and ARIES-ST. The properties of the ARIES-RS are as follows; A = 4, R_p = 5.5 m, I_p = 11.3 MA, f_{bs} = 88 %, β_N = 4.8, average neutron wall load of 4 MW/m^2, and a Toroidal field on the TF coils of $B_{\max}$ 16 Tesla. The aspect ratio, $B_{\max}$, the structural materials, and the cooling materials are the same as those applied of ARIES-II/IV. Properties for the ARIES-ST are described in chapter 3.

The Starlite-project evaluates five kinds of tokamak reactors in terms of economy [C.G.Bathke95]. The evaluated reactors are; FS (First Stability reactor which is referred to as ARIES-I), PU (Pulse operated reactor which corresponds the PULSAR reactor), SS (Second Stability derived from ARIES-II/IV), RS (Reversed Shear of ARIES-RS), and LAR(Low-Aspect-Ratio of ARIES-LAR). The ARIES-ST has not been formally evaluated because it is still being optimizing. The most current results indicate that both ARIES-RS and ARIES-ST have almost the same economic effectiveness. The total construction cost of the ARIES-RS (4224 M$) is higher than that of the ARIES-ST (4194 M$). In contrast, the COE of the ARIES-RS (75.8 mill/kWh) is slightly lower than that of the ARIES-ST (79.7 mill/kWh). The ARIES team evaluates the fusion economy compared with other energy sources [R.L.Miller97a]. Ref. [R.L.Miller97a] determines COE goal for fusion reactors to be 45 mill/kWh in 2040 ~ 2050, with a maximum requirement of 60 mill/kWh, with the condition that the COE of fission, coal, natural gas from present to 2010 are increased 1 ~ 2 % per year.

In Japan, the importance of fusion assessment studies has been recognized recently. Economic evaluation and cost-down studies have appeared. JAERI investigated the A-SSTR, with the aim of reducing the COE of the SSTR to that of the fission reactors. The properties of the A-SSTR are $B_{\max}$ = 20 Tesla, β_N = 4.2, f_{bs} = 80 %, R_p = 6 m, fusion power = 5.5 GW, electric output power = 1.7 GW. Two of the A-SSTR reactors are placed in the same plant space. At CRIEPI, the tokamak fusion systems code was developed with Hatayama in 1994 [T.Yoshida94]. This code consists of physics based upon the ITER PGL, constant tension D-shaped TF coil shape by the three-arch approximation which is obtained from TRESCODE by JAERI [TRESCODE], and the economic model by the Generomak model. Cost data are obtained from U.S./E.U. reactor cost data because of the lack of cost data experience in Japan. Some data like fixed charge rates are derived from Japanese fission experience.

Recently CRIEPI has investigated the requirements for fusion reactors that can be accepted by utilities, especially in terms of cost. The CREST-1 (Compact REversed Shear Tokamak) reactor, which uses the reversed shear profile, was proposed to demonstrate a highly cost effective reactor. The CREST is extremely compact with R_p = 5.4 m, A = 3.4, obtained by increasing β_N to 5.5, and f_{bs} to 88 % [K.Okano97a,b]. Since the physics performance is very high, a conservative engineering performance (e.g., 13 Tesla and water as a coolant, Ferrite steel as a structural material) is adequate. The COE of this CREST

can be successfully reduced to half that of the other ITER-level reactors. Problems caused by toroidal rotation that are inevitable for the reversed shear profile are resolved by the use of current profile control and conductor cells [K.Okano97c].

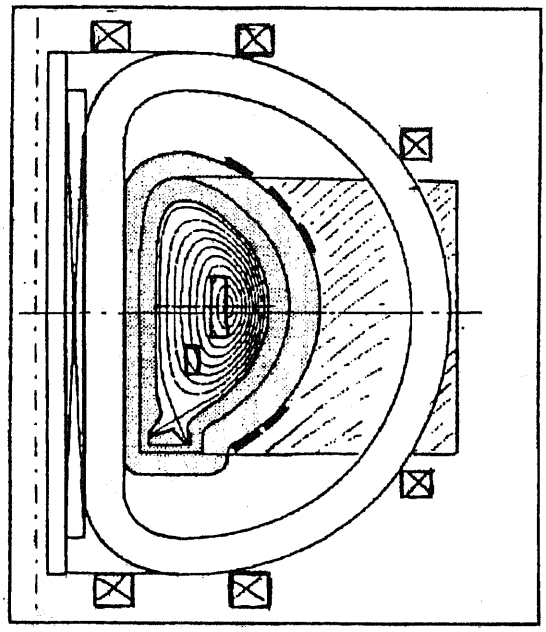

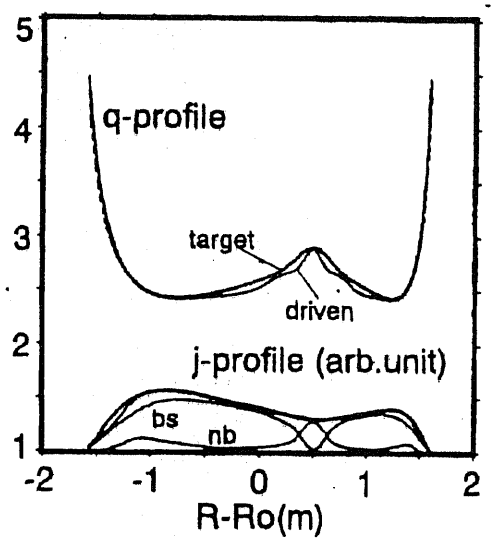

Major radius, R(m)	5.4
Aspect ratio, A=R/a	3.4
Minor radius, a(m)	1.59
Elongation, κ	2.0
Triangularity, δ	0.5
Safety factor, q_ψ	4.3
Pol. beta, β_p	2.5
Tor. beta, β_t (%)	7.6
Troyon factor, β_N	5.5
H factor(ITER 89L)	2.9
Plasma current (MA)	12.0
BSC fraction (%)	85
NBCD I_b (MA)	1.8
Beam power (MW)	94
$\langle T_e \rangle$ (keV)	15.2
$\langle T_i \rangle$ (keV)	15.5
$\langle n_e \rangle$ ($10^{20}m^{-3}$)	2.1
$\langle v_{rot} \rangle$ (10^6m/s)	0.93
Eff. charge, Z_{eff}	2.4
He accum. f_{He}(%)	15
τ_p^* (He)/ τ_E	9
B_{t0} (T)	5.6
B_t on coils (T)	12.5
Fusion power (MW)	2,970
Turbine inlet (MW)	3,378
Therm. efficiency(%)	41
Grs. elec.power(MW)	1,385
Net elec.power (MW)	1,163

Figure II-20 The CREST-1 power reactor conceptual design and its design parameters

5. Summary

5.1 The progress of the plasma physics experiments

(1) In the 1980s additional heating plasma experiments were begun. With this additional heating experiments, plasma experiments progressed from the ohmic region to confinement improvements, MHD stability, and beta improvements.

(2) A beta limit study developed beta limit scaling (Troyon scaling). Beta improvement studies were made for high aspect ratio, bean shape, elongation, and spherical torus. The ST (spherical torus) study has been carried out, however, the second stability region could not be attained by other plasma shape modifications.

(3) The Energy confinement study was proceeded from the H-mode by the ASDEX device to the PEP H-mode by the JET device, and the supershot-mode by the TFTR. After the TFTR experimentally revealed the existence of the bootstrap current, the JT-60U attained an 80 % bootstrap current fraction by high β_p experiments. The improved high β_p H-mode was deviated, by which the JT-60U attained the world record of the fusion triple product. Through the DIII-D devised VH-mode, β_t = 11 % and $\beta(0)$ = 44 % were obtained. Moreover it was reported that this VH-mode allowed for the attainment of the second stability region.

(4) Reversed shear operating mode evolved from the PEP H-mode by the JET, the VH-mode by DIII-D, and the high bootstrap current fraction experiment of high β_p H-mode by JT-60U. Simulation studies indicated the possibility of highly cost effective performance as well as superior physics performance. MSE measurements enabled to measure a detailed safety factor profile. The JT-60U attained break-even conditions through the use of this reversed shear profile.

(5) The JET device and the TFTR device have been used for DT experiments. The TFTR device carried out 50 % of the Tritium experiments, which resulted in a maximum 10.6 MW fusion power during a one second burning time.

(6) The ITER EDA activity has compiled physics knowledge based upon experimental research for a variety of factors including beta limit, density limit, and bootstrap current fraction scaling. Based on this compilation, the physics of reactor design were assessed as being highly accurate. However, the ITER's goal to sustain 1000 sec of 1.5 GW fusion power are greater than recent obtained data by three orders of magnitude, respectively.

5.2 Demo/commercial reactor design and their evaluation study

(1) Several power reactor designs were developed before the 1980s, which were based upon the physics knowledge at that time. It is clear, however, that these designs are inadequate compared with our present knowledge of physics, including such factors as beta and density limits. Engineering properties are almost the same as those applied to recent reactors, except that SUS and NbTi were used.

(2) Evaluation studies were carried out before the 1980s, although inconsistent results were obtained. For example, one study mentioned that fusion energy would be economically competitive, while another said that it would not. It was also suggested that fusion power's realization and introduction to energy systems would be delayed from the end of the 20^{th} century to the beginning of 21^{st} century.

(3) Reactors from the 1980s still had some inadequate physics design factors. Several issues are still valid, however, for recent reactor studies, including the use of steady state operation with non-inductive current, 12 ~ 3 Tesla with Nb_3Sn superconductor. The most prominent issues during this period were the development of economic evaluation guidelines and the Generomak model.

(4) Based on these developments, evaluation studies were promoted in the latter half of the 1980s. Reactor studies were carried our not only in the U.S. but also in EU, based upon beta limits, the Kaye-Goldston scaling advance from neo-Alcator scaling, and current drive efficiency. The cost evaluation systems code was developed in Japan, which could calculate the relative cost of the INTOR reactor. Such an evaluative study, however, was not emphasized.

(5) Physics knowledge, such as MHD stability, beta limit, energy time confinement time, bootstrap current fraction, were compiled through the ITER-EDA. This compilation enhanced the reliability of the physics design of reactors. As a result, SSTR or ARIES reactors using high physics/engineering performance were developed, such as superconductor coils, and advanced structural materials, and cooling. In contrast, the IDLT-study was carried out based upon the ITER-level physics/engineering knowledge. These reactor designs were evaluated by a bottom-up method. In Japan, the importance of economic evaluation was recognized, however, such an evaluative study was thought to be inadequate. This inadequacy results from the applied data.

(6) Analyses of the both energy and safety, except economy, had been carried out. Energy analyses were made for several reactor designs, including the STARFIRE. The results indicated that the energy gain of fusion reactors was excellent, however, the energy gain was reduced by one order in the case where Lithium was collected from seawater. Moreover, it was pointed out that the results were quite different each other depending upon the methodology used for energy analysis.

(7) A safety analysis was carried out. Evaluative studies examined 1) the reduction of the tritium inventory and radioactive levels, 2) volume and weight of radioactive waste, 3) exposure of neutrons, 4) accident analysis and so on. The SEAFP-study did not conclude that fusion must try to resolve these problems.

5.3 Low-Aspect-Ratio Tokamak

(1) M.Peng demonstrated several properties of Low-Aspect-Ratio tokamaks, such as high beta, low poloidal beta, high Troyon co-efficient, strong paramagnetism, strong plasma current, natural elongation. Several compact reactors with no complicated shaping coils were proposed based upon the ST reactors' physics characteristics.

(2) The START device begun to be used for ST physics experiments, by which the excellent physics performance was revealed experimentally. Recently, $\beta_{total} > 30\%$, $\beta(0) \sim 50\%$, were attained (world

record) by the START device. Moreover, several MA class experimental devices are now under construction.

(3) Pilot plant or reactor design, based upon ITER physics or experimental results, are proposed. Moreover, some studies to counteract the drawbacks of the ST reactor, such as neutron damage on the CP or plasma start-up by use of bootstrap current up to unity, have been carried out.

5.4 Recent power reactor design

Recently, reactor studies have investigated the use of advanced physics such as reversed shear or spherical torus. Comparative studies like the Starlite-study for evaluating reactor types, such as first stability, pulsed operated, second stability, reversed shear, spherical torus, have also been investigated. Both reversed shear and spherical torus appear to be somewhat more cost effective than other reactor types.

Part III

Study of Design Parameters for Minimizing the Cost of Electricity of Tokamak Fusion Power Reactors

1. Introduction

It is estimated that the International Thermonuclear Experimental Reactor (ITER) can be constructed about 6000M$ [ITER-IDR] in the year of 2008 [ITER-16thIAEA]. Although it will be a great milestone for fusion research and development if the ITER can fulfill its physics/engineering missions, it is possible that tokamak fusion reactors will remain expensive. Competition of cost is vital for fusion reactors to become a commercial energy source. It is therefore necessary to study the feasibility of fusion reactors in terms of cost (the construction cost and the cost of electricity; COE) as well as in regard to their physics/engineering. In particular, special attention should be paid to the research and development of tokamak fusion reactors based on or extrapolated from the ITER level physics/engineering databases in terms of their cost.

Several designs for demonstration reactors and commercial reactors to succeed the ITER have been proposed [SSTR,ARIES-I,PULSAR,DREAM,IDLT]. Their design is so highly precise and sophisticated that we are able to understand their design in detail. It is, however, difficult to evaluate which is the best suited for commercialization among the proposed reactors using a same framework. It is also difficult to know which design parameters have great impact on cost. In this study, design parameters means both basic parameters (i.e., aspect ratio A, safety factor on the 95% flux surface q_{95}, the Troyon beta coefficient β_N, maximum magnetic field at toroidal field (TF) coil $B_{\max}$) and FOMs which are derived from those basic parameters (i.e. the bootstrap current fraction f_{bs}, the fusion power density P_{fus}, the plasma volume V_p, and the volume of TF coils V_{TF}). The Starlite project paper [C.G.Bathke96] and the Galambos paper [J.D.Galambos] have attempted to address this cost issue; the Stacey paper [W.M.Stacey] did not.

However, the impact of design parameters (i.e., A, q_{95}, β_N, f_{bs}, V_{TF} etc.) on the COE are not fully investigated with regard to operating modes (e.g., First Stability (FS), Second Stability (SS) and Reversed Shear (RS)). The impact here means which design parameters are important in terms of cost, and how much value should be attained and/or is preferable to reduce the COE. It can be considered that these basic parameters are determined through FOMs by trade-offs and constraints like neutron wall load. For example, high aspect ratio increases f_{bs} which leads to low current drive power and cost. However it also increases V_p and V_{TF} which makes the reactor large and expensive. The basic parameters are restricted by some constraints. For example, high $B_{\max}$ results in a large cross section of TF coils which will be limited by radial build. High $B_{\max}$ may also result in high fusion power and high neutron power, which is limited by neutron wall load P_{wn}. Ref. [T.Yoshida96] did not addressed these operating differences.

The purposes of this study are; 1) to reveal which design parameters have strong impact on the COE for each operating mode, 2) to determine how much value should be chosen for those influential parameters, and 3) to know which operating mode is the best for reducing the COE.

2. Analytical Models

2.1 The COE calculation model

A global zero dimensional tokamak system code is used for the COE calculation. The details of this computer program are given in Refs. [T.Yoshida94,A.Hatayama]. Beta limit, power balance, current drive and bootstrap current, published in the ITER physics guidelines: 1989 [ITER-PGL], are considered in our system code. Overall energy flow, including current drive power, power for coils, cryogenics, and B.O.P.(balance-of-plant), is calculated by an energy flow model based on Ref. [Generomak] (See Fig. III-1). The plasma minor radius a_p is searched to satisfy the electric power at the bus bar (P_e) = 1000 MW.

The constant tension, D-Shaped TF coil is calculated to satisfy the required electro-magnetic force by use of a three-arc approximation. The allowable toroidal ripple and the number of TF coils are set at 1.5% and 16, respectively. The shapes of the blanket, and the shield are also calculated by setting their thickness to a constant value. Volumes of various components such as the PF (Poloidal Field) coils and their structures are estimated by the fraction of TF coils. The volume of the divertor is estimated from the plasma's major/minor radius and a input thickness. The weight of all of the components are calculated by multiplying their volumetric density.

Costs of all of equipment based on weight are calculated by multiplying a unit cost per weight constant. This calculation method is widely admitted and used in cost studies. We believe that the cost will depend largely upon the volume or weight of components at the time when the required processing techniques for building fusion components have matured. We referred to the volumetric density and the unit costs in Refs. [SSTR,STARFIRE,Generomak,R.A.Krakowski,RTR]. Costs of all the other equipment are calculated by a nonlinear scaling to a standard cost value either by volume or by power. This scaling method is the same as that of Ref. [Generomak]. The COE is calculated from eq.III-1 by a constant dollar mode. Detailed calculation formula are described in appendix.

$$COE = \frac{C_{ac} + C_{om} + C_{src} + C_{fuel}}{P_e \cdot 8760 \cdot f_{ave}} + C_{dis} + C_{dec} \quad \text{--- (III-1)}$$

The annual capital cost (C_{ac}) is calculated by multiplying a direct cost and factors such as an indirect cost multiplier, a capitalization factor, and a fixed charge rate together. We used achievements of fission power plants in Japan for these three factors. The annual maintenance cost (C_{om}) is calculated as a fraction of the value of the direct capital cost. The annual scheduled replacement cost (C_{src}) is calculated by considering the frequency of replacing the blanket, the divertor, and the heating equipment. The annual fuel cost (C_{fuel}) is calculated as a value proportional to the plant availability. C_{dis} and C_{dec} means the cost of disposal and the cost of decommission, respectively. Main parameters are listed in Table III-1.

2.2 The physics/engineering parameters

The COE depends greatly on the design parameters. Here we regard the COE as a function of the following eight basic parameters:

$$COE = COE(a_p, A, \kappa, \delta, q_{95}, T, \beta_N, B_{\max}) \quad \text{--- (III-2)}$$

where κ = the plasma elongation, δ = the plasma triangularity, and T = temperature of both the plasma's electrons and ions. These 8 parameters are, in turn, used to calculate other important parameters, such as the total plasma current I_p, the H-factor (energy confinement multiplying factor), and the plasma's electron/ion density. In this work, the parameters in eq.III-2 are surveyed within a range given in Table III-2. These values range from those obtained experimentally to limits predicted theoretically. The next four parameters (which we call FOM) expressed by the eight basic parameters in eq.III-2 can be considered to have a strong impact on the COE: (1) *Bootstrap current fraction*; high f_{bs} reduces active current drive power, which results in low cost of current drive. The f_{bs} is expressed as $f_{bs} \approx \varepsilon^{0.5} \cdot \beta_P \approx \beta_N \cdot q_{95} \cdot A^{0.5} \cdot \kappa$. (2) *Plasma volume*; small V_p may lead to compactness of the reactor and low construction cost. The V_p is expressed as $V_p = 2\pi^2 R_p a_p{}^2 \kappa \propto A \cdot a_p{}^3 \cdot \kappa$. (3) *Fusion power density*; large fusion power density (P_{fus}) results in a small V_p. P_{fus} is expressed as $P_{fus} \propto n^2 T^2 \propto \beta^2 B^4 \propto \left(\beta_N \cdot I_P \cdot B_0 / a_p\right)^2$. (4) *Volume of the TF coils*; the smaller TF coil volume (V_{TF}) reduces the cost of the coil system (including the structures of the coils). The V_{TF} is calculated by multiplying the total cross section of the TF coil (S_{tot}) and the length of the TF coil (C_{ling}) together. V_{TF} is expressed as $V_{TF} = C_{ling} \cdot S_{tot} = \cdots \approx (a_p \cdot A) \cdot (a_p \cdot A \cdot B_{\max})$. We note that the eight basic parameters in eq.III-2 have the trade-offs through the four FOMs as explained in the introduction. These trade-offs are summarized in Table III-3.

2.3 The operating modes

Three types of operating modes are considered in this work for steady state operation with aspect ratio from 3 to 4.5 which can be treated by our system code; namely, First Stability (FS), Second Stability(SS), and Reversed Shear (RS). We did not treat pulsed operated reactor nor consider a low aspect ratio (A from 1.1 to 2.0) tokamak reactor whose physics is quite different from that in Ref. [ITER-PGL]. In this study, FS and SS is distinguished by MHD (magnetohydrodynamics) stability expressed by M.E.Mauel [M.E.Mauel]. In Ref. [M.E.Mauel], the MHD instability region is given by

$$\varepsilon\beta_p\text{-}lowerlim < \varepsilon\beta_p < \varepsilon\beta_p\text{-}upperlim \text{--- (III-3)}$$

The $\varepsilon\beta_p$-*lowerlim* and $\varepsilon\beta_p$-*upperlim* means the lower boundary MHD instability and the higher boundary MHD instability, respectively. Therefore, the MHD stable region is expressed in the following way:

First Stability

$$\varepsilon\beta_p < \varepsilon\beta_p\text{-}lowerlim = 0.75\cdot\left(q^*/q_a\right)^2\cdot\left[\sqrt{q_a/q_0}-1\right] \text{--- (III-4)}$$

Second Stability

$$\varepsilon\beta_p\text{-}upperlim = 6.0\cdot\left(q^*/q_a\right)^2\cdot\left[\sqrt{q_a/q_0}-1\right] < \varepsilon\beta_p < 2.0 \text{--- (III-5)}$$

where q^*, q_a is defined in this study as

$$q^* \equiv \left(5a_p{}^2 B_0/R_P I_P\right)\cdot S^2$$

$$S \equiv \sqrt{\frac{1+\kappa^2\left(1+2\delta^2-1.2\delta^3\right)}{2}}$$

$$q_a \approx q^*\cdot\left(1+\varepsilon^2\left[1+0.5\left(l_i/2+\beta_P\right)^2\right]\right) = q_a(q_{95},\varepsilon,\beta_N,S)$$

$$\beta_p = \beta\cdot\left(q^*/\varepsilon\right)^2/S^2 = \left(q^*/\varepsilon\right)\cdot\beta_N/20$$

and $\varepsilon\beta_p$ is calculated as

$$\varepsilon\beta_p = q^*\beta_N/20 = \varepsilon\beta_p(\beta_N, q_{95}, \varepsilon) \text{--- (III-6)}$$

$$q_{95} = q^*\cdot\left(1.17-0.65\varepsilon\right)/\left(1-\varepsilon^2\right)^2$$

$\varepsilon, \beta_p, q_0, q^*, S, q_a, l_i$ are defined as the inverse aspect ratio, poloidal β, safety factor at center (= 1.1 in FS, 2.0 in SS), cylindrical safety factor, plasma shaping factor, safety factor at edge, and plasma internal inductance (= 0.5 in this study), respectively. By these equations, $\varepsilon\beta_p$ and $\varepsilon\beta_p$ *-lower/upper limit* are functions of $q_{95}, \varepsilon, \beta_N$, (κ and δ). Therefore, once $q_{95}, \varepsilon, \beta_N$, (κ and δ) are decided, each condition of eq.III-4 and III-5 is satisfied even if $B_{\max}$ and T is changed. In eq.III-5, we restrict $\varepsilon\beta_p < 2.0$ like Refs. [C.G.Bathke,Ramos91a&b]. The MHD (magnetohydrodynamics) stability of the RS operating mode is checked by the ERATO code only for the cost-minimized design point.

The safety factor/current profile cannot be included in our system code. Therefore, we used scalings of bootstrap current fractions for the FS and SS operating modes. In FS's case, f_{bs} is computed using the Cordey formula [J.G.Cordey]. In SS's case, f_{bs} is calculated using the formula given in Ref. [K.Okano93] (see appendix). This formula includes the effects of both the current profile and the plasma shape. In RS's case, f_{bs} is treated as a input parameter. The thing which f_{bs} is treated as an input parameter implies that the safety factor/current profile have to be changed to keep f_{bs} a constant. The safety factor/current profile of the cost-minimized RS design point is checked using DRIVER code [K.Okano90].

2.4 Parameter survey framework

This parameter survey is carried out to find the cost-minimized design point for each operating mode by changing the parameters in eq.III-2. The following conditions are used:

(1) The net electric power at the bus bar equals 1000 MW. The size of the tokamak reactor (A = from 3 to 4.5) will be inherently larger than that of a fission power plant. Therefore, its electrical output will be as large as that of a fission power plant. A 1000-1500 MW(e) output is assumed to be appropriate for future fusion power plants

(2) The NBI (Neutral Beam Injector) is acknowledged to be a practical device for either current drive heating or current profile control. The 2 MeV NBI proposed by Ref. [SSTR] is assumed to be the technical limit of the NBI.

(3) The plasma major radius R_p is more than 5 m by a radial build requirement. We treated A = from 3 to 4.5 tokamaks for which center cores like ohmic heating (OH) coils are indispensable. Therefore, we believe that the plasma major radius cannot be less than 5m for a radial build requirement. Actually system code solutions of $R_p < 5$ m are never found in FS and SS mode. Solutions of $R_p < 5$ m are found whose costs are lower than the cost-minimized RS design point by 2 mill/kWh. However, the neutron wall load of those solutions all exceed 5 MW/m^2. Considering plant availability, we believe it no good for $R_p < 5$ m with more than 5 MW/m^2 neutron wall load just for 2 mill/kWh.

(4) The neutron wall load must not exceed 5 MW/m^2. Advanced low activation materials, such as vanadium alloys or SiC/SiC, have at the most 20 $MW \cdot y/m^2$ neutron fluence. Therefore, these low activation materials can be used for about four years at a 5 MW/m^2 neutron wall load. 75% of the plant's availability can be attained at 5 MW/m^2 of neutron wall load because it is assumed to take at least one year for replacement of in-vessel components. Of course, the same 75% plant availability can be attained by shortening the replacement time if the neutron wall load exceeds 5 MW/m^2. However, since we have no prospect to reduce the time for replacement greatly, we did not apply such idea.

(5) The thermal to electricity conversion effect in the water cooling system is set at 34.5%. Water cooling should be chosen in the early type (including 10^{th} kind) of commercial tokamak reactors because of its practical use in fission power plants. Advanced technologies such as helium-cooling or lithium-cooling can be used as we gain more experience with them. At that time, powering up to 1500 MW(e) might be possible.

(6) Plant availability is set at 75% for all the operating modes. 75% of the plant availability is assumed to be required to make practical power plants. We assume all operating modes can attain 75% plant availability; i.e., in this study, the difficult operating mode such as SS or RS also can attain this availability. The results are, therefore, subject to change if this plant availability cannot be realized.

(7) The number of TF coils or other parameters listed in Table III-1 are fixed. These parameters are fixed to make the parameter survey easier. It is also assumed that the results we obtained do not change greatly if those parameters are changed. The outer shield with the blanket of the coils is about 1.8 m. The total multiplying rate of the breeder is assumed to be close to the limit of its practical use.

Table III-1 Summary of fixed parameters

Physics	
Effective charge of background plasmas	1.8
Atomic mass of NBI-CD beam species	2
Charge number of NBI-CD beam ion	1
Engineering	
Current Density of TFcoil winging pack	2.4 kA/cm^2
Current Density of TFcoil structure pack	1.2 kA/cm^2
Volume fraction of PFcoil/TFcoil	0.2
Volume fraction of Structure/TFcoil	0.75
Width of inside-blanket	0.5 m
Width of inside-gap	0 m
Width of inside-shielding	0.65 m
Width of outside-blanket	0.6 m
Width of outside-gap	0 m
Width of outside-shielding	1.22 m
Weight density of Blanket	4.8 ton/m^3
Weight density of Shielding	7.8 ton/m^3
Weight density of TFcoil	7.9 ton/m^3
Weight density of PFcoil	7.9 ton/m^3
Weight density of Structure	6.0 ton/m^3
Weight density of Diverter	6.9 ton/m^3
Multiplying factor of breeder	1.36
Blanket Covering factor	0.9
Cost	
Plant availability factor	0.75
Factor of indirect multiplication	1.05
Factor of construction interest multiplication	1.1
Factor of maintainance	0.04
Unit cost of Blanket	96.6$/kg
Unit cost of Shielding	17 $/kg
Unit cost of TFcoil	50 $/kg
Unit cost of PFcoil	50 $/kg
Unit cost of Structure	29 $/kg
Unit cost of Diverter	140$/kg
Cost of disposal	1.0 mill/kWh
Cost of decomission	0.5 mill/kWh

Table III-2 The range of main parameters

	Minimum	***Maximum***
A	3.0	4.5
κ	1.4	2.0
δ	0.2	0.5
β_N	2.0	6.0
q_{95}	3.0	5.0
T	10	20
n_{20}	1.0	3.0
B_{max}	10	20

Table III-3 Trade off of basic parameters

	the larger the better for	**the smaller the better for**
a_p	———	V_p, P_{fus}, V_{TF}
A	fbs	V_p, V_{TF}
κ	fbs	V_p
q_{95}	fbs	P_{fus}
β_N	fbs, P_{fus}	———
B_{max}	P_{fus}	V_{TF}

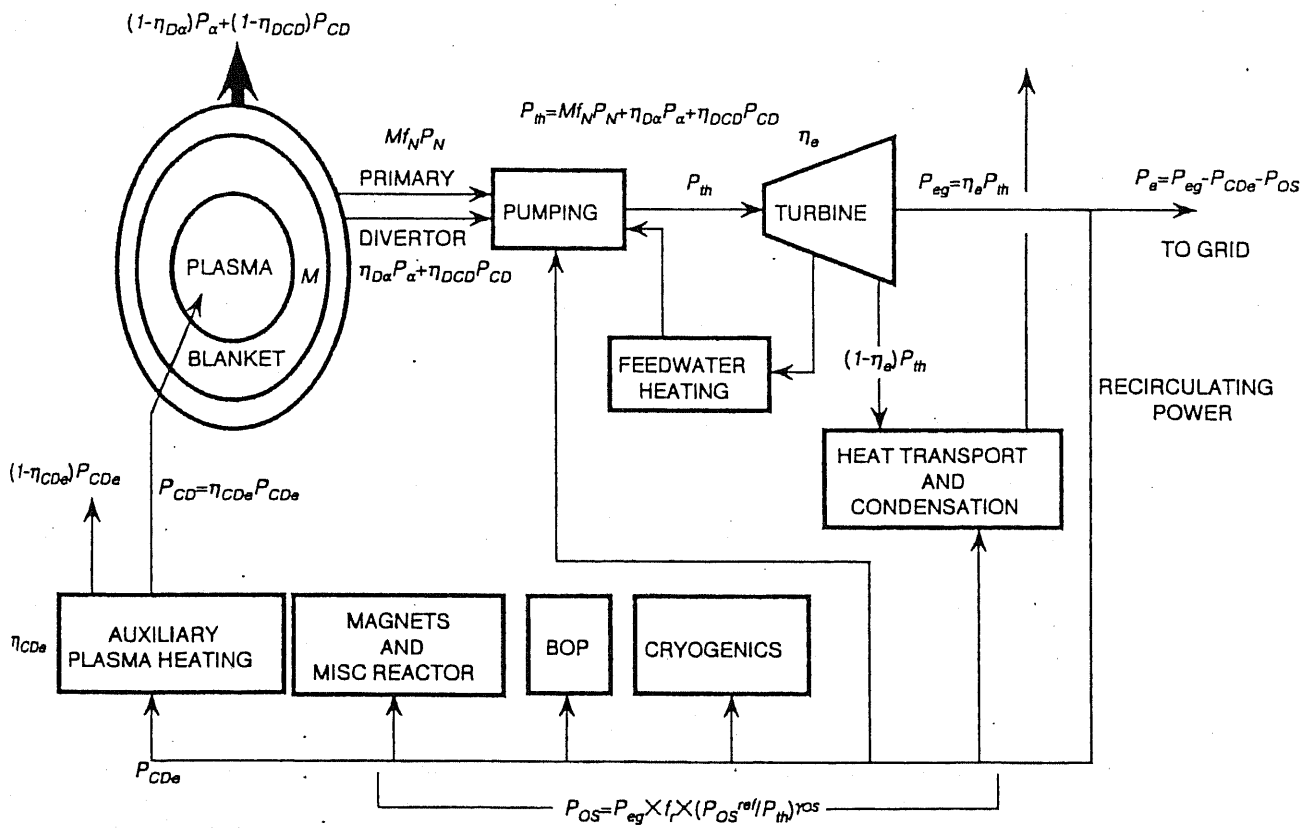

Figure III-1 Thermal flow model of the reactor system. This model is used on Ref. [T.Yoshida, A.Hatayama] referred from the Generomak model on Ref. [Generomak].

3. Minimization of the COE of each operating mode

3.1 First Stability operating mode

In the case of the FS operating mode, the most effective parameter to reduce the COE is considered to be β_N. However, β_N is limited by MHD stability, as described by eq.III-4 and eq.III-6. Hence β_N must be decided at its maximum within MHD stability by fixed A, κ and q_{95}. After finding the maximum β_N, the sensitivity of the B_{max} and T is checked. In this survey, the condition expressed by eq.III-4 and eq.III-6 is satisfied unless q_{95}, A, κ and δ are fixed. Therefore our parameter survey is concluded as follows:

Step 1) T, κ, and δ are fixed at 15, 2.0, 0.5, respectively. *Step 2)* q_{95} is chosen to be either q_{95} = {3.0, 4.0, 5.0}. *Step 3)* The combination of (B_{max}, A) is chosen with B_{max} = {12,14,16,18,20}, A = {3.0, 3.5, 4.0, 4.5}. *Step 4)* β_N is increased from 1.0 to 6.0 to find the cost-minimized point for all the combinations of (B_{max},A). *Step 5)* At the combination of (β_N, A) of the cost-minimized point in step 4, sensitivity of (B_{max},T) and (κ,δ) is checked. *Step 6)* The procedure from step 1 to step 5 is repeated for all q_{95} until the overall cost-minimized point is found.

Fig. III-2 shows the result of the procedure from *Step 1)* to *Step 4)* at q_{95} = 5.0. This figure indicates that (1) β_N > 3.0 results in a MHD instability region, and if the MHD stability should be insured, (2) the aspect ratio decreases as β_N increases, (3) both high β_N and high B_{max} do not satisfy the radial build and/or neutron wall load. Therefore, it can be concluded in FS operation that (1) β_N will be limited around 3.0, (2) the aspect ratio go up to 4.5 of this study's upper limit in order to obtain high bootstrap current fraction because high β_N cannot be achieved, and (3) the B_{max} increase in order to decrease the plasma volume. Therefore, it is worth developing B_{max} = 20 Tesla TF coils in FS operation mode to cover its poor physics performance.

Fig. III-3 shows dependency of the COE on temperature T at each B_{max} (*Step 5*). This result indicates that the higher both T and B_{max} are, the better for reducing the COE. It can be concluded that because β_N is small in the FS operating mode, T and B_{max} should be raised as much as possible to obtain a high P_{fus}.

Fig. III-4 shows the overall results (till *Step 6*) of this analysis. This result indicates 1) q_{95} need not be so high, 2) there is a 6.5 mill/kWh value between the B_{max} = 20 Tesla and B_{max} = 16 Tesla TF coils at q_{95} = 4.0. The cost-minimized detail design parameters are shown in Table III-4.

3.2. Second Stability operating mode

In the case of the SS operating mode, we treated β_N and A as input parameters and changed q_{95} to satisfy the SS region. Our parameter survey is calculated as follows: *Step 1)* The combination of (β_N, A) are chosen with β_N = {4.45, 4.95, 5.45, 5.95} and A = {3.0, 3.5, 4.0, 4.5}. *Step 2)* The combination of (B_{max}, T) is chosen from all combinations of B_{max} = 12 ~ 20 at every 0.5, T = 10 ~ 20 at every 2.5. *Step 3)* (κ,δ) are fixed at κ = 2.0, δ = 0.5. *Step 4)* q_{95} is increased every 0.05 from 6.5 to 10.0 to find the cost-minimized design point. *Step 5)* At q_{95} of this cost-minimized point in Step 5, the sensitivity of all combinations of (B_{max},T) is checked. *Step 6)* At the cost-minimized combination of (B_{max},T) in Step 5, the sensitivity of (κ,δ) is checked for all the combinations of κ = 1.4 ~ 2.0 at every 0.2, δ = 0.2 ~ 0.5 at every 0.1. *Step 7)* The procedure from Step 2 to Step 6 is repeated for all combinations of (β_N, A) until the overall cost-minimized point is found.

To find a q_{95} which satisfies the MHD second stability, the dependency of q_{95} on $\varepsilon\beta_p$, $\varepsilon\beta_p$-lim (the upper boundary of the MHD unstable region in this figure), and the COE is shown in Fig. III-5 for β_N = 4.95, A = 3.0, B_{max} = 16, and T = 12.5 (from Step 1 to 4). The calculated points where $\varepsilon\beta_p > \varepsilon\beta_p$-lim are in the SS region. This result shows that $\varepsilon\beta_p$ increases and $\varepsilon\beta_p$-lim decreases by raising q_{95}, respectively. The COE is also increased by raising q_{95} because of reduction of P_{fus}.

Fig. III-6 shows the dependency of the COE when the combination of (B_{max},T) is changed for β_N = 4.95, A = 3.0, and q_{95} = 8.6 (Step 5). The combination for cost-minimized is (B_{max},T) = (17,15). The reason why B_{max} does not increase in low T can be explained as follows: The low T raises the plasma electron/ion density. The high plasma density also raises the P_{fus}. Therefore, a small V_p is sufficient to satisfy 1000 MW(e) because of both the high P_{fus} and a small current drive power are needed. For this reason, the small V_p causes a radial build so small that the required cross section of the TF coils cannot be satisfied. This figure also shows that it is worth developing the TF coils with a B_{max} = 17 Tesla, but not necessarily 20 Tesla.

Fig. III-7 shows the dependency of the COE on (κ,δ) which is decreased from (κ,δ) = (2.0,0.5). This indicates that a low κ and δ increases the COE. Surprisingly, when κ is decreased from 2.0 to 1.4 with δ = 0.2, the COE is increased about 35 mill/kWh. Decreasing δ from 0.5 to 0.2 also increases the COE about 20 mill/kWh. This result indicates that κ and δ may have strong impacts on the COE.

Fig. III-8 provides each cost-minimized point for all combinations of (β_N, A) (Step 7). The cost-minimized combination of (B_{max},T) is chosen at these calculated points. The cost of all these points are also minimized for all combinations of (κ, δ). The COE and the active current drive power by the NBI is

minimized close to $\beta_N = 4.95$ at A = 3.0. In the SS region, a high q_{95} increase f_{bs} is so large that the A results in a small reduction of V_p and V_{TF}. A high β_N (e.g., $\beta_N = 5.45$) exceeds f_{bs} 100%, which increases an active current drive counter to plasma current, power/cost and the COE. The cost-minimized detail design parameters are shown in Table III-4.

3.3. Reversed Shear operating mode

Recently, the reversed shear mode has been investigated by simulation studies [J.Manickam,C.Kessel,A.D.Turnbull] and experimentally obtained [E.J.Strait95, F.M.Levinton, B.W.Rice]. Its major features are that it has a high f_{bs} and a high β_N obtained by reversed shear profile. In this reversed shear case, both f_{bs} and β_N are treated as input parameter. One reason is because the DRIVER code cannot treat f_{bs}, β_N, and $B_{\max}$ as input parameters and the other reason is because these f_{bs} and β_N give great influence to the COE. Therefore, we checked the safety factor/current profile at the cost-minimized design point by the DRIVER code. Costs of other design points, if they satisfy the reversed shear profile, are higher than that of the cost-minimized design point.

The cost-minimized point is obtained through a parameter survey using the following procedure. *Step 1)* combination of (β_N, f_{bs}) is chosen from the following five combinations; (β_N, f_{bs}) = (4.5, 0.9), (4.95,0.9), (4.95, 0.935), (4.95, 0.865), and (5.45, 0.9). *Step 2)* The combination of ($B_{\max}$, A) is chosen within all combinations of $B_{\max}$ = 10 ~ 16 at every 1.0 and A = 3.0, 3.5, 4.0, 4.5. *Step 3)* T, κ and δ are fixed at T = 15, κ = 2.0, and δ = 0.5. *Step 4)* q_{95} is increased every 0.25 from 3.5 to 6.0 to find the referenced cost-minimized point. More than 3.5 of q_{95} is assumed because the minimum q ($q_{\min}$) = 2.0 is assumed to obtain reversed shear. *Step 5)* At this cost-minimized point in Step 4, sensitivities of T, κ and δ are checked within T = 10 ~ 20 keV at every 1.0, κ = 1.4 ~ 2.0 at every 0.2, δ = 0.2 ~ 0.5 at every 0.1. *Step 6)* This procedure is undertaken for all combinations of (β_N, f_{bs}) and ($B_{\max}$,A) until the overall cost-minimized point is found.

Fig. III-9 gives the dependency of the COE on ($B_{\max}$,A) at (β_N, f_{bs}) = (4.95,0.935) (Step 1 to 4). This figure demonstrates that the COE is minimized at $B_{\max}$ = 13, A = 3.0 ~ 3.5. It is considered that a higher $B_{\max}$ (until 13 Tesla) results in a small V_p which reduces the COE, and that a smaller A (e.g. 3.0) results in a small V_p and small V_{TF}, both of which reduces the COE. Fig. 10 shows the reason why the COE increases for $B_{\max}$ > 13 in Fig. III-9. Fig. III-10 illustrates how each neutron wall load P_{wn}, plasma major radius R_p, and the COE is changed by q_{95} at $B_{\max}$ = 16 Tesla. We recognize that restriction of P_{wn} raises q_{95}, which also results in a high COE. It can be assumed that for a high $B_{\max}$, a higher q_{95} results in a low P_{fus}, which in turn increases R_p and the COE.

Fig. III-11 shows the dependency of the COE on each (β_N, f_{bs}) combination where the COE is minimized. All the calculated points are cost-minimized for (B_{max},A), q_{95}, T, κ and δ. This figure indicates that the higher f_{bs} contributes to the reduction of the COE more than the higher β_N does. A sufficiently high β_N creates small difference on the COE. This result implies that cost reduction obtained by a high f_{bs} (e.g., 0.935) is more effective than that obtained by a high β_N (e.g., 5.45). The cost-minimized design parameters which correspond to the black circle in Fig. III-9 are listed in Table III-4.

Fig. III-12 shows the temperature and density/safety factor/current profiles calculated by the DRIVER code as $T \sim (1-r^2)^2, n \sim (1-r^4)$. Almost all parameters of the cost-minimized design point on the system code and those of the DRIVER code are in very good agreement. MHD equilibrium and stability are checked by an EQLAUS code and an ERATO code, respectively, at a design point (β_N = 5.5, A=3.4) [K.Okano97a] close to the cost-minimized design point.

Table III-4 Summary of cost-minimized design parameters

		ITER-like	FS	SS	RS
Plasma major radius	Rp[m]	8.4	6.4	5.7	5.1
Plasma minor radius	ap[m]	2.87	1.42	1.9	1.7
Plasma aspect ratio	A=Rp/ap	2.91	4.5	3	3
Plasma elongation	κ	1.8	2	2	2
Plasma triangularity	δ	0.24	0.2	0.5	0.5
Plasma volume	VP[m^3]	2451.1	500.4	805.4	581.2
Safety factor on the 95%	q95	3	4	8.85	3.75
Stability parameter	$\varepsilon\beta p$	0.333	0.509	1.779	0.769
Beta parameter	$\beta/\varepsilon*1/S^2$	0.055	0.041	0.033	0.08
Total beta	β-total[%]	4.291	2.406	3.527	8.494
Poloidal beta	βp	0.968	2.292	5.336	2.308
Normalized beta	βN[%mT/MA]	2.7	2.89	4.85	4.95
ITER-89P confinement factor	H-factor	1.424	1.85	3.3	2.289
Plasma confinement time	τ[sec]	2.038	1.382	1.971	1.401
Plasma current	Ip[MA]	27.6	13.5	10.1	15.5
Bootstrap current	Ibootstrap[MA]	8.0	7.8	10.2	14.5
Current by beam	Ibeam[MA]	19.6	5.7	-0.1	1.0
fraction of bootstrap current	fbs	0.289	0.581	1.012	0.935
Current drive efficiency	γ[10^{20} A/Wm^2]	0.534	0.506	0.285	0.402
Beam energy	Eb[MeV]	2	2	2	2
Current drive power	Pb[MW]	263.1	123.0	5.0	23.5
Plasma temperature	Te=Ti[keV]	20	20	11	15
Plasma electron density	ne20[*10^{20} m^{-3}]	0.856	1.729	2.102	1.843
Greenwald limits	nGreenwald	0.904	1.829	0.759	1.446
Borrass limits	nBross	0.47	0.866	0.565	0.454
Magnetic field on axis	Bt[T]	6.06	11.49	7.33	5.30
Maximum toloidal field	Bmax[T]	12.5	20	17	13
average neutron wall load	Pw[MW/m^2]	2.371	4.904	3.342	4.287
Fusion power	Pf[MW]	4034	3359	2790	2879
Fusion power density	Pfus[MW/m^3]	1.646	6.713	3.464	4.954
Electric power at bus bar	Pe[MW]	1000	1000	1000	1000
Direct construction cost	Cconst.[M$]	5061.4	3627.8	2572.2	2273.4
Cost of Electricity	COE[mill/kWh]	129.6	96.0	67.0	60.6

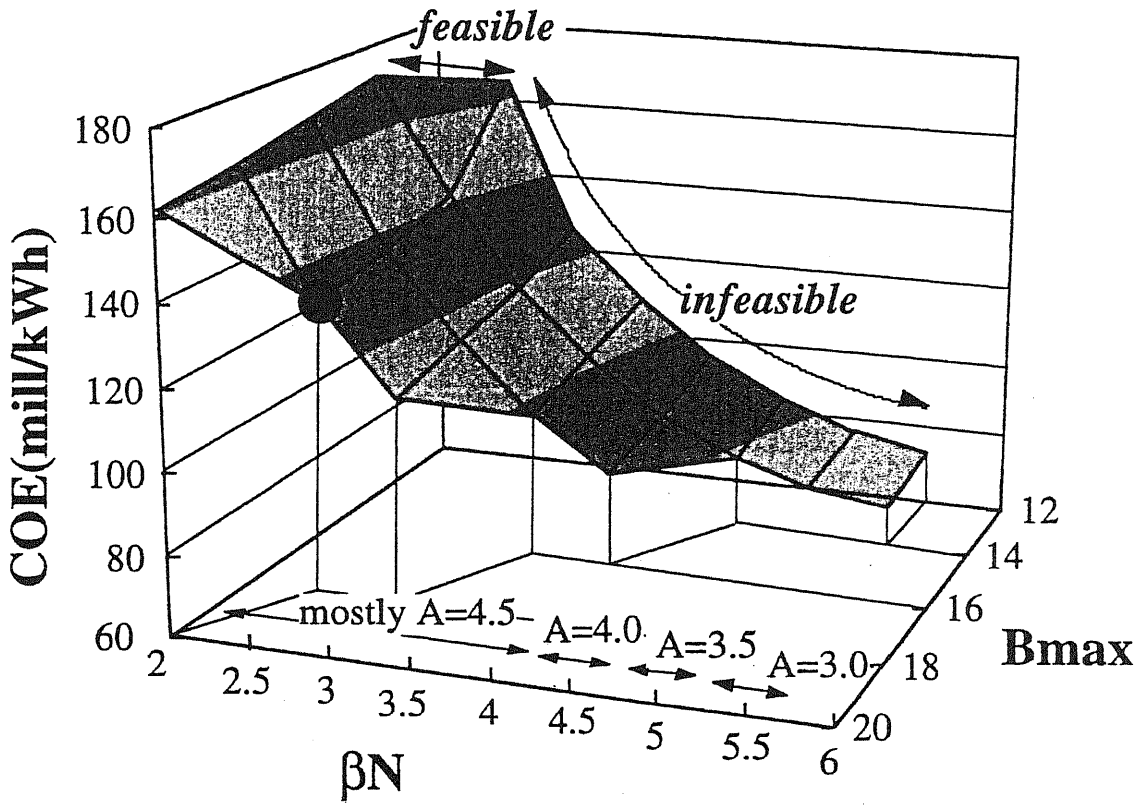

Figure III-2 Dependency of the COE on β_N, B_{max}, and aspect ratio in FS operating mode at q_{95} = 5.0, T = 15 keV, κ = 2.0, and δ = 0.5. The COE and aspect ratio decreases gradually as higher β_N, higher B_{max}. β_N > 3.0 is an unstable region. The black circle corresponds to the minimized COE in this survey.

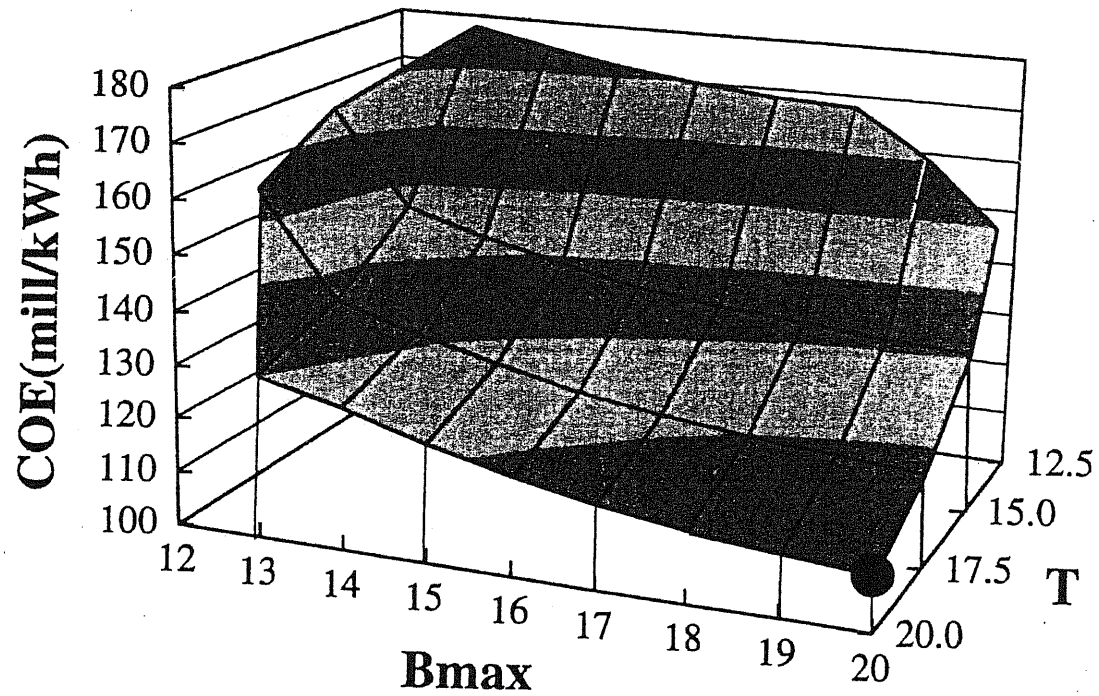

Figure III-3 Dependency of the COE on T and B_{max} at q_{95} = 5.0, A = 4.5, β_N = 2.5, κ = 2.0, and δ = 0.5. The COE gradually decreases in higher B_{max} and higher T.

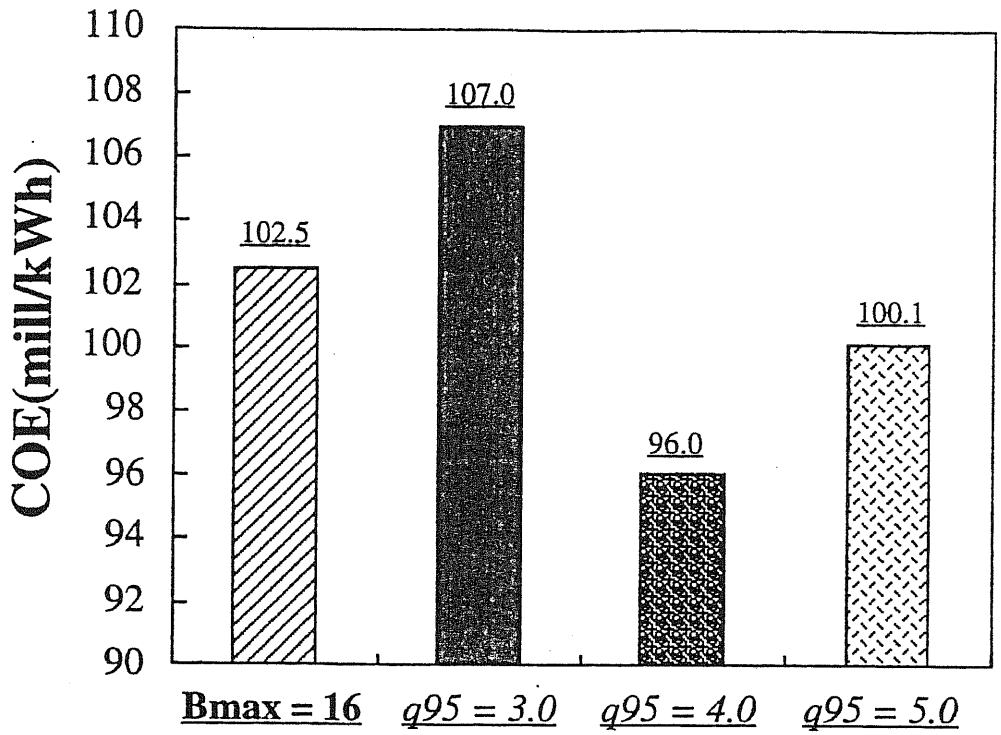

Figure III-4 Overall results within the FS operating mode.

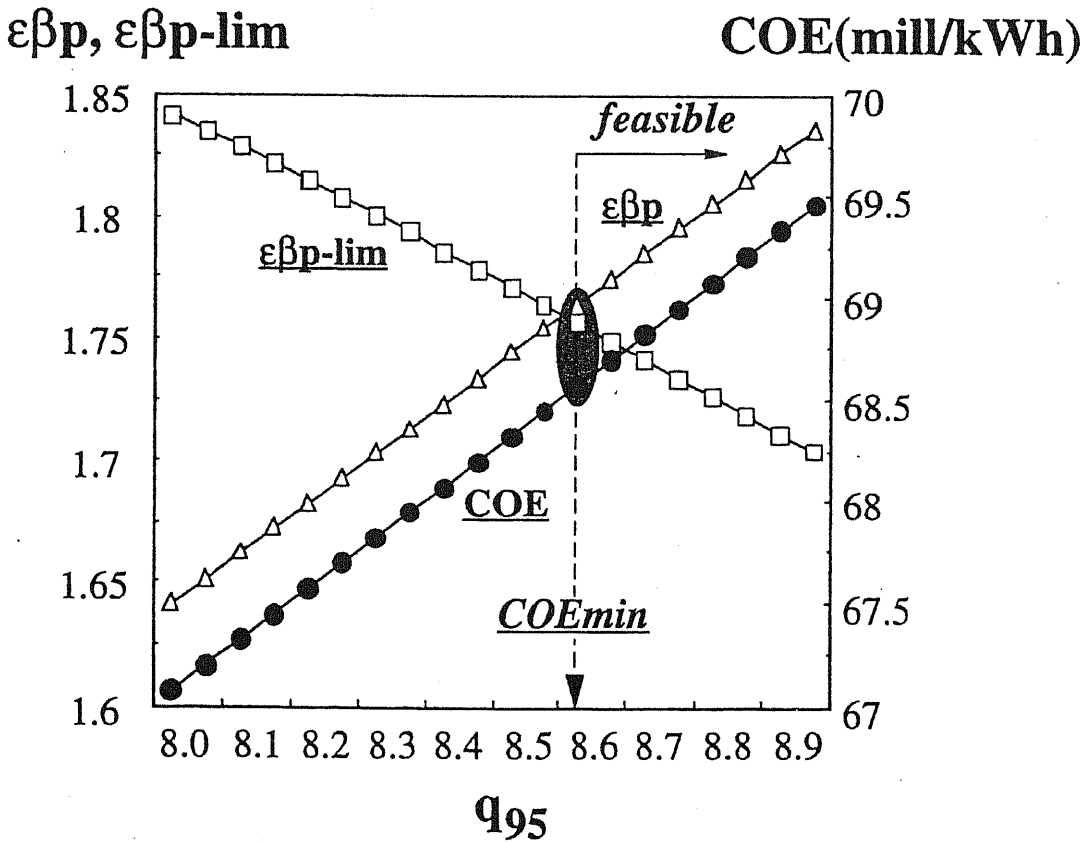

Figure III-5 Variation of $\varepsilon\beta_p$, $\varepsilon\beta_p$-lim, and the COE by change of q_{95} in the SS operating mode at $\beta_N = 4.95$, $A = 3.0$, $B_{max} = 16$, $T = 12.5$, $\kappa = 2.0$, and $\delta = 0.5$. q_{95} of more than 8.6 is a stable region where the COE is increasing.

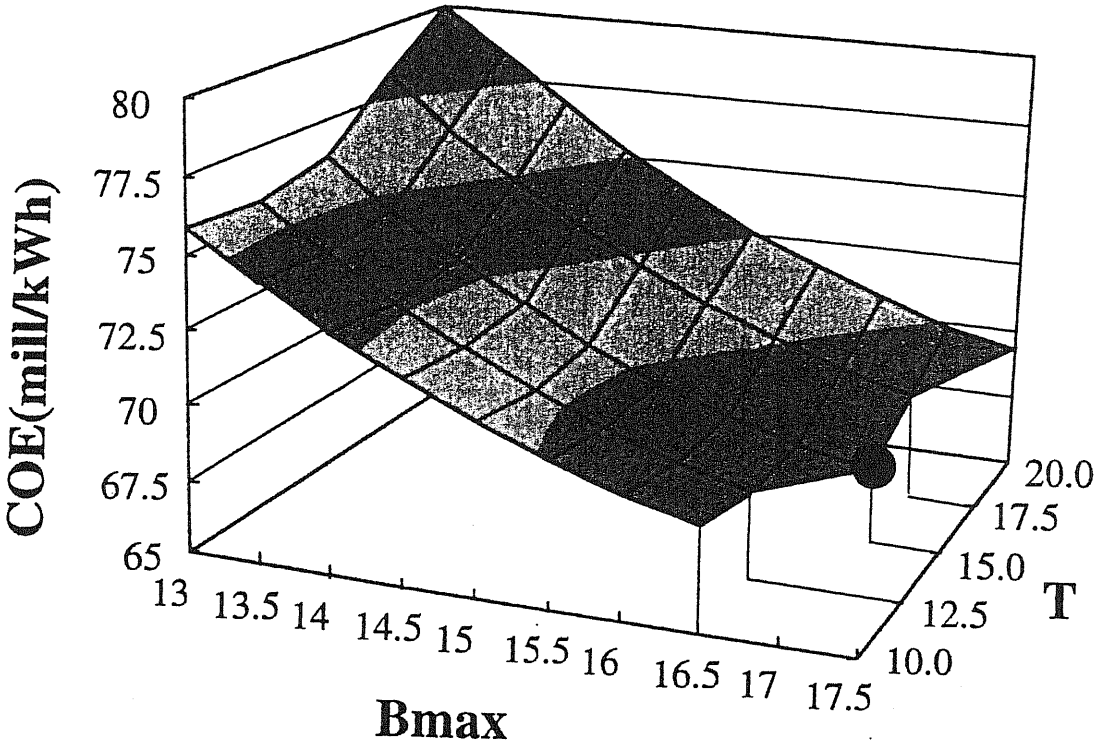

Figure III-6 Dependency of the COE on T and B_{max} at β_N = 4.95, A = 3.0, q_{95} = 8.6, κ = 2.0, and δ = 0.5. The COE decreases in higher B_{max}, and the COE is minimized at T = 15.

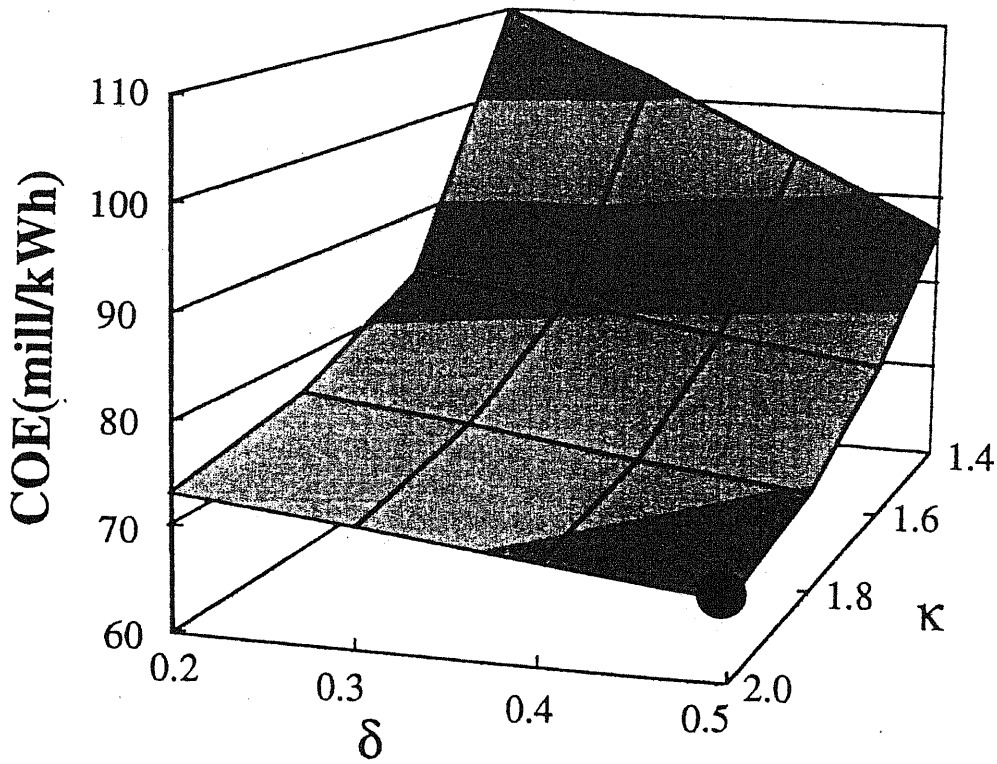

Figure III-7 Dependency of the COE on κ and δ at β_N = 4.95, A = 3.0, q_{95} = 8.6, B_{max} = 17, and T = 15.

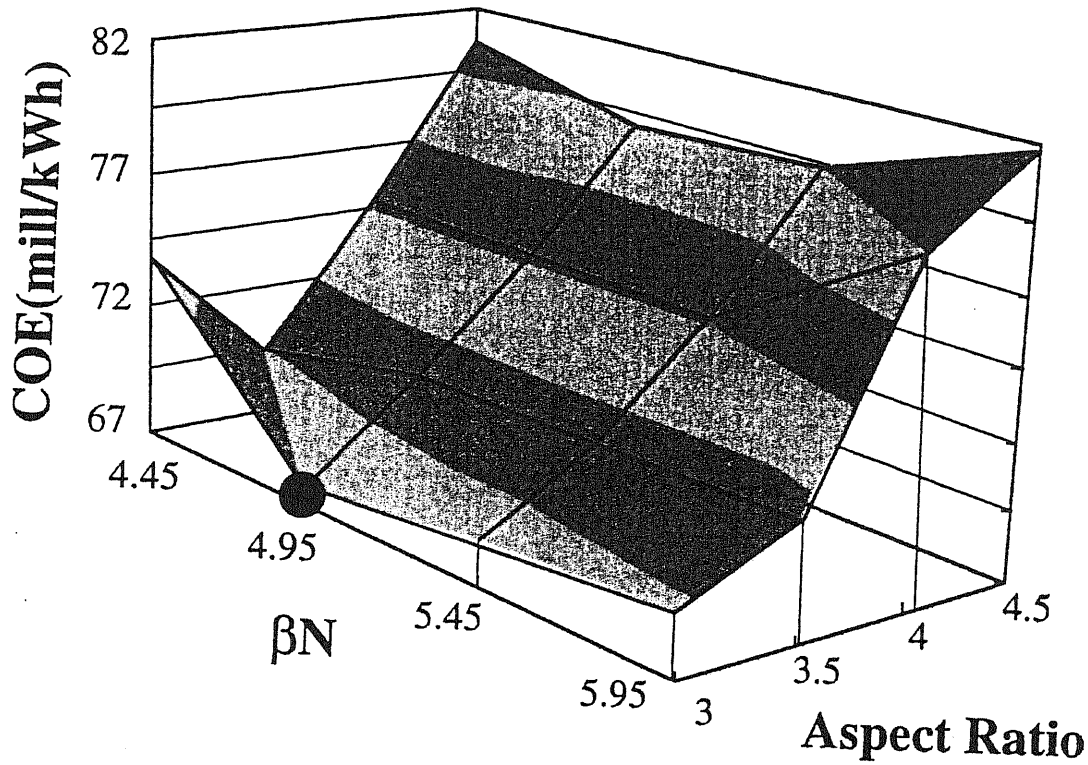

Figure III-8 Dependency of the COE on β_N and aspect ratio at $\kappa = 2.0$ and $\delta = 0.5$. q_{95}, T, B_{max} are optimized for each calculated point.

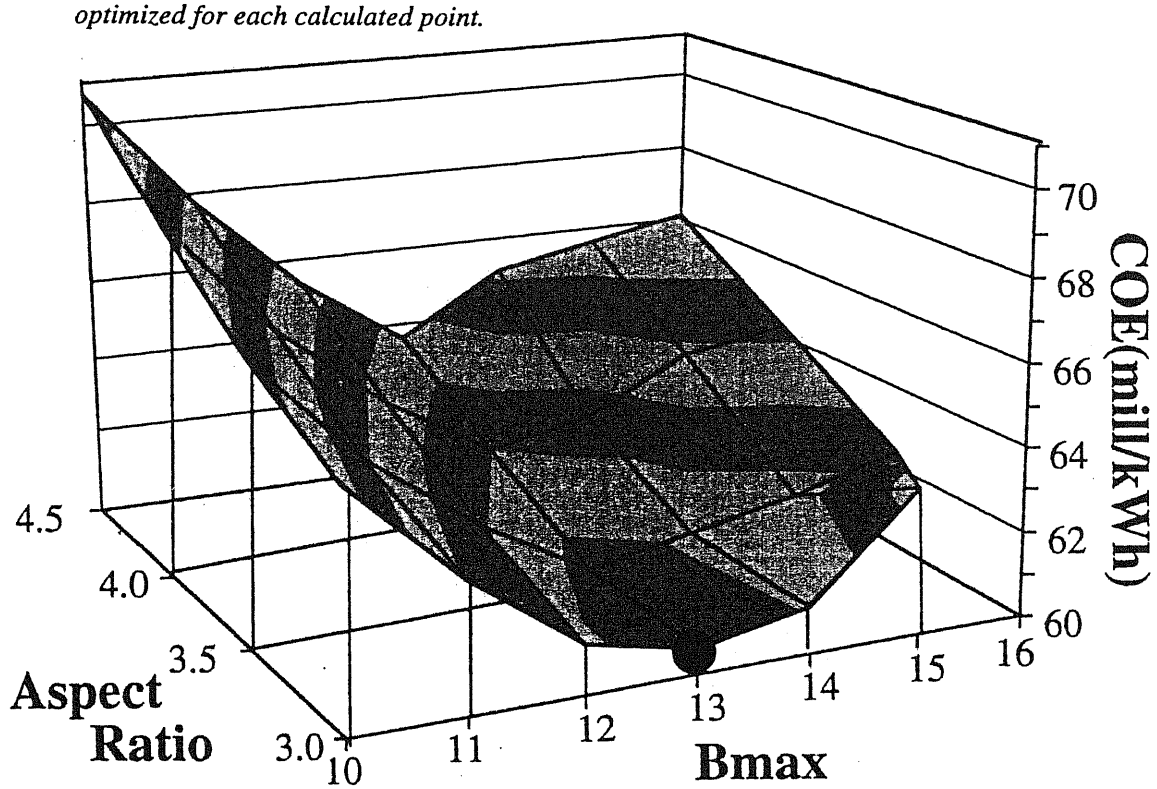

Figure III-9 Dependency of the COE on B_{max} and aspect ratio in the RS operating mode at $\beta_N = 4.95$, $f_{bs} = 0.935$, $q_{95} \geq 3.5$, $T = 15$, $\kappa = 2.0$, and $\delta = 0.5$. The COE is minimized at $B_{max} = 13$, $A = 3.0 - 3.5$. The COE gradually decreases from $B_{max} = 10$ to 13, and increases from $B_{max} = 13$ to 16. The COE decreases in lower aspect ratio for all B_{max} (except $B_{max} = 15$).

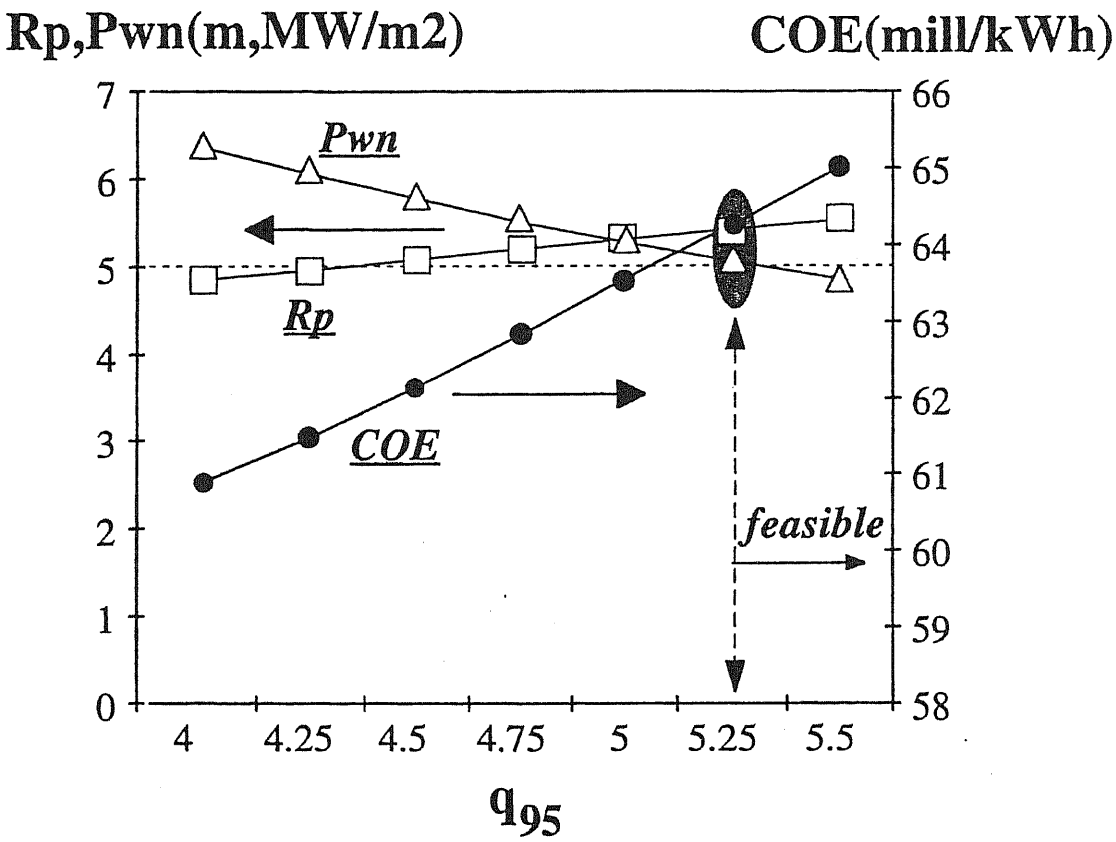

Figure III-10 Variation of P_{wn}, R_p, and the COE by changing of q_{95} at B_{max} = 16, A = 4.0. The restriction of P_{wn} and R_p cause the COE to increase by increments of q_{95}.

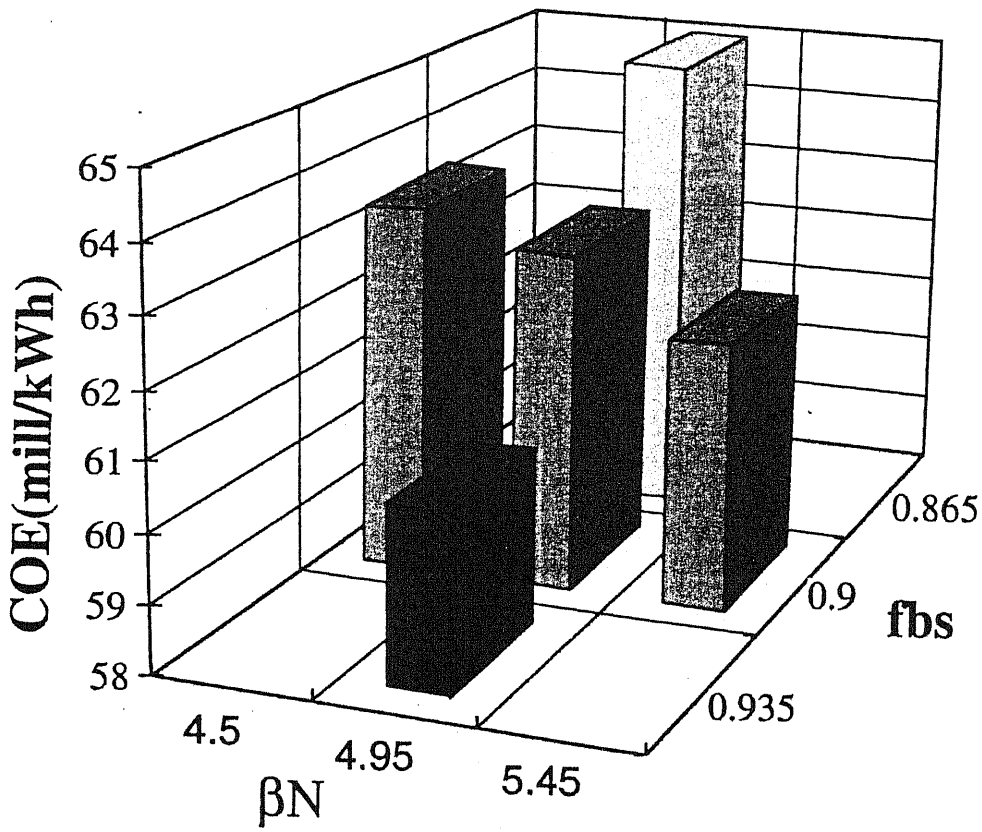

Figure III-11 Dependency of the COE on β_N and f_{bs}. The COE is minimized at each calculated point.

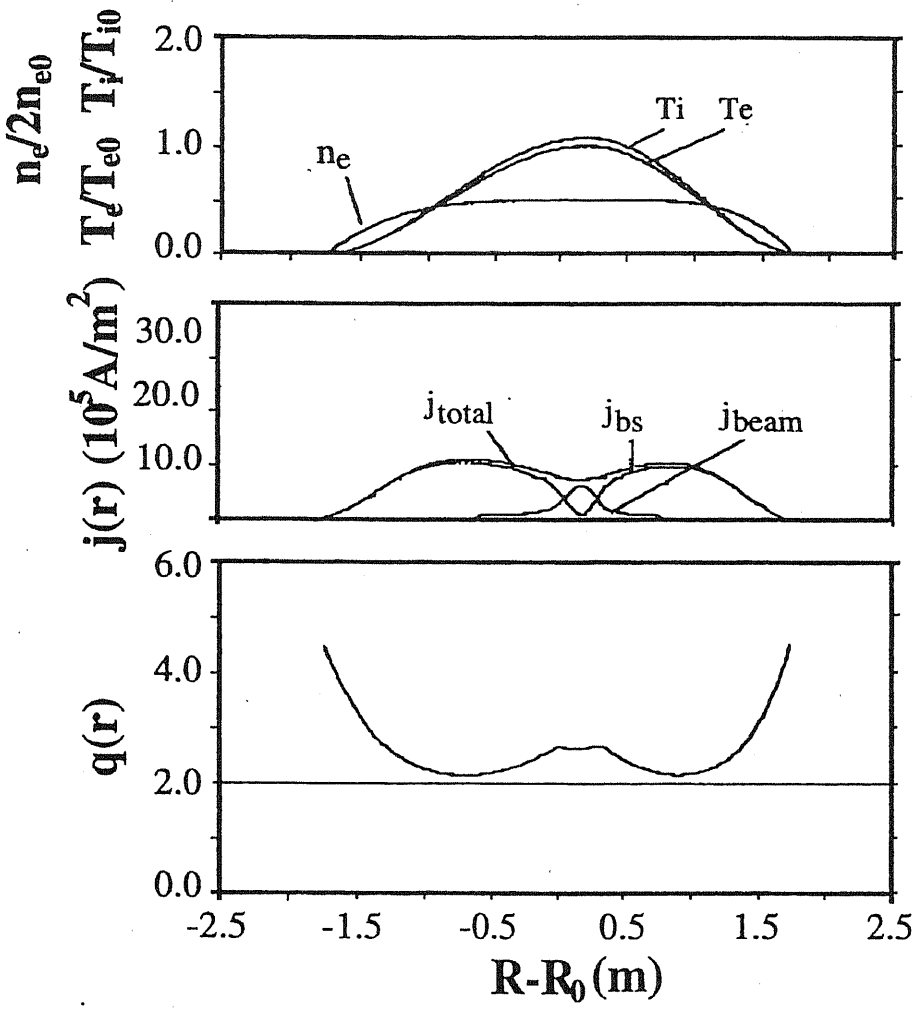

Figure III-12 The plasma temperature/density, current, and safety factor profile at the cost-minimized RS design parameter. The reversed shear profile is confirmed by this safety factor profile

4. Comparison among operating modes

The COE-minimization of each operating mode was explained in the previous chapter. To compare the operating mode, the ITER-like reactor is computed as a reference reactor. The ITER-like reactor design point is chosen using a minimum modification of the ITER parameters to satisfy 1000 MW(e). The ITER-like parameters are the following:

$$A = 2.91,\ \underline{\kappa = 1.8\ (1.6)},\ \delta = 0.24,\ q_{95} = 3.0,\ \underline{\beta_N = 2.7\ (2.4)},\ \underline{T = 20\ (10)},\ B_{max} = 12.5.$$

(The underlined parameters are modified values; original values are given in parentheses.)

Fig. III-13 illustrates the figures of merit for each operating mode in terms of their β_t/ε vs. $\varepsilon\beta_p$ diagram. This figure of merit representation, which is used by the Starlite team, has the advantage of illustrating $\varepsilon\beta_p$, β_t/ε, q^*, and β_N in one figure. The oblique curve represents a boundary between the MHD stable and unstable region. The white squares denote the cost-minimized design point of each operation region. This diagram shows that there are two ways to increase β_N in FS. One is to go into the SS region by raising both q_{95} and β_p while avoiding MHD instability. The other is to go into the RS region by raising β_t.

Fig. III-14 shows a comparison of the COE. The COE of the cost-minimized RS reactor is the lowest and is almost half that of the reference ITER-like reactor. This result indicates that the cost-minimized RS reactor is less expensive than the cost-minimized FS reactor with a high aspect ratio and B_{max} or the cost-minimized SS reactor using a high q_{95}.

Fig. III-15 shows a comparison of the total construction costs. The construction cost of the cost-minimized RS reactor is the lowest. This result demonstrates that the construction cost can be reduced by reducing the cost of both current drive and the coils/structures, and that other costs like the B.O.P, the reactor building (R.B.) do not show much change.

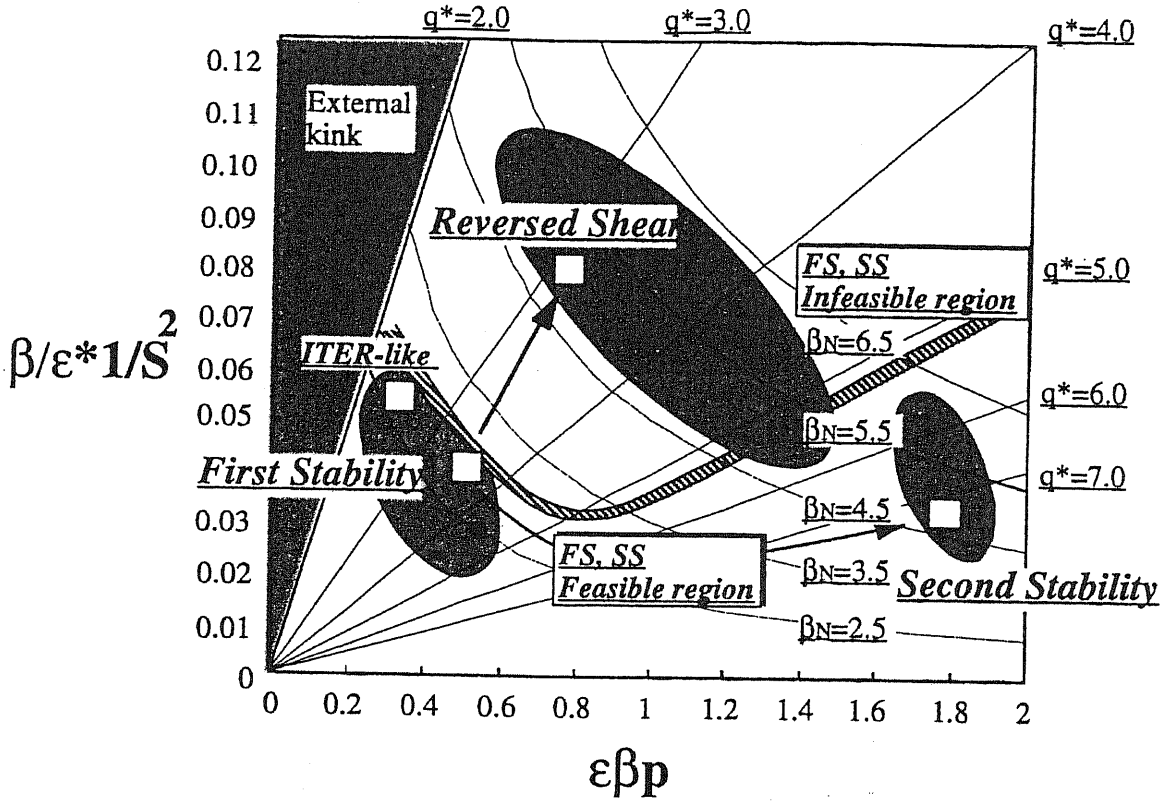

Figure III-13 Figure of Merit of three operating modes. White squares indicate the cost-minimized points, and the oblique curve indicates a boundary between MHD stability and instability

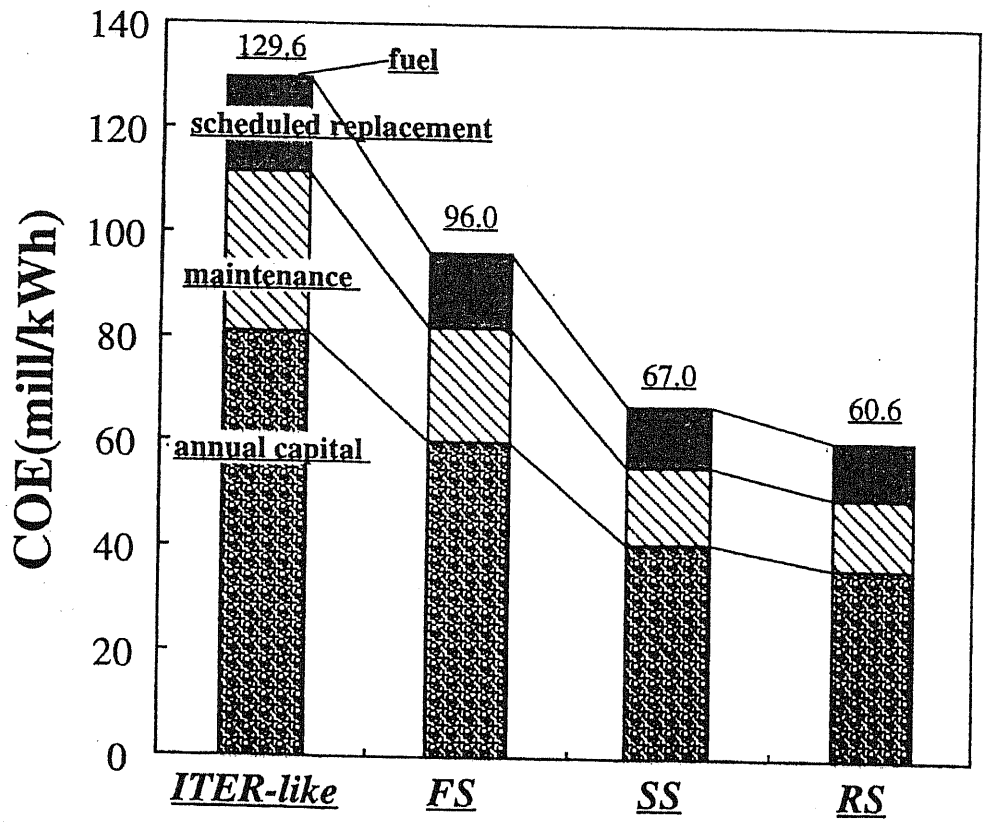

Figure III-14 Comparison of the COE among the cost-minimized reactors of three operating modes and the ITER-like reactor.

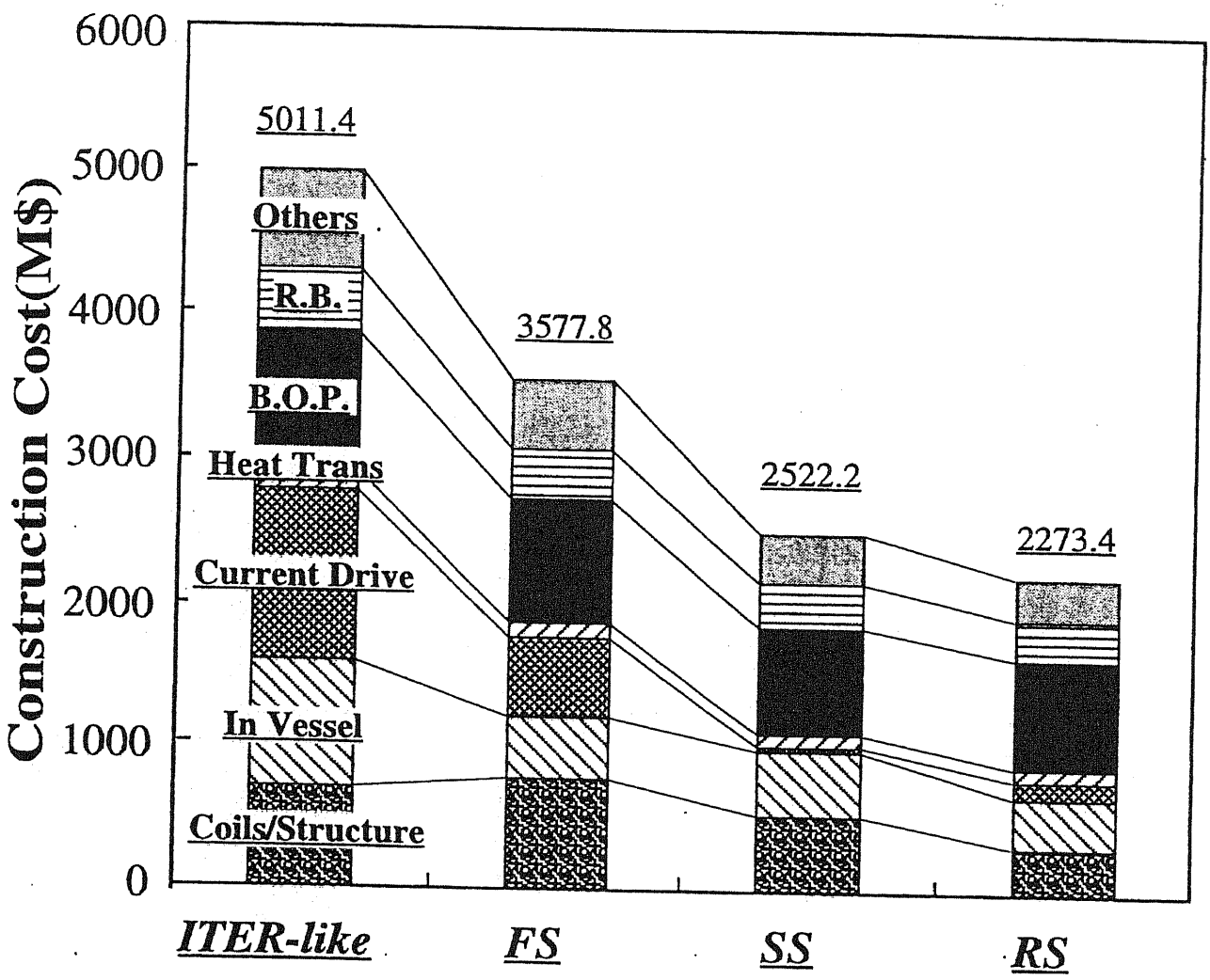

Figure III-15 Comparison of the construction cost among the reactors of three operating modes and the ITER-like reactor.

5. Discussion

In this chapter, we emphasize (1) the originality of the cost-minimized RS design point (which corresponds to the black circle in Fig.III-9), (2) the reason of the RS design point can be the cost-minimized, and (3) the validity of the parameters set for the cost-minimized RS design point.

5.1 The originality of the cost-minimized RS design point

We assert that lower aspect ratio (e.g., A =3.0) and lower $B_{\max}$ (i.e. 13 Tesla) is best to minimize the cost of water cooled RS reactor in our parameter survey. The aspect ratio may be increased if the clearance for the replacement of inner-vessel components is not enough. $B_{\max}$ is restricted by the neutron wall load limit (5 MW/m^2) and our design point for the electric output, i.e., 1 GWe. A larger $B_{\max}$ may be possible by assuming 1) a higher thermal-electric conversion efficiency with a lower fusion output and a higher aspect ratio (Ref. [C.G.Bathke96]), or 2) a larger electric output and a larger wall load. However, both cases deviate our basic constraints in the present study where the conventional water cooling system (i.e., 34.5 % thermal-electric conversion efficiency) and 1 GWe electric output are assumed.

5.2 Reasons of the cost-minimized RS reactor can be the most cost-minimized among all the three operation modes in this study, especially less expensive than the-cost minimized second stability

5.2.1 About the cost-minimized RS reactor can be the most cost-minimized among all the three operation modes

There are two reasons why the cost-minimized RS reactor is the cost-minimized of all operating modes. The first reason is that low current drive power (P_{CD}) results in a low cost of current drive, and also results in a low cost of B.O.P. ($C_{B.O.P.}$). $C_{B.O.P.}$ is calculated by scaling the thermal power (P_{th}) which , in turn, is converted to electric power P_{eg} ($\approx P_e + P_{CD}$, where P_e is constant). Thus a small P_{CD} results in a small P_{eg} and P_{th}. Reversed shear can attain a high f_{bs} close to 100%, which results in a low P_{CD} and a low cost current drive.

The second reason is that small V_{TF} lowers the cost of coils/structure and reactor building expenses ($C_{R.B.}$) since the volume of coils/structure is proportional to V_{TF} in our model and that $C_{R.B.}$ is calculated by scaling the volume of the fusion island which is dependent on V_{TF}. Small V_{TF} can be obtained by both a small cross section of TF coils (S_{tot}) and a short length of TF coils (C_{ling}). A low $B_{\max}$ of TF coils is required for a small S_{tot}. Both a low A and a small a_p is needed for a short C_{ling}. Reversed shear can attain low $B_{\max}$, low A, and short a_p simultaneously because reversed shear can

attain high β_N, low q_{95}, and high f_{bs} at the same time. High f_{bs} results in low A. High β_N and low q_{95} result in high P_{fus} which ,in turn, results in low $B_{\max}$ and small V_p (i.e., short a_p).

In short, it must be emphasized that the reversed shear can attain high β_N, low q_{95}, and high f_{bs} at the same time. This characteristic of reversed shear causes a low P_{CD} and allows for a compact reactor (small V_{TF} and V_p via high P_{fus}), both of which results in cost-minimization. On the contrary, although the SS mode can attain high β_N and high f_{bs}, MHD stability requirement does not allow a low q_{95} which, in turn, results in a low P_{fus}, high $B_{\max}$, and a large reactor size.

5.2.2 Skepticism to an existence of electron density/temperature profile which satisfies global parameters of the cost-minimized SS reactor found in this study, and also to that the profile, if found, turned out to be a reversed shear profile.

The safety factor profile of SS type reactors in our study is assumed to be a monotonic profile whose center value is more than 2.0, and not assumed to be a reversed shear profile. In this study, reactors using reversed shear profile are all categorized as reversed shear operation even if they are in second stable region because only monotonic safety factor profile can be treated by MHD determination of equation (III-5). If safety factor profile of the cost-minimized SS reactor is turned out to be a reversed shear by any electron density/temperature profile, (1) additional heating power might be required for safety factor as well as current profile adjustment which results in increment of the cost or (2) another second stability global parameters which satisfy equation (III-5) should be chosen. Any case of (1) or (2), the cost of the SS reactor is more expensive than that of the cost-minimized RS reactor as Fig. III-15 indicates. Therefore, the cost-minimized RS reactor is ALWAYS less expensive than any SS reactors which have monotonic safety factor profile assumed in this study.

5.3 Validity of the parameters and the constraints set for the cost-minimized RS design point.

5.3.1 About the β_N and H-factor

The value of β_N used in the RS case is decided according to the recent MHD simulation results. The ideal MHD calculations assuming a closed conducting shell [C.Kessel, K.Okano97, A.Bonderson] have been shown that the β_N up to about 5.5 will be possible. We also calculated the H-factor (the plasma confinement factor) using the confinement time by the ITER89P and by calculating by the plasma thermal energy and additional heating power. The H-factor of the cost-minimized RS reactor is 2.3, which is obtained from recent experimental results and can be fully attainable in the future.

5.3.2 About the bootstrap current fraction

The bootstrap current fraction f_{bs} can usually be calculated by the β_N, the safety factor, and the aspect ratio. However, simple scaling of the f_{bs} for the RS case does not exist, the f_{bs} has to be treated as a constant value. We believe there are no other means except treating the f_{bs} as a constant. The f_{bs} used in our study are fully attainable when we consider recent numerical simulation. This is because close to 90% of the f_{bs} are attainable if the β_N is close to 5. Moreover, we also checked the f_{bs} = 93.5% at the $\beta_N = 4.95$ of the cost-minimized design point by the DRIVER code which can calculate to satisfy the current profile and safety factor profile self-consistently. Furthermore, the f_{bs} is decided not only by poloidal beta β_p but also by the current/safety factor profile, hence, we think the profile should be adjusted to attain those f_{bs} used in RS case. Even if the f_{bs} should exceed 93.5% to reach 100%, the cost does not change much because the 93.5% f_{bs} is already large enough.

5.3.3 About the B_{max} treatment

It is true that there is a relation between current density of TF coil (j_{st}) and the B_{max}; higher B_{max} reduces the j_{st}, which we did not consider in our system code. We used the j_{st} of the SSTR in Ref. [SSTR-JAERImemo] whose B_{max} at 16.5 Tesla. Within our study of B_{max} from 10 to 20 Tesla, the j_{st} is the underestimated of the RS case as B_{max} < 16.5 Tesla. Therefore, the width of the TF coil (ΔTF) may further be decreased in RS case, which in turn reduces the plasma major radius and reactor size. On the contrary, not only the ΔTF but the reactor size of the FS reactor may increase as B_{max} is 20 Tesla. The SS reactor size may not change much because its B_{max} is close to 16.5 Tesla. Therefore, even if we consider the relation between j_{st} and B_{max}, the conclusion that the RS reactor is the cost-minimized among the three operating modes does not change.

5.3.4 About the constraints of plasma major radius and neutron wall load

We set constraints $R_p > 5$ m and neutron wall load > 5 MW/m^2 in our survey. No solution was found because of the lack of radial build for the center cores or ΔTF, or MHD instability in FS and SS case. In the RS case, solutions are found which satisfy $R_p > 5$ m, the radial build requirement, and whose costs are less expensive than by not more than 2 mill/kWh. However, all those neutron wall load exceed 5 to reach 7 or 8 MW/m^2. As we have no prospect of reducing the replacement and maintenance greatly, we did not chose such reactors just for the sake of reducing 2 mill/kWh.

6. Summary and Conclusion

6.1 The impact of the design parameters on the COE in each operating mode

(1) FS operating mode

It can be concluded that (1) β_N should be raised as much as possible within the MHD stability limit (e.g. ≈ 3.0). However, β_N cannot be raised high enough, the following three conditions are further required. (2) High A (e.g. 4.5) and high κ (e.g. 2.0) are preferable to raise f_{bs} which reduces the cost of current drive. (3) High $B_{\max}$ (e.g. 20 Tesla) is desirable to reduce the V_p with high P_{fus}, although high $B_{\max}$ results in large V_{TF}. (4) High temperature (e.g. 20 keV) can more effectively obtain high P_{fus}. The SSTR-like reactor with a high $B_{\max}$ and a high aspect ratio is superior to the ITER-like reactor with a low $B_{\max}$ and a low aspect ratio.

(2) SS operating mode

In the SS operating mode, high q_{95} (e.g. 8.6) is required. The high q_{95} allows (1) SS region, (2) high f_{bs} close to 100% which results in low A (e.g. 3.0), and (3) high β_N (e.g. 4.95). However a too high β_N (e.g. more than 5.45) requires a counter current drive, which in turn requires a current drive power/cost and raises the COE. Moreover, high q_{95} results in a low plasma current and P_{fus} which requires a high $B_{\max}$ (e.g. 17 Tesla). The cost-minimized temperature (e.g. 15 keV) is dependent on $B_{\max}$. Both a high κ and a high δ (e.g. 2.0, 0.5, respectively) are more cost-effective.

(3) RS-like operating mode

The RS operating mode results in (1) a high f_{bs} close to 100% with low A (e.g. 3.0), (2) high β_N (e.g. 4.95). It must be emphasized that a high f_{bs} can be obtained even for low q_{95} (e.g. 3.75) using a reversed shear profile. By high β_N and low q_{95} (which result in high P_{fus}), a high $B_{\max}$ is not required. Surprisingly, because of the restriction of P_{wn}, a high $B_{\max}$ (more than 13 Tesla) increase the COE because the plasma minor radius a_p increases in order to reduce the P_{fus}. A high f_{bs} is more effective in reducing the COE than β_N. Cost-minimized temperature (e.g. 15 keV) is dependent upon $B_{\max}$. Both high κ and δ (e.g. 2.0, 0.5, respectively) are more cost-effective.

6.2 The superiority of the cost-minimized RS reactor

(1) It was demonstrated that (i) the cost-minimized RS design point can most reduce the COE and the construction cost among three operating modes, (ii) the construction cost can be reduced by reducing *the costs of both current drive and coils/structures*, and (iii) other costs like the B.O.P and the R.B. do not change much. Therefore, the FOMs which have the most direct impact on the COE are both *high* f_{bs} *and small* V_{TF}. It must be emphasized that *only the RS operating mode can attain a high* f_{bs} *and a small* V_{TF} *at the same time by high* β_N, *low* q_{95}, *and high* f_{bs}.

(2) It can be concluded that *the cost-minimized RS reactor can no longer reduce the cost* in our parameter survey and system code model. This is because the cost-optimized RS reactor has a small $B_{\max}$ (i.e., 13 Tesla), low A (i.e., 3.0), small a_p (i.e., 1.7 m, R_p = 5.1 m), all of which cannot be further reduced.

(3) This cost-minimized RS reactor has *two advantages:* one is because the B_{max} = 13 Tesla TF coil (which is adapted to this reactor) can be obtained *by use of ITER coil technology,* and the other is because *the same cooling technology of the ITER (water cooling)* can be used. The former advantage means that advanced coil technology like the 16 Tesla is not required. The latter advantage means that advanced technology like He-cooling or Li-cooling are not required.

Part IV

Economy, Energy Analysis, and Environmental Impact of Tokamak Fusion Power Reactors

1. Introduction

The status of tokamak fusion research and development (R&D) has reached a point wherein not only physics or engineering matters but also matters of economy, energy gain, environmental impact, or safety. All matters of economy, energy gain, environmental impact, and safety, are the tokamak reactor's properties as a socially responsible energy source, required characteristics for fusion reactors to be put to commercial use. Fusion R&D have been carried out to attain break-even condition for about 45 years since Dr. L.Spitzer,Jr. had devised fusion power generation. The break-even condition had been attained by the JET device experiment [JET92] and by the JT-60U device experiment [JT-60U97]. The JET device [F.B.Marcus] and the TFTR device [M.G.Bell] are now investigating physics/engineering matters of Deuterium-Tritium (DT) experiments. Furthermore, a detailed design of the International Thermonuclear Experimental Reactor (ITER) which aims self-ignition condition has been compiled [ITER-DDR], as well as conceptual designs of a demo reactor [IDLT-DEMO], and some power reactors [SSTR,ARIES,PULSAR,DREAM,SEAFP] had been proposed based upon present physics/engineering knowledge and databases.

It is indispensable and not at all premature to assess tokamak fusion reactors as an energy source, since tokamak fusion research had attained the break-even condition experimentally, compiled the detailed design of the ITER, and created conceptual reactor design. Since the beginning of fusion research, fusion researchers have asserted that fusion reactors are a source of "dream energy", i.e., clean, safe, and eternal. One result of this assertion that fusion energy is expected to be an important future energy supplier in the re-construction of "Geo Resuscitation Plan" [MITI] advocated by Japanese Ministry of International Trade and Industry (MITI). (See Part I)

Based upon these assumptions, we have studied the feasibility of minimizing the cost of electricity (COE) of tokamk power reactors [K.Tokimatsu97a&b] and re-assessed construction cost and the COE following the ITER cost. Our most important finding is that the construction cost and the COE of a reactor using reversed shear profile which has been recently experimentally obtained [F.M.Levinton,E.J.Strait,B.W.Rice], can be half of that of an ITER-like reactor whose electric power at a bus bar (P_e) is up to 1000 MW by minimum modification of plasma shape.

The parameters of the RS (reversed shear) reactor in Ref. [K.Tokimatsu97a&b] are almost the same of those of the CREST (Compact REversed Shear Tokamak) [K.Okano97a&b] designed Dr. Okano et al., at CRIEPI (Central Research Institute of Electric Power Industry). The assertion that the cost can be reduced by half in Refs. [K.Tokimatsu97a&b] is the same as that in Ref. [K.Okano97a&b]. The major radius of the RS reactor in Refs. [K.Tokimatsu97a&b] is reduced to 5.1 m by raising the Troyon factor (β_N) up to nearly 5, based upon present reversed shear simulation results [J.Manickam,C.Kessel,A.D.Turnbull]. The reason for the RS reactors' high cost performance is that the plasma shape and TF (Toroidal Field) coils of these RS reactors become compact by attaining the high $\beta_N \approx 5.0$, high bootstrap current fraction ($f_{bs} \approx 0.9$) with a low safety factor using reversed shear profile.

In these studies, we used various unit cost -- assumed to be attainable in the future -- of U.S. and E.U. reactor components [SSTR,STARFIRE,Generomak,R.A.Krakowski,RTR]. The absolute value of cost (construction cost and the COE) is uncertain, although relative value is meaningful. Instead of using those unit costs, we believe it is appropriate to make use of cost assessments based upon the ITER technology and its cost estimation as much as possible. This is to eliminate future uncertainty when fusion reactors are compared with other energy sources, even if this comparison might make fusion reactors disadvantageous. Through this comparison, however, we see present "possibilities" of tokamak fusion reactor costs and a "gap" between fusion reactor costs and those of other energy sources. Following this idea, we will propose arguments in favor of fusion reactors' possibilities not only in terms of cost, but also in terms of energy gain and environmental impact, compared with those of other present energy sources.

In this study, we estimate the ITER's volumetric densities and weight costs based upon their component weight and costs. Next, we explore the reactor's cost estimation, energy analysis (i.e., energy gain which is calculated as a ratio between input and output energies), CO_2 emission, and waste disposal, in taking into consideration of scheduled replacement of degraded within the plant's lifetime from construction to decommission. The aim of this study is to assess of fusion as an energy source in light of these properties, compared with those of fusion reactor types, along with fusion reactors' structural materials and those of other energy sources.

2. Reactor parameters used in this study

In this study, reactor parameters of the experimental reactor ITER, the power rectors; the ITER-like reactor, the RS reactor using reversed shear whose reactor parameters are almost the same of those of the CREST, and the ST (spherical tokamak), are listed in Table IV-1. In assessing the ST reactor, we used the plasma parameters and the volume data of the ARIES-ST reactor [ARIES-ST] (whose fusion power is about 3.8 GW, He-cooling, and of Vanadium-alloy structure) as a ST reactor model. The ST reactor is called a Low-Aspect-Ratio tokamak because the aspect ratio of the ST reactor is reduced as much as from 1.1 to 2.0. The possibility of the high physics performance of ST reactors had been demonstrated by theoretical studies [Y.K.-M.Peng86]. Recent experiments made by the START (Small Tight Aspect Ratio Tokamak) device in Culhum laboratory demonstrated the high physics performance of ST, i.e., $\beta_N = 4.0$, total β more than 30 %, $\beta(0)$ about 50% [START97]. The status of ST research is yet in its initial experimental phase; however, several Mega Ampare (MA) class experimental reactors are being designed or constructed. These will also reveal the possibility of small, high economic level reactors using ST physics.

1000 MW of P_e, 75% of plant availability, 30 years of plant life are characteristics ascribed to all power reactor types in this reactor comparison study. The fusion power is from 3 to 4 GW with the thermal to electricity conversion efficiency of 34.5 % using water as a coolant. Ferrite steel is assumed to be used for the structural material of the ITER-like reactor and the RS reactor. A shield blanket for the ITER, and a breeding blanket for power reactors is assumed, respectively. Weight fractions of structural materials, Tritium breeder Li_2O, and neutron multiplier Be in the breeding blanket are set as described in Table 2 for each replacement blanket and permanent blanket which are referred from the SSTR (Steady State Tokamak Reactor) [24]. Weight calculation of PF (Poloidal Field) coils, miscellaneous, and support structures is set as described in Table IV-3, and are referred from the ITER-TAC4 report [ITER-TAC4].

Energy gain and CO_2 emission of the ITER-like reactor and the RS reactor are also evaluated when structural materials, i.e., Ferrite steel, Vanadium-alloy, and SiC/SiC (Silicon carbide composite), are changed, i.e., cases (Fe1.0) (V1.5) (V1.0) (SiC1.5) (SiC1.0) are compared in Table IV-1. Those reactor parameters, including plasma physics, energy flow, TF coil shape, and cost, are calculated using zero-dimensional system code [T.Yoshida94]. In the design identification code (XY), X = Fe, V, SiC means structural materials, Y = 1.0, and 1.5 means P_e (unit: GW). The symbol (Fe1.0) corresponds to "Ferrite steel, electric bus bar 1.0 GW", which is used in comparing the ITER with the ST. This is the base case fusion power close to 3 GW. Thermal to water conversion efficiency is assumed to be 34.5 %, and Ferrite steel is used as a structural material in these cases.

(V1.5) case corresponds to "Vanadium-alloy, electric bus bar 1.5 GW", which is applied He-cooling, Vanadium-alloy with the same reactor parameters with those in the (Fe1.0) except the cooling and structural material. The electric bus bar is increased up to 1.5 GW because thermal to electrical conversion efficiency increased up to the 46.5% with the fusion power still being at about 3 GW. In (V1.0) case, He-

cooling and Vanadium-alloy is also applied as in the (V1.5) case, while P_e is adjusted to be 1 GW (fusion power 2.8 GW) by changing the minor radius with the same aspect ratio. In the ITER-like case, plasma shape bears almost no change, however, a high aspect ratio (aspect ratio A = 4.0) and a high magnetic field (16 Tesla on the TF coils) are applied to the RS case like ARIES-RS [C.G.Bathke96].

The same concept is applied to (SiC1.0)(SiC1.5) cases. The inner/outer blanket gap, and shield thickness are increased from those of other structural materials. The thickness of these material cases are described in Table IV-4 and derived from ESECOM (The Senior Committee on Environmental, Safety, and Economic Aspects of Magnetic Fusion Energy) study reactor design [ESECOM].

Table IV-1 Design parameters in this study.

	Comparison of reactor types				Comparison of structural materials							
	ITER	ITER-like (Fe1.0)	RS (Fe1.0)	ST	ITER-like				RS			
					(V1.5)	(V1.0)	(SiC1.5)	(SiC1.0)	(V1.5)	(V1.0)	(SiC1.5)	(SiC1.0)
structural material	SUS	Fe[a]	Fe	V[b]	V	V	SiC[c]	SiC	V	V	SiC	SiC
Coolant	Water	Water	Water	He	He	He	He	He	He	He	He	He
conversion efficiency (%)	34.5	34.5	34.5	46.5	46.5	46.5	46.5	46.5	46.5	46.5	46.5	46.5
plasma major radius (m)	8.4	8.4	5.1	2.9	8.4	8.55	8.95	9.05	5.1	5.1	5.68	5.65
aspect ratio	2.91	2.91	3.0	1.6	2.91	2.91	2.91	2.91	3.0	4.0	3.0	4.0
elongation	1.6	1.8	2.0	3.4	1.8	1.6	1.8	1.8	2.0	2.0	2.0	2.0
triangularity	0.24	0.24	0.5	0.59	0.24	0.24	0.24	0.24	0.5	0.5	0.5	0.5
toroidal field on TF coil (T)	12.5	12.5	13.0	14.2	12.5	12.5	12.5	12.5	13.0	16.0	13.0	16.0
Toroyon coefficient	2.2	2.7	4.95	6.3	2.7	2.7	2.7	2.7	4.95	4.0	4.95	4.5
H-factor	~2.6	1.424	2.289	2.6	1.424	1.639	1.374	1.738	2.289	2.31	2.196	2.48
plasma temperature (keV)	10.5	20	15	12	20	20	20	20	15	15	15	15
safety factor on 95%	3.0	3.0	3.75	11.2[d]	3.0	3.0	2.75	3.5	3.75	4.34	3.25	4.34
plasma current (MA)	21.0	27.6	15.5	28.9	27.6	23.8	29.4	23.5	15.5	10.89	17.1	10.5
bootstrap current fraction		0.289	0.935.	0.990	0.289	0.273	0.289	0.289	0.935	0.91	0.935	0.91
current drive power (MW)	70	263.1	23.5	41.9	263.1	200.9	272.5	175.3	23.5	27.5	24.6	25.3
neutron wall load (MW/m^2)	1.5	2.371	4.287	6.247	2.371	1.68	2.094	1.334	4.287	4.2	3.46	3.47
fusion power (MW)	1500	4034	2879	3490	4034	2749	4079	2662	2879	2160	2885	2150
Total thermal power (MW)		4699	3239	3845	4699	3218	4756	3102	3239	2431	3246	2421
electric output power (MW)	---	1000	1000	1000	1564	1000	1571	1000	1389	1000	1390	1000

(a): Ferritic steel, (b): Vanadium alloy, (c): Silicon Carbide , (d): on edge

Table IV-2 Weight fraction of structure, Li_2O, and Be of replacement/permanent blankets. These values are assumed from Ref. [SSTR-JAERImemo]

	Structure	Li_2O	Be
Replacement	0.1	0.12	0.2
Permanent	0.1	0.38	0
Total	0.2	0.5	0.2

Table IV-3 Volumetric fraction, volumetric density of components. Volumetric fractions are assumed from Ref. [SSTR-JAERImemo,ITER-TAC4].

	PF coil	Support structures	Misc.
Weight fraction	25% of TFcoils	1/15 of total reactor components* weight	20.2% of TFcoil cost
Cost ($/kg)	200	11.33	

*Coils, Blanket, Shield, Divertor

Table IV-4 Thickness of the each component. Thickness of SiC is assumed from Ref. [ITER-TAC4], others are assumed from Ref. [SSTR-JAERImemo]

	Inner Components			Outer Components		
Materials	Blanket	Gap	Shield	Blanket	Gap	Shield
SiC	0.56	0.2	0.85	0.67	0.4	1.59
Others	0.5	0.0	0.65	0.6	0.0	1.22

unit: m

3. Evaluation method

3.1 Economy

3.1.1 Calculation method of construction cost

The method of calculating construction cost in this study is based upon the ITER cost calculation, which will be used as a point of reference. Construction cost is calculated by summing the cost of (1) reactor components (superconductor coils, support structures, shield, blanket divertor), (2) current drive (CD), (3) heat transportation (Heat Trans), (4) reactor building (RB), (5) balance of plant (BOP), and (6) allowance for indeterminates (AFI). The cost of reactor components is the sum of all component cost. Each component cost is calculated by multiplying volume, volumetric density, and unit cost together. Cost of current drive is a product of heating power and unit heating cost. Cost of Heat Trans, RB, and BOP is a product of standard cost and scaling factor. The scaling factors are scaled from standard thermal power or standard Fusion Island (FI) volume. Thermal power is total thermal power gained from the fusion reactor, which is converted into electricity at turbines. The FI volume is the sum of the volumes of the reactor components. AFI in this study is 5 % of total costs of the others. This 5 % value is estimated from the ITER-IDR report [ITER-IDR].

The volumetric densities (t/m^3), unit costs ($/kg), manufacturing costs of reactor components -- all of which are listed in Table IV-5 -- are evaluated from the ITER-TAC4 report [ITER-TAC4] in which weights and unit costs are explained in detail. Unit cost data of Ferrite steel, Vanadium alloy, SiC which have asterisks (*s), are assumed by multiplying unit of SUS in the ITER with fractions between the unit cost of the material and the unit cost of SUS. These fractions are evaluated in from those unit costs in the ARIES system code [ASC].

Cost calculation methods of Current drive, Heat Trans, RB, and BOP are listed in the Table IV-6. The unit cost of heating power is set 4.6 $/W [T.Yoshida] referred from the SSTR. The standard costs of Heat Trans, RB, and BOP are decided by re-categorizing the ITER-IDR cost items following the Generomak model [Generomak]. Detailed items of RB and BOP are listed in Table IV-7. Costs of main reactor building, vacuum systems, coil power supply, cryostat -- all of which are in the ITER-IDR -- are included in the standard cost of RB. The standard cost of the BOP includes some costs from the ITER-IDR and the others from the Generomak model.

The categories from the ITER-IDR are the following: cost of waste treatment, fuel handling, instrumentation and controls, gas/liquid distribution, machine assembly, remote handling, and general test equipment. The costs from the Generomak model are land, buildings (except the main building), turbines, and other equipment including the electrical plant. The cost of buildings in the BOP is calculated by multiplying the cost of the main building (building in the ITER-IDR report) with fraction between costs of the main building and the other buildings in the Generomak model. Since the standard costs of the Generomak model and the ITER-IDR reflect the dollar values of '83 and '89, respectively, these standard costs are adjusted to US '93$ as is the ITER-TAC4, derived from the Implicit Price Deflator (IPD) in the ASC. The standard thermal power and the Fusion Island volume, which is 4699 and 5553, respectively, as described in the Table IV-6, are those of the ITER-like reactor.

3.1.2 Calculation method of the cost of electricity

The cost of electricity is calculated following formula.

$$COE = \frac{C_c \cdot F_{cr} + C_{om} + C_{scr} + C_{fuel}}{P_e \cdot 8760 \cdot f_{ave}} + C_{dis} + C_{dec}$$

$C_c, F_{CR}, C_{om}, C_{src}, C_{fuel}, P_e, f_{ave}, C_{dis}$, and C_{dec} means total capital cost, fixed charge rate, cost of maintenance, cost of scheduled replacement, cost of fuel, electric power at a bus bar, plant availability, cost of decontamination, and cost of decommissioning, respectively. The C_c is the sum of construction cost, indirect cost, and interest during construction. In this study, C_c is a product of construction cost, indirect multiplying factor, and construction multiplying factor. The construction cost used for the COE follows the Generomak model, which is different from that in previous section 3.1.1. In the construction cost based on the Generomak model, (1) coil cost includes 20 % of the contingency, (2) 75 % of total current drive cost is included in the construction cost (i.e., the remaining 25 % of the total current drive cost goes to replacement), and (3) initial tritium cost for the first three months is accounted for. Cost of maintenance is calculated by multiplying the sum of the "construction cost + initial replacement component cost" with a factor. The indirect multiplying factor, construction multiplying factor, fixed charge rate, and a factor used for cost of maintenance are derived from Japanese fission power plant experiences, set as 1.05, 1.1, 0.12, and 0.04, respectively.

Generomak model for replacement cost methodology is used in this study. In a blanket case, replacement frequency is calculated by dividing neutron fluence by neutron wall load. Replacement frequency of the current drive is half of the blanket. The divertor and the CP (center post) of the ST reactor are assumed to be replaced every year. Blanket replacement blanket cost is assumed as a single expenditure. The replacement cost for current drive corresponds to 25 % of the total current drive cost. Total divertor cost and total CP cost is used for a divertor and a CP, respectively. Moreover, both inflation and frequency between replacement interval are also considered part of the replacement cost.

Deuterium consumption is considered proportional to the numbers of DT reactions (i.e. fusion power). Additional tritium, except that initially installed for reactor operation, is assumed to be self-sufficient. Therefore, fuel cost is only the expenditure required for the consumed deuterium necessary for reactor operation. The cost of decontamination and decommission is "U.S. fission experience" 1.0, and 0.5 (mill/kWh), each of which follows the Generomak model.

3.2 Study of Energy Analysis and CO_2 emission

3.2.1 Background of this study

The energy analysis for power plants compares all energy following directly/indirectly into the power plant (input energy) and produced energy (output energy) by the plant system. This study shows one aspect of power plant quality in terms of energy. P.F.Chapman's study for nuclear power plants [P.F.Chapman] is the most prominent energy analysis. Many other power plant studies followed this study.

Some energy analysis studies have been made for fusion reactors [R.Bunde,D.Firsh, Y.Kozaki,Y.Shimazu86,Y.Shimazu88]. Disagreement regarding energy accounting occur between Ref. [R.Bunde] and Ref. [D.Firsh]. Ref. [Y.Kozaki] is the first Japanese energy analysis, treated fusion power reactor UWMAK-II and III. Ref. [Y.Shimazu86,Y.Shimazu88] and compared various fusion power reactors. The energy analysis results must be updated because (1) fusion power reactor designs evolve owing to the progress of plasma physics and engineering, (2) energy intensities derived from an input-output (I/O) matrix have changed because of industrial changes; where the energy intensity means required energy per unit weight, electricity, and/or price. In Japan, Life Cycle Assessment (LCA) is currently taking place. The energy analysis comparison studies [Y.Uchiyama95,Y.Uchiyama96] have been made for all other kinds of power plants except for fusion power plants. Following the current study trend, we have investigated fusion power reactors in order to measure their energy gain quantitatively in comparison with other energy sources. Our methodology of fusion reactor energy analysis is based upon Ref. [Y.Uchiyama95] in order to use a consistent standard to evaluate with other power plants.

As shown in Fig. IV-1, there are two streams, fuel and material, which compose the input of energy plant. In these two streams, processes consist of mining, refining, manufacturing, disposal, and the transportation connecting these four processes. All the materials and energy have to be considered in each process. We used the bottom up method which sums up all the energies used for fuel and materials. Fuel energies include fuel mining, refining, manufacturing, and transporting. Material energies include mineral mining, material refining, material/component manufacturing/transport, and component construction/building.

Energy gain is defined as the ratio of output/input energy. Although output energy is electricity, it is "second energy (i.e., electric energy)"; however, both "first energy (i.e., thermal energy)" and "second energy" are included in input energy. In this study, all the input energy is regarded as first energy and energy gain is calculated as second energy. 2250 kcal/kWh conversion efficiency [Y.Uchiyama95] according to Japanese experience is used, which is considered efficient for Japanese electrical generation.

3.2.2 Premises for energy analysis in this study

Input energies regarding fuel and materials, inclusions, and methods are summarized in Table IV-8. In this study, reactor construction, replacement within lifetime, and fuel consumption are considered, as well as waste disposal storage whose time span can be as long as 100 years. Deuterium is assumed to be sourced from nitrogen and hydrogen by an ammonia-hydrogen dual temperature exchange process in ammonia plants. Therefore, only fuel manufacturing energy is considered, i.e., no consideration is given to mining. Energy for fuel refinement and transportation, because of the difficulty of evaluating this energy, is assumed to be 20 % of fuel refinement energy, as in Ref. [Y.Uchiyama95]. Self-sufficient initial tritium and deuterium consumption (about 0.3kg/day for the 1 GWe reactor) are assumed as energy, similar to the cost method described in section 3.1.2. Energy intensity for deuterium is based upon Ref. [Y.Kozaki], and the energy intensity of tritium is assumed to be the same as that of deuterium.

Regarding material flow, energy for raw mineral mining and refining cannot be considered because of a lack of existing data. Energy necessary for manufacturing materials (material energy) from raw material, via intermediate material, to final material is calculated by multiplying weight and energy intensity together. Energy necessary for manufacturing (manufacturing energy) from final material to component is evaluated by manufacturing cost [ITER-TAC4]. Energy necessary for construction and transportation is assumed to be 20 % of the sum of material energy and manufacturing energy.

Reactor lifetime, replacement, and replacement frequency calculation follows the same as the cost evaluation described in 3.1.2, respectively. Input energy for one blanket replacement, current drive, and divertor equals to the input energy for a replacement blanket is 25 % of the total input energy for a current drive, and the input energy of a divertor. All the other components are assumed to be wholly replaced within 30 years of reactor operation. This assumption is to make same comparison with other plants' energy gains [Y.Uchiyama95] using the same standard.

3.2.3 Data for material energy

Input energy per unit cost and weight for calculating material energy is listed in Table IV-9. Energy intensities for superconductor strands, SUS, Ferrite steel, and copper alloy all of which are used for superconductor coils, blanket shield, and divertor are derived from data contained in a report [Super-GM] describing the energy analysis of a Super-GM (a motor-generator using superconductor). These data are appropriate because (1) the data used in Ref. [Super-GM] are detailed enough to be analytically reliable, (2) components of the super-GM resemble to those of reactor components, and (3) the data relatively recent. Input energy for Li_2O which is used for the blanket is evaluated using the latest data of Li extraction from sea water (10000 kWh for Li_2CO_3 1 ton) [K.Ohi]. Energy intensity of titan in Ref. [Y.Shimazu86] is applied for Vanadium-alloy. Energy intensity data for Be and SiC are sourced from Ref. [Y.Kozaki].

In the evaluation of the Heat Trans, the reactor building (RB), and the balance of plant (BOP), the sum of whose components cannot be calculated in detail, the amount of materials and electrical equipment are

considered. For RB, unalloyed steel used in the reactor plant equipment in Ref. [R.Bunde] (2086 ton) is included in the reactor building. High-alloyed steel in the reactor is not included since we consider that it has already been included in the reactor components. For the BOP, both unalloyed steels and high alloyed steels for "structure + site facilities", turbine plant equipment, and miscellaneous. plant equipment (total amount = 43656 ton) are considered. In addition to the steel, concrete (Japanese fission experience = 983390 ton) is counted as a part of the BOP. The energy intensities of blister steel and concrete described in Ref. [H.Hondo] are applied to these types of steels and concrete.

Evaluation of the necessary amount of material cost for current drive is very difficult because no detailed information exists regarding the material and its amount in the NBI (neutral beam injector) of the ITER, SSTR, and other reactor designs. The only weight data we could obtain about the NBI are those of components for the NBI device (0.5 MeV, 10 MW) in the JT-60U of JAERI (Japan Atomic Energy Research Institute) [JT-60U-NBI]. Because a 2 MeV NBI applied for the SSTR is assumed in our study, we tried to compare the NBI components in the JT-60U and those in the SSTR. In this study, Fig. IV-10 shows the weight of the NBI components of the SSTR as estimated from the volume and weight of the NBI components of the JT-60U, corresponding to the volume of the SSTR components known from detailed design of the SSTR [SSTR-JAERImemo]. Based upon this, we assemed the following values: 5 MW output per an ion source tank based Ref. [SSTR-JAERImemo,JT-60U-NBI], 8 ion sources per beam line based upon Ref. [SSTR-JAERImemo], and one vending tube, one beam dump + ion neutralizer cell, a NBI port, a measuring system. By use of these assumptions for components, a relation between current drive power and weight is formulated. Another problem is that we have no data describing materials used in the NBI and input energy data for manufacturing the NBI. It does not seem to be enough evaluation if all the input energy for the NBI is the necessary energy only for SUS yet no input manufacturing energy to the NBI is considered. We therefore used the second highest energy intensity data described in Ref. [H.Hondo] for the NBI (85.2 Gcal/ton as an electric computer) in order to make a severe assessment. Electric equipment for the electric power station, which corresponds to transformer equipment, transmission equipment in Ref. [H.Hondo], is also included in energy cost and the costs for Heat Trans, CD, RB, and BOP.

3.2.4 CO_2 emission and CO_2 reduction cost

CO_2 emission

Environmental impact, besides energy analysis, should be assessed in order to evaluate the tokamak reactor as an energy source. In this study, CO_2 emission, CO_2 reduction cost and waste disposal within the lifetime of tokamak fusion reactors are described. In this section, methodologies of calculating CO_2 emission and CO_2 reduction cost are also explained. The premises of evaluating CO_2 emission are the same as that of the energy analysis shown in the Table IV-8. In order to calculate the CO_2 emission from a component, all the energies such as oil, gas, and electricity -- input into the component have to be known. CO_2 emission by one kind of input energy is calculated by multiplying the input energy quantity with CO_2 emission intensity. Total CO_2 emission from the components is the sum of all CO_2 emissions from the components. Table IV-11 shows the quantities and CO_2 emission intensities of all the input energies of every component. Total CO_2 emission intensities, shown in Table IV-9, of the components treated in Table IV-11 can be calculated by summing all products of input energy and CO_2 emission intensity. The CO_2 emission intensity data of electrical equipment, blister steel, concrete, and electrical computers in Table IV-9 are derived from the I/O method described in Ref. [H.Hondo]. The CO_2 emission intensities of special materials such as Vanadium-alloy, SiC, and Be are products of each energy intensity with 0.28 ($t\text{-}CO_2/Gcal$), which is a ratio total energy consumption to total CO_2 emission in Japan in 1990 [H.Hondo].

CO_2 reduction cost

It is rational to compare energy sources in terms of costs for reducing unit ton of CO_2. This cost is the CO_2 reduction cost, which is calculated by a ratio of the "difference between the COE of the energy source and the average COE consisted of the existed energy sources" and the "difference between CO_2 emission from the energy source and the average CO_2 emission".

$$CO_2 \text{ reduction cost} = \text{COE increment} / CO_2 \text{ reduction}$$

The COE increment = The COE of each power plant – The average COE in total energy system

(#8.86 yen/kWh)

The CO_2 reduction = The average CO_2 emission intensity of the total energy system (#468 $g\text{-}CO_2/kWh$)

– The CO_2 emission intensity of each energy source. # Japanese experience in 1992

The CO_2 reduction cost is high when the COE of the energy source is high and the CO_2 emission intensity is high.

3.3 Radioactive waste

Radioactive waste disposal is a significant issue in the public acceptance of the fusion reactors as an energy source. Radioactive wastes from fusion power reactors do not include long-lived nuclides such as Pu (plutonium), TRU (Transuranic Element) which are included in radioactive waste from fission reactors. However, in-vessel components such as blanket divertor, and shield which carries radioactivity by 14 MeV neutron result in radioactive waste. Moreover, it is evident that they contain long-lived ($10^3 \sim 10^6$ years) nuclide such as ^{14}C、^{10}Be、^{53}Mn、^{186}Re [T.Tabara]. In this study, the volume of radioactive waste from the fusion power reactors during their plant lifetime is evaluated in comparing with (1) reactor types and (2) fission reactors. In this section, calculation methodology for volume of radioactive waste disposals is described in terms of reactor type comparison.

Total volume of radioactive waste disposals is the sum of the installed reactor component (blanket divertor, and shield) volume over the reactor's lifetime. Following radioactive waste disposals are not considered because of the difficulty in evaluation, i.e., those from front end such as reactor construction and manufacturing/transportation/installation of the initial tritium, and those from back end such as decommissioning of reactors. It is assumed that that shield can ideally protect neutrons from plasmas, and also assumed that all the components outside the shield can be used within the reactor's lifetime with no replacement. The methodology for calculating the replacement frequency of the replacement blanket divertor, and the CP is the same described in the cost methodology of section 3.1.2.

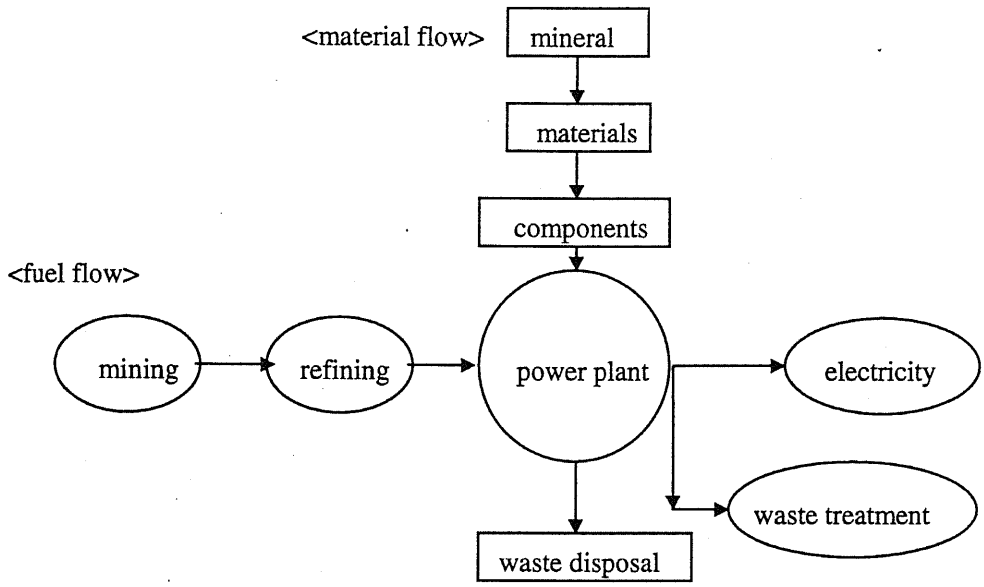

Figure IV-1 Energy analysis and CO_2 emission analysis flow

Table IV-5 Volumetric density, volumetric fraction, and unit cost used in this study. Most of them are estimated from Ref. [ITER-TAC4], Unit costs of Ferrite steel, Vanadium, SiC are assumed from Ref. [ASC].

Components	Items	Materials	Volumetric density[(a)]	Volumetric fraction	Unit cost ($/kg) [(b)]	ASC[(c)]'s unit cost[(d)]
TF coil[(e)]	Winding	Nb_3Sn	5.1	0.368	321.6	92.7
	Can	SUS etc.	16.4	0.632	8.38	
	Manufacturing cost	68.68 ($/kg) for total TF coil weight				-
	Cost factor	Multiplying 1.015 by total cost (for bus work and cooling)				-
Blanket	Structure	SUS	8.0	0.61	30	61.6
		Ferritic steel	8.0	0.2	33*	67.7
		Vanadium alloy	6.1		146*	300
		Silicon Carbide	3.2		195*	400
	Cu-alloy/Breeder	Copper/Li_2O	8.96/2.02	0.019/0.5	10/500	67.7/68.5
	Coating/Multiplier	Beryllium	1.87	0.003/0.2	625	615.6
			Tooling		587.1	-
	30000 ($/m^2) for First Wall (including tooling)					-
	60600 ($/m^3) for assembly, testing and inspection					-
Shield	Structure	SUS	8.0	1	35.5	61.6
		Ferritic steel	8.0		39.1*	67.7
		Vanadium alloy	6.1		172.1*	300
		Silicon Carbide	3.2		230.4*	400
Divertor	Structure	SUS	8.0	0.928	20	61.6
		Ferritic steel	8.0		22*	67.7
		Vanadium alloy	6.1		97.4*	300
		Silicon Carbide	3.2		129.8*	400
	Cu-alloy	Copper	8.96	0.0464	12.25	67.7
			Assembly and tooling		285.5	-
	Be brush	Beryllium	1.87	0.0258	843.9	615.6
			Associated tooling		843.9	-

(a) unit: t/m^3, (b) '93US $ (c) ARIES system code [ASC], (d) as a reference by '92US$,

(e) Copper coil is assumed in ST case, whose volumetric density and unit cost are same in those of ASC.

Table IV-6 Cost calculation formulas and contents of Current Drive, Heat Trans, Reactor Building, and Balance of Plant

Items	ITER	Formulas	Contents
Current Drive	901	calculated by 4.6 \$/W	Current Drive and its power supply etc.
Heat Trans	264	$264 \cdot \left(\frac{P_{th}}{4699}\right)^{0.6}$	Heat transportation and Heat tank etc.
Reactor Building	1834	$1834 \cdot \left(\frac{V_{FI}}{5553}\right)^{0.67}$	Main reactor building, Vacuum system, Coil power supply, Cryostat etc.
Balance of Plant	872	$2189 \cdot \left(\frac{P_{th}}{4699}\right)^{0.6}$	Land*, Buildings*, Fuel&Waste treatment, Instrumentation and Control, Liq./Gas Distribution, Turbine*, Machine assembling, Remote handling, other reactor plant equip.*, etc.

Unit; M\$, V_{FI} , P_{th} means Volume of Fusion Island and thermal power of fusion reaction, respectively.

*s are not included in ITER

Table IV-7 Standard cost breakdown of reactor building and balance of plant.

Reactor Building		
Items	**Reference**	**Cost** [a]
Main building	ITER[b]	1014
Vacuum Systems	ITER	69
Coil power	ITER	386
Cryostat	ITER	81
Thermal shield	ITER	22
Cryoplant/Cryodistribution	ITER	262
Balance of Plant		
Land	Generomak[c]	5.6*
Buildings (except main reactor)	Generomak/ITER	529*
Waste treatment	ITER	79
Fuel handling		
Fueling	ITER	32
Tritium plant	ITER	72
Instrumentation and controls		
Control and Data Acquisition System	ITER	63
Interlocks and alarms	ITER	2.3
Poloidal control	ITER	0.6
Diagnostics	ITER	168
Radwaste Monitoring	ITER	4.6
Gas/Liquid Distribution		
Liquid Distribution	ITER	64
Gas Distribution	ITER	23
Sampling	ITER	4.6
Turbine plant and main heat reject	Generomak	366*
Machine assembly, equipment		
Machine asse'y and tools	ITER	92
Remote handling equip.	ITER	239
General test equip.	ITER	28
Spare parts allowance	Generomak	111*
Electrical plant equip.	Generomak	171*
Other reactor equip.	Generomak	74*
Miscellaneous equip.	Generomak	60*

(a) Unit: '93 US M$, (b) ITER-IDR, (c) Generomak, *s are not included in ITER

Table IV-8 Inclusion and method of input energy for fuel and materials. "20% of (material and) manufacturing " method and "replacement method except blanket, current drive, and divertor" in this table are referred from Ref. [Y.Uchiyama95].

Fuel			Materials		
Process	Inclusion	Method	Process	Inclusion	Method
Mining	no		Mining and Refining of minerals	no	
Manufacturing	yes	Energy Intensity x Energy consumption	Material	yes	Energy Intensity x volume
Refining	yes	20% of manufacturing	Manufacturing	yes	cost
Transport			Transportation	yes	20% of material and manufacturing
Consumption	yes	Deuterium : 0.3 kg/day Tritium : self-sufficient is assumed	Replacement	yes	Blanket/Current Drive : considering Neutron wall load and neutron fluence
					Divertor : replacement of every year
					Others : one time of whole replacement within plant life time

Table IV-9 Energy intensity and CO_2 emission intensity of each component. Energy intensity of superconductor strands,SUS, and Ferrite steel are referred from Ref.[Super-GM], Vanadium, SiC, and Be are referred from Ref. [Y.Kozaki,Y.Shimazu86], the others are referred from Ref.[H.Hondo]. CO_2 emission intensities are calculated following by Table 10 or referred from Ref. [H.Hondo].

Items	Materials for reactors		Materials appried for this study	Energy[a] Intensity	CO_2 Emission[b] Intensity
Superconductor Coils	Nb_3Sn strand		NbTi strands[e]	49.2	30.7
	SUS316 (Fe66, Ni22, Cr18, Mn2, Mo2)		SUS alloy[e] (Fe31.2, Ni33, Cr30.7)	35.2	7.5
Blanket Shield Divertor	Structural Materials	SUS316	SUS alloy	35.2	7.5
		Ferrite (HT-9) (Fe87, Cr8, W1)	Fe-Ni-Cr alloy[e] (Fe86.5, Ni9, Cr3)	82.3	8.7
		Vanadium (V-5Cr-5Ti) (V90, Cr5, Ti5)	Ti64[f]	299	83.7
		SiC (Si50, C50)	SiC[g]	50	14.0
	Cu-alloy		Cu99, Cr1[e]	9.2	3.2
	Li_2O		Li2, O1[h]	21.2	9.68
	Be		Be[g]	860	240.8
Reactor Building	Unalloyed steels (2086 ton)		Blister steel[i]	4.68	1.41
	Electrical equipment		Electrical equipment[i]	1112[c]	344.3 [d]
Balance of Plant	High alloyed steels (43656 ton)		Blister steel	4.68	1.41
	Concrete (983390 ton)		Concrete[i]	0.15	0.11
Heat Trans	Electrical equipment		Electrical equipment	1112[c]	344.3 [d]
Current Drive	SUS etc.		electric computer[i]	85.2	21.3

Unit: (a) t-CO_2/t-material, (b) Gcal/t-material, (c); Gcal/M$, (d); t-$CO_2$/M$

References: (e) Ref.[Super-GM], (f) Ref.[Y.Shimazu], (g) Ref.[Y.Kozaki], (h) Ref.[K.Ohi], (i) Ref.[H.Hondo]

Table IV-10 Weight assumption of SSTR NBI components from those of JT-60U. (Unit; (a):m, (b):ton)

JT-60U				SSTR			
Components	Specification[(a)]	Weight [(b)]		Components	Specification[(a)]	Multiply	Weight [(b)]
Ion Source Tank	ϕ3 x 6	97.4	→	Ion Source Tank	ϕ 3 x 15	x 2.5	250
Neutralizer Cell	~ 10	59.3	→	Bending Tube	25	x 2.5	150
Ion Dump Tank	ϕ 4 x 3.5	62.2	→	Beam Dump + Neutralizer	ϕ 7 x 9	x 4.5	280
NBI port		2.2	→	NBI port		(x 2.5)	5.5
Measurement		30	→	Measurement		(x 2.5)	75

Table IV-11 CO_2 emission intensity of energy sources and energy consumption of each component. CO_2 emission intensities are referred from Ref. [H.Hondo]. Energy consumption breakdown is referred from Ref. [Super-GM, Y.Kozaki]. ((a) : g-CO_2/unit energy)

Energy			Energy Consumption for each component				
Items	Unit of Items	CO_2 Emission Intensity [(a)]	SC coils	SUS	Ferrite steel	Copper alloy	Deuterium
volatile oils	litter	2358.6			0.0		
lamp oils	litter	2528.3	1.5	5.8	4.2	1.9	
light oils	litter	2644.3	0.3	3.1	0.7	0.4	
A type heavy oils	litter	2697.7	38.7	1.6	3.8	1.8	
B type heavy oils	litter	2885.6	6.2	34.1	0.9	124.2	
C type heavy oils	litter	2885.6	126.2	257.2	93.6	161.0	1135000
hydro-carbon oils	litter	3162.5			0.0		
coals	kg	2795.0	132.9	133.5	45.1	169.5	
oil coke	kg	3307.4	6708.0			8.6	
coal coke	kg	3247.2	31.0	382.5	615.7	46.7	
LPG	kg	3006.6	5.5	145.9	6.2	67.1	
coke gas	m^3	809.6		27.5	78.9		
butane gas	m^3	2041.7		600.0	634.0		
natural gas	m^3	2026.2		1.5	4.3		
refined gas	m^3	2141.0	0.0	0.3	0.8		
fireplace gas	m^3	877.1		124.5	356.9		
electricity	kWh	392.3	19200	8000	11700	3006.1	2260000

4. Results

4.1 Reactor comparison

Reactor comparisons in terms of construction cost, the COE, input energy, CO_2 emission, and waste disposal are shown in Fig. IV-2 (a) ~ (e). In figures of (a) construction cost, (c) input energy, and (d) CO_2 emission, breakdowns of the bar graphs are from the bottom (1) coils and their support structure, (2) blanket/shield/divertor, (3) current drive (CD), (4) heat transportation (Heat Trans), (5) reactor building (RB), and (6) balance of plant (BOP). 5 % of the AFI in the case of construction cost, while both replacement (blanket divertor, and current drive from the bottom) and fuel in the case of input energy and CO_2 emission, are added. The breakdowns in (b) the COE is also from the bottom of the capital cost, maintenance cost, replacement cost, fuel cost, disposal treatment cost, and decommission cost. All these are principal in the COE, while rest are the fuel cost, decontamination and decommission cost. The breakdown categories in (e) the radioactive waste disposal are blanket shield, divertor, and CP for the ST reactor.

4.1.1 Characteristics of fusion reactors

Fuel can be neglected since it can be known from (b), (c), and (d). Almost all the input energy into or CO_2 emission from components (not fuel) are accounted for. The initial installation fraction, corresponding to capital cost in the COE and all the breakdowns except fuel and replacement in the input energy and CO_2 emission, becomes almost 60 to 70 %, while operational cost, input energy, and CO_2 emission equals 30 to 40 %. Moreover, the initial installation, cost, input energy, and CO_2 emission for the reactor components (coils/structure + blanket/shield/divertor) occupy half of the total cost, input energy and CO_2 emission, while the others (reactor buildings, balance of plant) are also equivalent to half of the total.

4.1.2 Comparison of fusion reactors

From (a) to (e), it can be inferred that construction cost, the COE, input energy, CO_2 emission, and radioactive waste disposal of both the RS reactor and the ST reactor can successfully be reduced in comparison of the ITER-like reactor. The reason for this is that the RS and the ST reactor can reduce reactor volume by use of high physics performance. Although the ST reactor by use of the low plasma aspect ratio can be more compact than the RS reactor, all the results are almost the same because of the cost increase and quantity of replacement along with the frequency of replacement due to the increment of the neutron wall load. We cannot draw general conclusions of comparison between an RS reactor and an ST reactor due to the differences of structural materials and varying cooling methods between the reactors. Both of the RS reactors based upon the CREST reactor and the ST reactor based upon the ARIES-ST reactor can both be prominent models for future fusion R&D if both reactors can attain the same 75 % plant availability.

4.2 Structural materials comparison

Construction cost, the cost of electricity, input energy, CO_2 emission, and the radioactive waste of the ITER-like and the RS reactor, whose structural materials are changed from Ferrite steel to Vanadium alloy and SiC, are investigated. Results of these properties for the ITER-like reactors are shown by unit electricity (or electric power) in Figure IV-3 (a) ~ (e). Breakdowns are the same of those of section 4.1. Scale merit affects the case (V1.5) and (SiC 1.5) whose electric power is larger than the cases.

To make comparisons fair, in comparing (Fe1.0) (V1.0) (SiC 1.0) whose electric power is the same at a bus bar, (a) construction cost, (b) the COE, (e) radioactive waste disposal are greater as Fe < Vanadium < SiC, while (c) input energy and (d) CO_2 emission are greater as SiC < Fe < Vanadium. Input volume quantities to the fusion reactor components increase in the reactor cases made from Fe, Vanadium, to SiC structural materials. This inclination is true to (a)(b)(e); however, this is not true to (c)(d). Two reasons account for this. (1) Components weight in the reactor case made of SiC is light because of the lightness of the volumetric density even though the number of reactor components is higher. (2) Both input energy and CO_2 emission are small because the energy intensity and CO_2 emission intensity (in terms of unit weight) is also small. In the SiC reactor case, energy gain increases slightly and CO_2 emission intensity (in terms of unit electric power at a bus bar) decreases slightly in comparison with a Ferritic reactor.

These inclinations seen in the ITER-like cases are almost identical to the RS reactor cases whose results are shown in Figure IV-4 (a) and (b). However, volume of superconductor coils increases by the modification to ARIES-RS type, which results in increment of CO_2 emission intensity in the case of (SiC 1.0).

Radioactivity level of radioactive waste in comparison with structural materials is also mentioned. However, radioactivity calculation by use of detailed codes is beyond our study. Therefore, radioactive level of structural materials is referred from data in Ref. [AESJ]. In Table IV-12, radioactive waste disposal levels and definitions are summarized from Ref. [JAIF,IAEA-Safety111,P.Rocco,B.L.Cohen]. Class C waste disposal, structural material recycling, and natural background is referred from 10FCR50, Ref. [P.Rocco], Ref. [B.L.Choen], respectively. All these Class C, material recycle, and natural background radioactive levels are indicated in contact dose rate. In this study, we indicate these levels in activity level in becquerel (Bq) by use of $1\times10^{8}(\mathrm{Bq\cdot h/Sv\cdot cm^{3}})$ conversion efficiency [AESJ] which have order accuracy. This conversion efficiency can be calculated by use of 1 cm constant dose rate ($\mu\mathrm{Sv\cdot m^{2}\cdot MBq^{-1}\cdot h^{-1}}$) of a nuclide, radiation emission energies and their decaying factor ($\mathrm{m^{-1}}$) obtained from emission fraction of gamma-ray from the nuclide [K.Shibata, JRIA]. This value of Ferrite steel, Vanadium alloy, and SiC are all in order of 10^{8}.

Table IV-13 indicates that radioactivity level decay of Ferrite steel (assumed HT-9), Vanadium alloy, and SiC from Ref. [AESJ] in the case of 5 MW/m^2 of neutron wall load and 2 years neutron radiation time. From this table, Ferrite steel is classified HLW even after 100 years cooling. SiC is classified as Class C radioactive waste disposal, however, it can not be cooled to the level capability of recycling and natural background. Vanadium alloy is still classified as HLW after 1 year cooling, however, its radioactive level is decreased to natural background level after 100 years cooling. It is enough to satisfy Class C disposal standard for radioactive waste disposal treatment, however, it is much attractive for radioactivity to reach natural background level because environmental impact is negligible and also public acceptance can easily be obtained.

Moreover Ref. [AESJ] mentioned possibilities of radioactivity reduction of structural materials by use of isotope separation. By this method, there are possibilities to drastically reduce radioactive level in the case of low activate Ferrite steel, resulted in satisfying natural background level in Table IV-13 after 100 years cooling. We do not evaluate cost, energy gain, and CO_2 emission of these isotopic separated materials because there are no data of cost, energy gain, and CO_2 emission for those materials. This evaluation is left as a future study.

In conclusion, Ferrite steel should be used if cost is the top priority; Vanadium alloy for radioactive level after 100 years cooling; and SiC for energy gain, CO_2 emission intensity, and radioactive level after 1 year cooling. Shortcomings for these cases, radioactive level is high in the case of Ferrite steel, energy gain and emission get worth in Vanadium case, and expensiveness in SiC case.

4.3 Comparison with other energy sources

Construction cost per unit electricity, the COE, energy gain, CO_2 emission, and CO_2 reduction cost in comparison with other energy sources are listed in Table IV-14. Ferrite steel as a structural material, with a 1 GW electric bus bar case is applied to the ITER-like reactor, the RS reactor. Data except that of fusion reactors' are referred from Ref. [Y.Uchiyama95,EnergyData97]. Data for the once-through, gas diffusion method of the uranium condensation fission rector type is listed in this table. Other candidates of future energy sources, such as a FBR (fast breeding reactor) or a fission rector using plutonium recycling or centrifugation for uranium enrichment, are not listed in this study because we will compare fusion energy with other present energy sources in the contemporary energy system. Electric power and plant availability of the fission rector, the coal fired power plant, and the LNG fired power plant is all 1 GW and 75 % is assumed, respectively. 10 MW and 45 % for the hydro-electric generation plant, 3 kW and 15 % for a house-use PV (photo voltaic) are also assumed. An exchange rate of 1$ = 125 yen, which is used in Ref. [EnergyData97], is also applied to fusion reactor costs.

4.3.1 Economy

Although scale merit is effective for fusion reactors, the costs of fusion reactors, even for the ST reactor, are much higher than the costs of the others except PV. This is because the fusion reactors are FOAK (first-of-a-kind) reactors because the costs are based upon the ITER cost estimate. However, unit costs of reactor components can be considered as TOAK cost data compared with those of ASC shown in Table IV-5. The large difference between this study's results and those of TOAK results (e.g., by ARIES-study) come from the standard cost data of RB and BOP used in this study. Such a cost assessment difference had also pointed out the SSTR cost evaluation results in the value between by JAERI case and by IFT (Institute for Future Technology) case [IFT]. Ref. [IFT] shows about 120 billion yen difference came from the cost of RB and BOP. Therefore, such difference is inevitable.

We consider the range of "present economic competitiveness" as one between the maximum cost and minimum cost of other energy sources in Table 14; from 10 to 14 (yen/kWh) in terms of the COE. Therefore, by this definition of competitiveness, fusion reactors cannot be presently economically "competitive" although it can be said to possess some degree of competitiveness. Economic competitiveness can be regarded as a necessary aspect of fusion reactor's ability to become a viable energy source. Therefore, three things are required (1) the RS reactor and the ST reactor, which utilize high physics performance, should be utilized for their value in fusion R&D. (2) The reactors based upon the ITER physics are not cost effective. (3) Moreover, possibilities of further cost reduction have to be demonstrated even by use of the ITER cost estimation applied to this study.

4.3.2 Energy analysis, CO_2 emission, and CO_2 reduction cost

Manufacturing energy is not included in the results of the fusion energy gain because this manufacturing energy is not included in all the other energy sources in Table 14. Therefore, the figures for fusion reactors are different from those shown in Figure 2. The energy gain of the ITER-like reactor exceeds that of the coal fired power plant and PV; however it is below that of fusion. The energy gain of the RS and the ST reactors slightly exceeds that of fission. CO_2 emission intensity (CO_2 emission per unit electricity) exceeds only that of PV in the case of the ITER-like; however, both the RS reactor and the ST reactor are close to a hydro-electric generation or a fission reactor in terms of CO_2 emission intensity. The CO_2 reduction cost of the fusion reactors is more expensive than that of fission or hydro-electric generation since fusion reactor's CO_2 emission intensity is higher and their COE is more than those of fission or hydro-electric generation. However, the CO_2 reduction cost of fusion reactors is less than those of PV and CO_2 recovery devices in coal fired plants.

4.3.3 Radioactive waste disposals

In this section, radioactive waste volumes of fusion reactors are compared with those from fission reactors. However, it is beyond our study to carry out detailed radioactivity calculation for evaluating radioactive waste level. The structure and components of blanket and shield of the ITER-like and the RS reactor are referred from those of SSTR, divertor is from referred from ITER in this study. Therefore, we proceed our arguments referring from those radioactivity calculation results Ref. [T.Tabata,AESJ] of the blanket and shield of the SSTR, and the divertor of ITER [K.Maki]. Table IV-12 shows classification of HLW, ILW, and LLW of Japanese Nuclear Safety Committee [JAIF], IAEA [IAEA-Safety111], and P.Rocco [P.Rocco].

No HLW disposals are emitted from fusion reactors following to the classification of the Japanese Nuclear Safety Committee. In the other two classifications, heat and dose rates are required for classification of radioactive waste. After 50 years cooling time, first blanket of the SSTR (the most inner blanket) is not classified as HLW by the IAEA definition, however, classified as HLW by P.Rocco. After 100 years after cooling time, no SSTR components are classified as HLW. Moreover, long-lived nuclide radioactive level is almost negligible in SSTR radioactive waste disposals.

As we see, there is no confirmed classification for radioactive waste, and classification for radioactive waste of fusion reactors are different in terms of cooling time. Radioactive level of fusion reactor components is changed by cooling period after removal from fusion reactors. In this study, cooling period is assumed as 100 years during which radioactive waste disposals from fusion reactors are not classified as HLW; i.e., ILW/LLW by IAEA and P.Rocco definition. Reasons of this classification are (1) radioactive level of long-lived nuclide is negligible in radioactive waste disposal from fusion reactors, (2) no radioactive waste disposals are classified for HLW at burying the disposals after long cooling period.

We admit that this classification is provisional and detailed classification of radioactive waste disposals for fusion reactors including fission reactors is desired. The ST reactor is not treated as we have no radioactive waste level of the ST reactor.

Next, radioactive waste disposal volume from fission reactors is described. Classification and volume of radioactive conditioned waste disposals from fission reactors (therefore they are considered to be solid) are derived from Table X in Ref. [IAEA-Tech366]. There is no explanation about a classification standard in Ref. [IAEA-Tech366], therefore the classification used in Ref. [IAEA-Tech101] is unknown whether it is derived from IAEA classification of Ref. [IAEA-Tech101] or is referred from classifications of references in Ref. [IAEA-Tech366]. However, since radioactive waste that can be classified as HLW is only a part from back end reprocessing, this part is classified as HLW, the others are classified as LLW/HLW.

Figure IV-5 indicates comparison of volume, dominant nuclide, and radioactive level of radioactive waste of fusion reactors with those of a fission reactor, following the described classification. Largest part of radioactive waste disposal volume from a fission reactor is originated from Uranium mining process of front end, whose volume is not less than 6×10^5 m^3 and its dominant nuclide is ^{238}U whose half-life is very long (4.5×10^9 years). This amount is quite huge, however, its radioactivity level is 10^8 [Bq/m^3]. Volume of the HLW from the fission reactor is less than 1000 m^3, however it contains TRU or ^{239}Pu whose half-life is also quite long (2.4×10^4 years). Moreover, radioactive level of the HLW from the fission reactor is around 10^{15} to 10^{16} [Bq/m^3]

In contrast, radioactive waste total volume from fusion reactors, in the cases of Ferrite steel, is about 10000 m^3 for the ITER-like case and about 5000 m^3 for the RS case. Therefore, it can be said that fusion reactors can reduce radioactive waste disposal volume at least by two orders less than that from fission reactors. Furthermore, it can be inferred that much more reduction of radioactive waste disposal volume can be expected if low activation materials such as Vanadium alloy or SiC, are applied for structural materials. It is clear that radioactive level of radioactive waste disposal from fusion reactors is still high (up to $10^{15} - 10^{16}$) even after 100 years of cooling in the case of Ferrite steel applied reactors, however, this level also can be greatly reduced in Vanadium alloy or SiC cases.

To clarify equality, this comparison between fusion reactors and a fission reactor are not completely impartial in following points. In this study, radioactive waste volume by decommissioning is not included for neither fusion reactors nor a fission reactors because there is no experience of decommissioning. It can be considered to be fair in that decommissioning is not considered for both fusion reactors and a fission reactor, however, result is unknown nor unclear if the actual radioactive waste disposal volume includes decommissioning. Moreover, radioactive waste disposals from fission reactors includes all the disposals except decommissioning, such as tailings from mining, filter or ion exchanger sludges, evaporator contamination, all of which are due to reprocessing. Furthermore, there are possibilities

to reduce volume of mining tailings through Pu recovery by reprocessing or by Pu use through FBRs (Fast Breeder Reactor).

On the other hand, radioactive waste disposals from fusion reactors will include those from current drive components, some components contaminated by Tritium or other radioactive nuclides, or miscellaneous due to tritium refining, installations etc.. These radioactive waste disposals are not considered here because there is no reliable estimations for the volume of these radioactive waste disposals. Therefore, further detailed comparison study of radioactive waste disposals from fusion reactors and from fission reactors should be made in future.

Table IV-12 Summary of Radio waste disposal levels, their definitions. Waste disposal level (HLW, ILW, LLW) is referred from Japanese definition (Ref.[JAIF]), IAEA (Ref.[IAEA-Safety111]), P.Rocco (Ref.[P.Rocco]), Class C radioactive waste (Ref.[10FCR50]), hands on recycle level (Ref. [P.Rocco]), background level (Ref. [B.L.Cohen]).

Definition			Level				
			HLW	ILW	LLW	VLLW /EW	others
Japan			Waste liquid from reprocessing process	All the other waste disposals except the HLW. They are classified α disposal, β/γ disposal, and RI disposal.		-	
IAEA	Radioactivity	Bq/g	-	Short lived waste (LILW-SL) Restricted long lived radionuclide concentrations (4000 Bq/g in individual waste package and an overall average of 400 Bq/g per waste package) Long lived waste (LILW-LL) Long lived radionuclide concentrations exceeding limitation for short lived waste		10^4-0.1	
	Dose equiv.	mSv/h	-			0.01	
	Heat	kW/m^3	>2 including long lived radio-nuclide concentrations exceeding limitations for short lived waste			-	
Rocco	Radioactivity	Bq/g	-			0.4>	
	Dose equiv.	mSv/h	>20	20-2	2>	0.01	
	Heat	W/m^3	>10	10-1	1>	-	
Class C	Dose equiv.	μSv/h					Class C disposal level: $5*10^3$ >
Rocco	Dose equiv.	μSv/h					Hands on Recycle level: 25 >
Cohen	Dose equiv.	μSv/h					Background level: 0.1 >

> x ; more than x, x > ; less than x

Table IV-13 Radio waste disposal levels, their definition, and induced radioactivity of structural material dependence for cooling time. Induced radio activity is assumed from Ref.[AESJ] in the case 5 MW/m^2, 2years. Waste disposal level (HLW, ILW, LLW) is referred from Japanese definition, Class C radioactive waste level is from 10FCR50, recycle level from Ref. [P.Rocco], background level from Ref. [B.L.Cohen]. Conversion efficiency from radioactivity to dose equivalent is referred from Ref. [AESJ, K.Shibata, JRIA].

Level	Definition	Induced radioactivity								
		Material	Ferrite			Vanadium			SiC	
		Time	24h	1y	100y	24h	1y	100y	24h	1y	100y
		Radioactivity	$7*10^{12}$	$4*10^{12}$	$3*10^{8}$	$9*10^{11}$	$3*10^{9}$	$1*10^{-22}$	$3*10^{10}$	$3*10^{4}$	$3*10^{4}$
		Contact Dose rate	$7*10^{4}$	$4*10^{4}$	3	$9*10^{3}$	3*10	$1*10^{-30}$	$3*10^{2}$	$3*10^{-4}$	$3*10^{-4}$
HLW	More than 20 (mSv/h)	no	no	no	no	no	yes	no	yes	yes
ILW	2-20 (mSv/h)	no	no	no	no	no	yes	no	yes	yes
LLW	Less than 2 (mSv/h)	no	no	no	no	no	yes	no	yes	yes
Class C	$5*10^{3}$ (μSv/h) after 100 years	no	no	no	no	no	yes	no	yes	yes
Recycle	25 (μSv/h) after 100 years	no	no	no	no	no	yes	no	no	no
Background	0.1 (μSv/h)	no	no	no	no	no	yes	no	no	no

Table IV-14 Comparison of energy gain and CO_2 emission with other power plants. ITER's properties are no so excellent; cost is four times higher than that of a fission, energy gain is worth than that of coal fired, CO_2 emission intensity is slightly better than that of PV (Photo-Voltaic). On the contrary, properties of the RS and the ST reactors are excellent. Although cost is expensive, e.g., two times than that of fission, energy gain and CO_2 emission intensity is close to those of fission.

	Fusion			Fission (once-through)	Coal fired	Water powered	Photo-Voltaic (for a house use)
	ITER-like (Ferrite)	RS (Ferrite)	ST				
tal output electric power (MW)	1621	1117	1788	1000	1000	10	0.003
-circulation power fraction (%)	38.3	10.5	44.1	3.4	7.4	0.25	0
lectric power at bus bar (MW)	1000	1000	1000	966	926	9.975	0.003
Plant availability (%)	75	75	75	75	75	45	15
Construction cost per t electric power [10^4 yen/kW[(c)]]	121	61	53	31	30	60	200(80[(d)])
ost of electricity [yen/kWh[(c)]]	44	21	20	10	11	14	222(89[(d)])
Energy gain	14	28	28	24	17	50	9
emission intensity [g-CO_2/kWh]	46.5	22.5	24.0	20.9	990	17.6	58.7
CO_2 emission reduction cost [10^4 yen / t-CO_2[(c)]]	8.25	2.76	2.51	0.26	4.8[(a)]	0.93	52(18[(d)])

(a) (b) CO_2 recovery facility on coal and LNG fired power plant, respectively. (c) 1$ = 125 yen is assumed, (d) prospective value in future, * All the data except fusion are derived from Ref. [Y.Uchiyama95, EnergyData97]

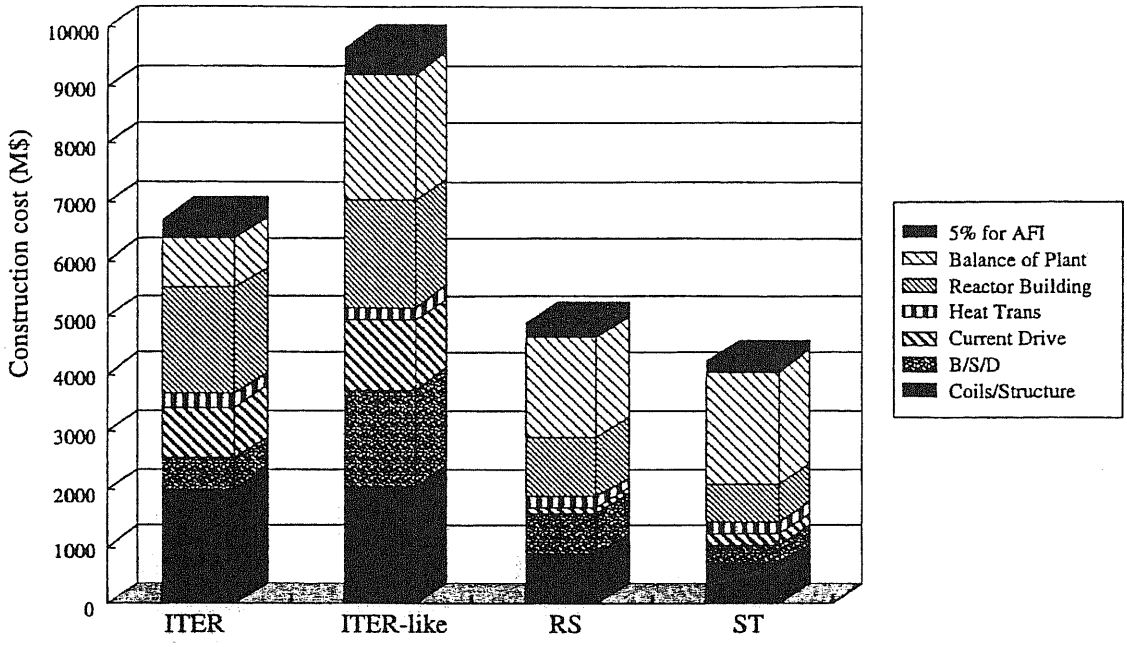

Figure IV-2(a) Comparison of the direct construction cost for the ITER, the ITER-like, the RS, and the ST reactors. These construction cost is calculated by the ITER cost data basis and cost estimation. The construction cost of the RS reactor and the ST reactor is less than half of that of the ITER-like reactor. The construction cost of the ST reactor is slightly less expensive than that of the RS reactor.

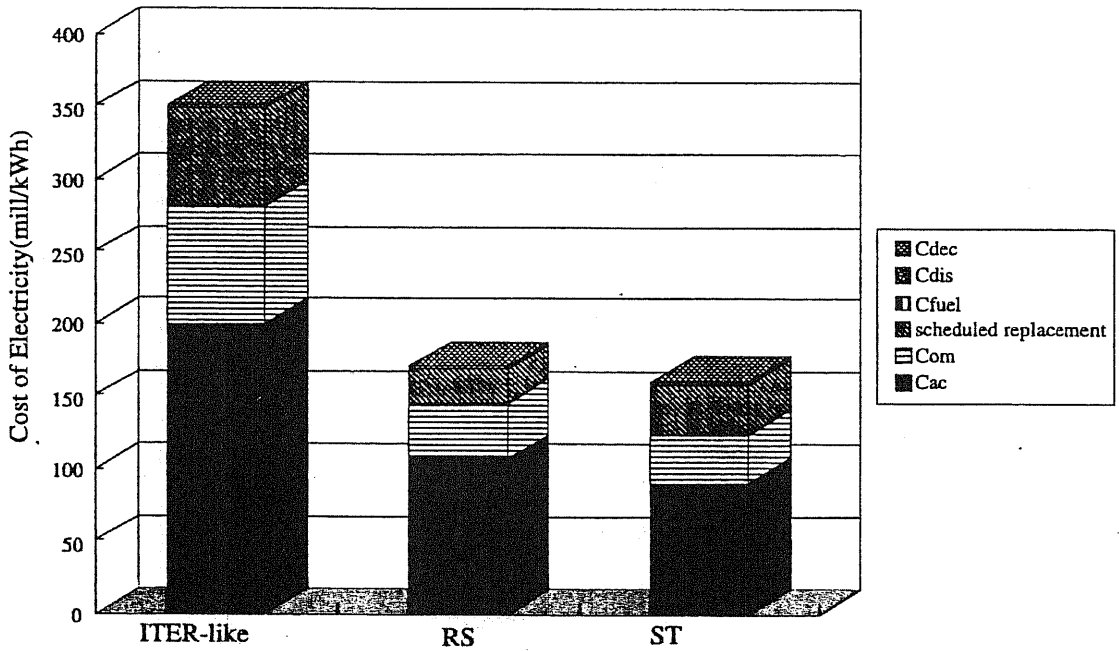

Figure IV-2(b) Comparison of the cost of electricity (COE) for the ITER, the ITER-like, the RS, and the ST reactors. The construction cost for calculating this COE is based upon the Generomak model. The COE of the ST reactor is almost the same of that of the RS reactor. The reason of the cost difference between the RS reactor and the ST reactor in the COE is less larger than that in the construction cost is because the ST reactor increases the number of replacement of scheduled replacement, which results in the increase of the COE.

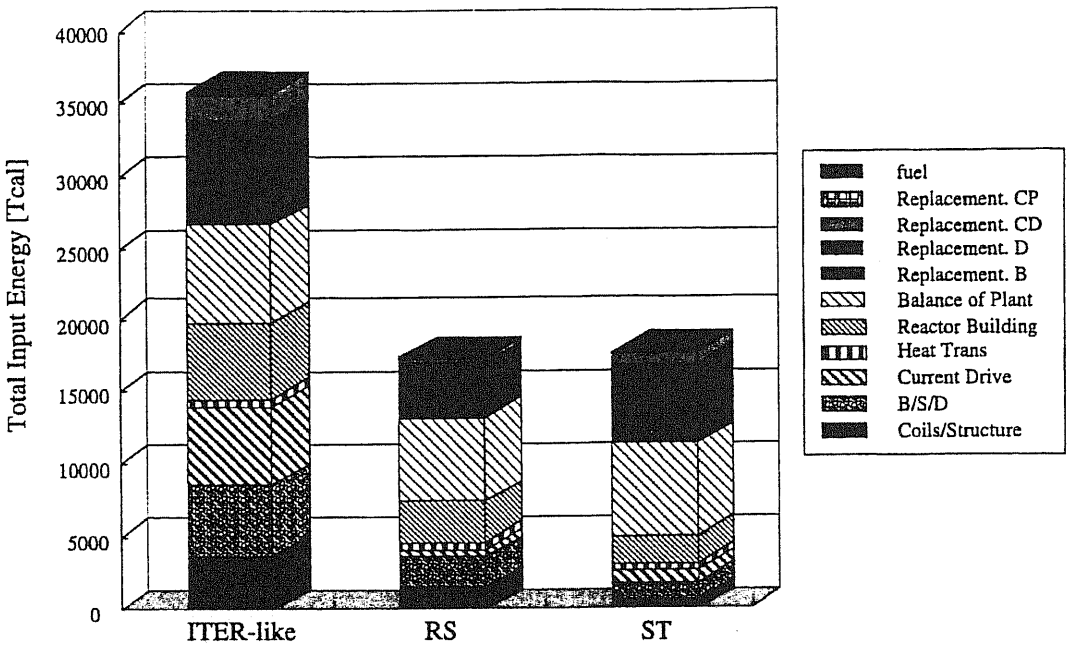

Figure IV-2(c) Comparison of the input energy for the ITER, the ITER-like, the RS, and the ST reactors. Following two things are characteristic for these tokamak reactors; the input energy for fuel can be neglected, the input energy related to the upper three columns correspond to replacement increase up to 30 to 40 %. The input energy for the RS reactor and the ST reactor is less than half of that of the ITER-like reactor. The total input energy for the ST reactor is almost the same as that for the RS reactor. The ST reactor can success to reduce the input energy for Coils/Structure and B/S/D by its compactness, however, the input energy for replacement of the ST reactor is larger than that to the RS reactor which, in turn, yields the result.

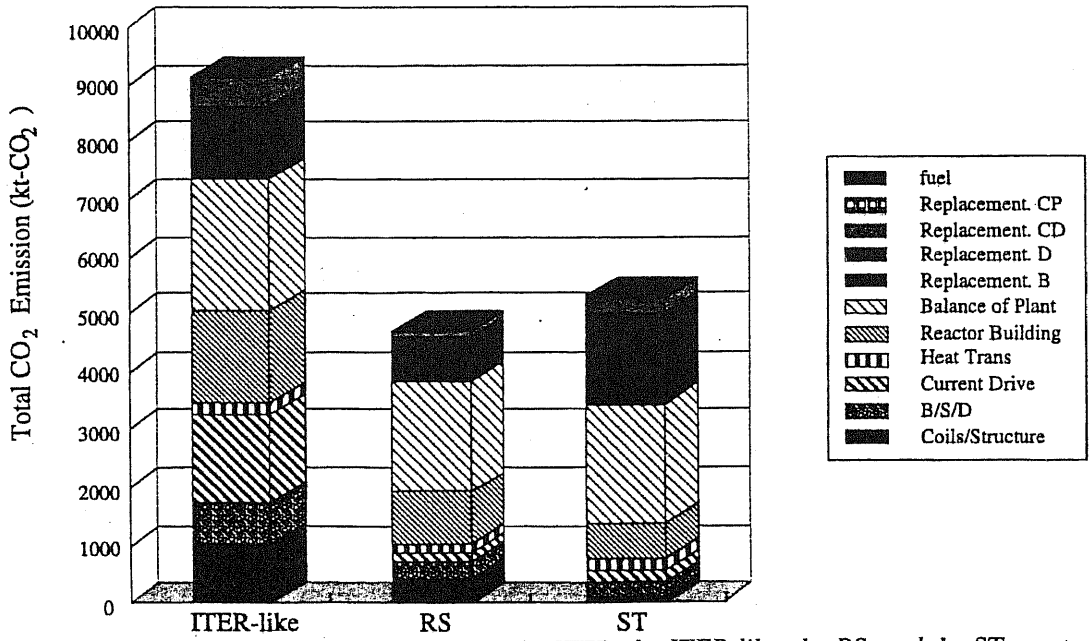

Figure IV-2(d) Comparison of the CO_2 emission for the ITER, the ITER-like, the RS, and the ST reactors. The same tendency can be seen as that observed for the input energy. However, the total CO_2 emission owing to replacement of the ST reactor is larger than that of the RS reactor, which results in the larger CO_2 emission from the ST reactor.

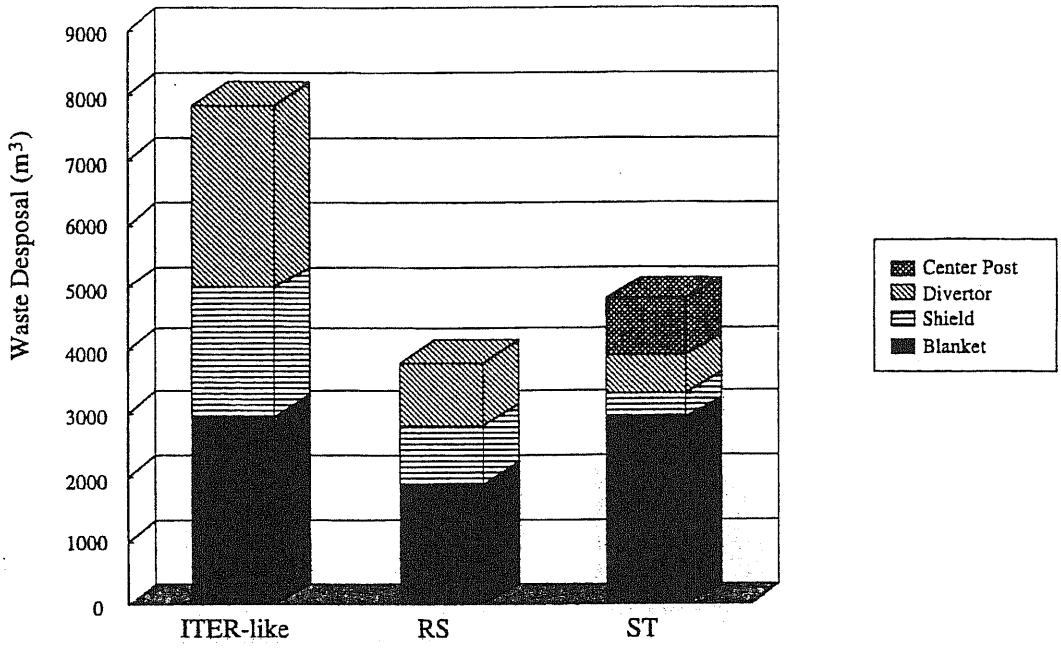

Figure IV-2(e) Comparison of total waste disposal volume disposed within plant life time for the ITER, the ITER-like, the RS, and the ST reactors. The disposal amount volume from the RS reactor is half of that of the ITER-like reactor, which is also smaller by the center post volume from the ST reactor.

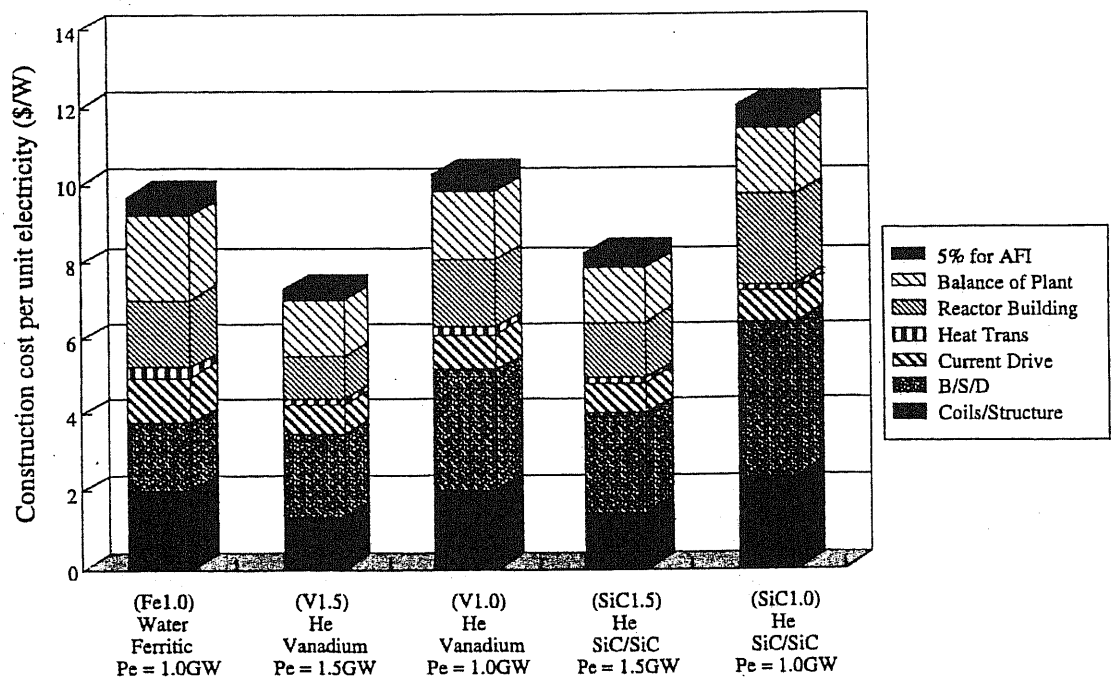

Figure IV-3(a) Comparison of direct construction cost per unit electricity for the structural material variations of Ferrite steel, Vanadium alloy, and SiC of the ITER-like reactor. The direct construction cost per unit electricity is getting larger as Ferrite < Vanadium < SiC. Scale merit is effective for effective for cost down.

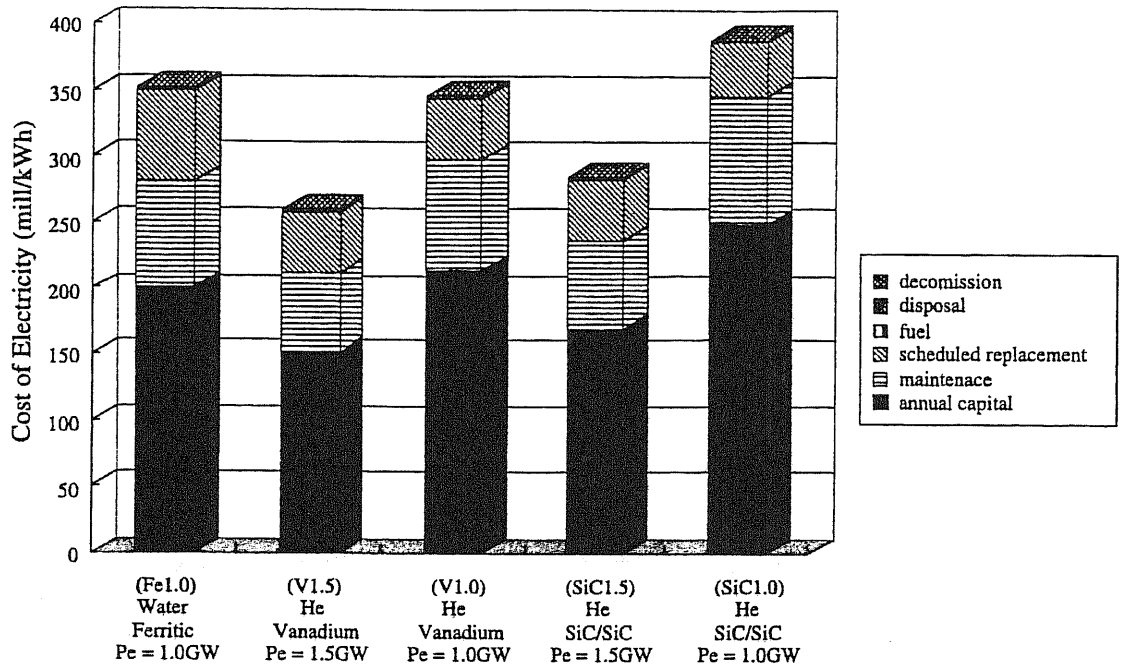

Figure IV-3(b) Comparison of the COE for the structural material variations of Ferrite steel, Vanadium alloy, and SiC of the ITER-like reactor. The tendency is the same of that of the direct construction cost per unit electricity. The reason why the COE of the Vanadium case (V1.0) is a slightly little than that of the Ferrite case (Fe1.0) is that current drive power of (V1.0) case is a little bit smaller than that of the (Fe1.0).

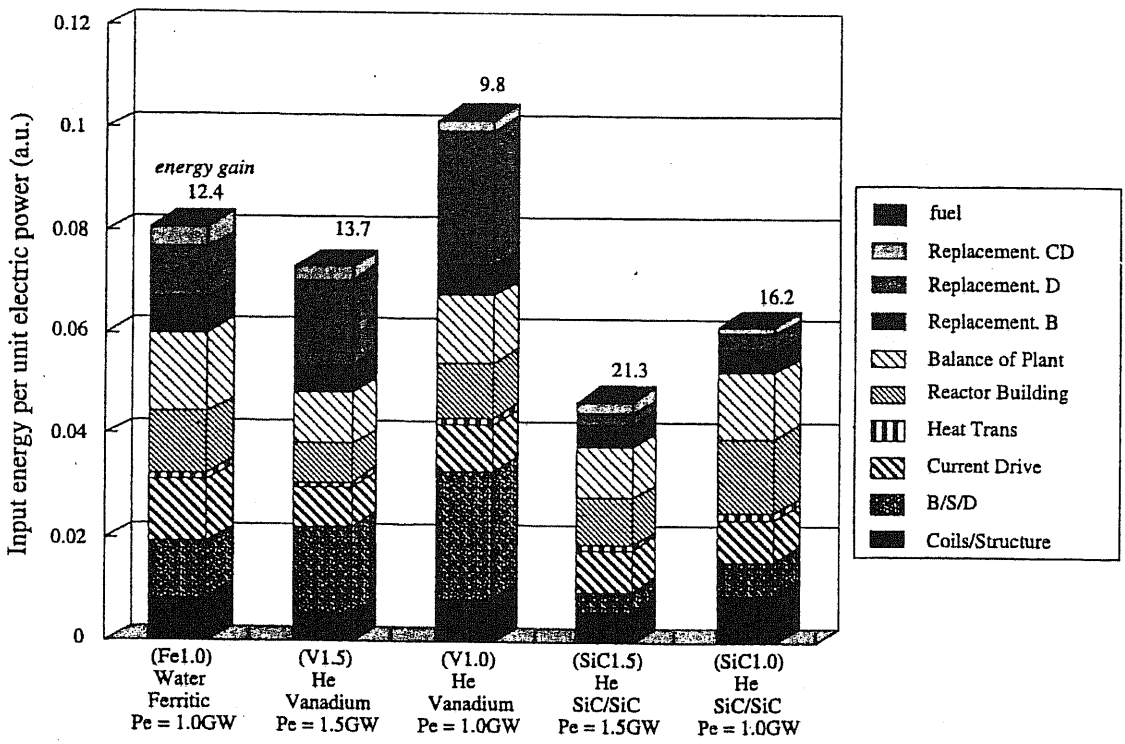

Figure IV-3(c) Comparison of the input energy for the structural material variations of Ferrite steel, Vanadium alloy, and SiC of the ITER-like reactor. The energy gain is getting better as Vanadium < Ferrite < SiC. Although the component volumes of the SiC case are larger than the others, the energy intensity for SiC is smaller than other structural materials.

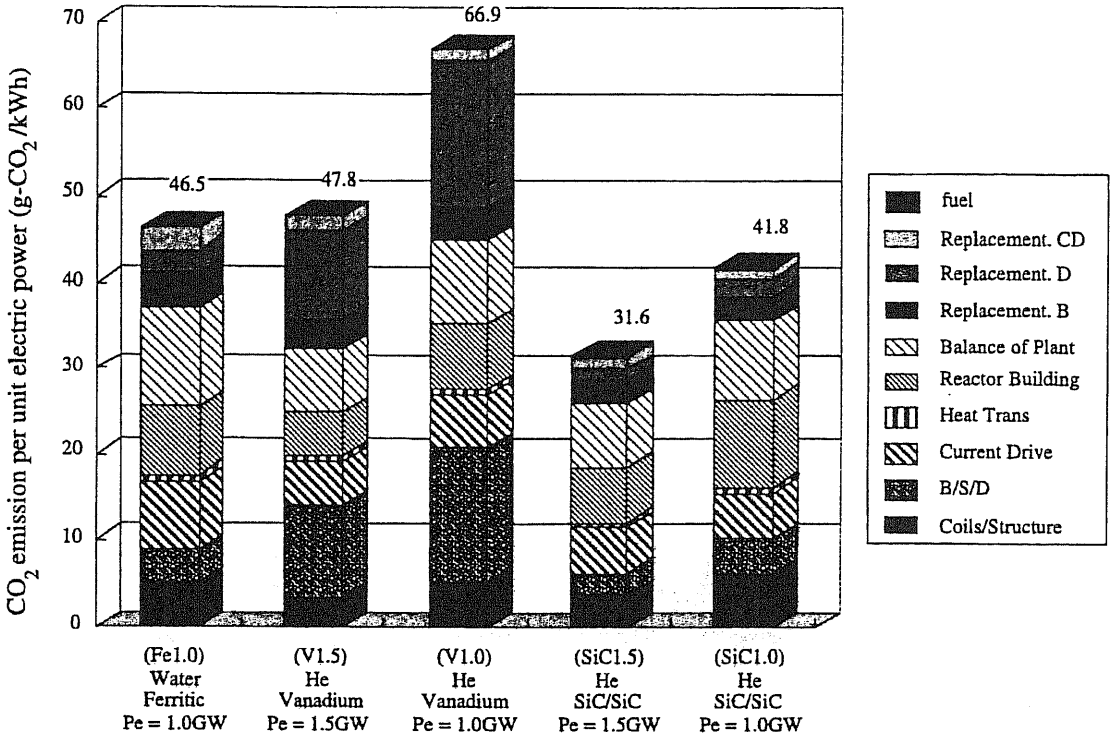

Figure IV-3(d) Comparison of the CO_2 emission for the structural material variations of Ferrite steel, Vanadium alloy, and SiC of the ITER-like reactor. The same tendency can be seen as that observed for the input energy.

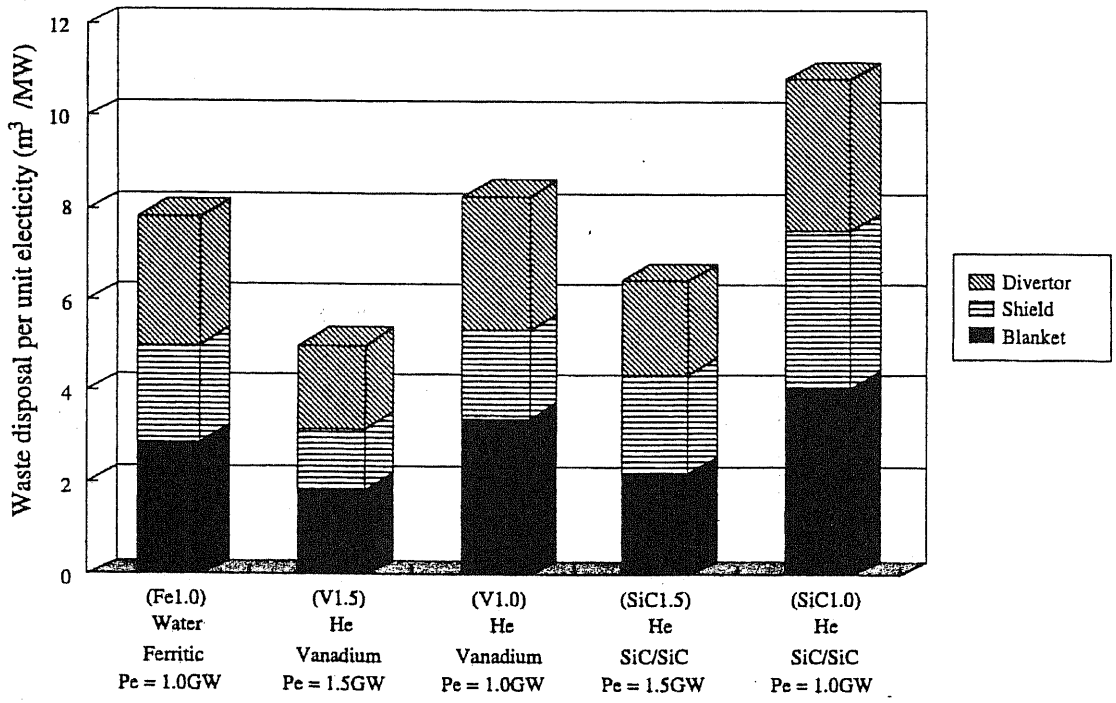

Figure IV-3(e) Comparison of the total radioactive waste disposal after removal from every reactor case of the ITER-like reactor. It cannot be said that the superiority of structural materials in terms of radioactive waste should be discussed only by this result.

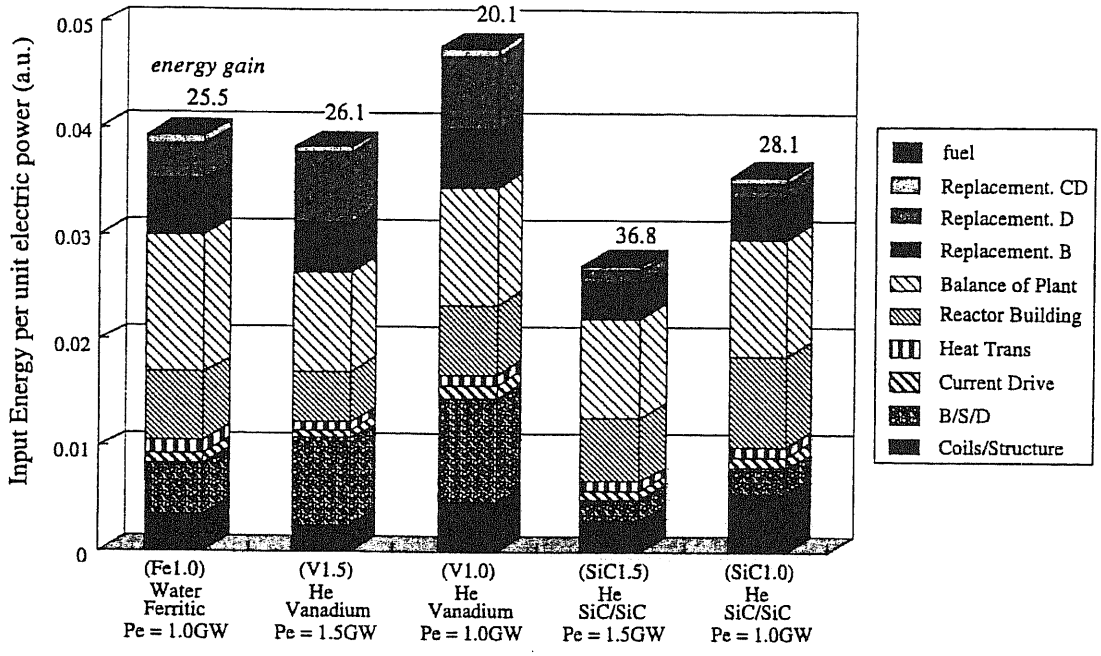

Figure IV-4(a) Comparison of the input energy for the structural material variations of Ferrite steel, Vanadium alloy, and SiC of the RS reactor. The same tendency like the ITER-like reactors are seen, however, the absolute value of these values are larger than those of the ITER-like cases.

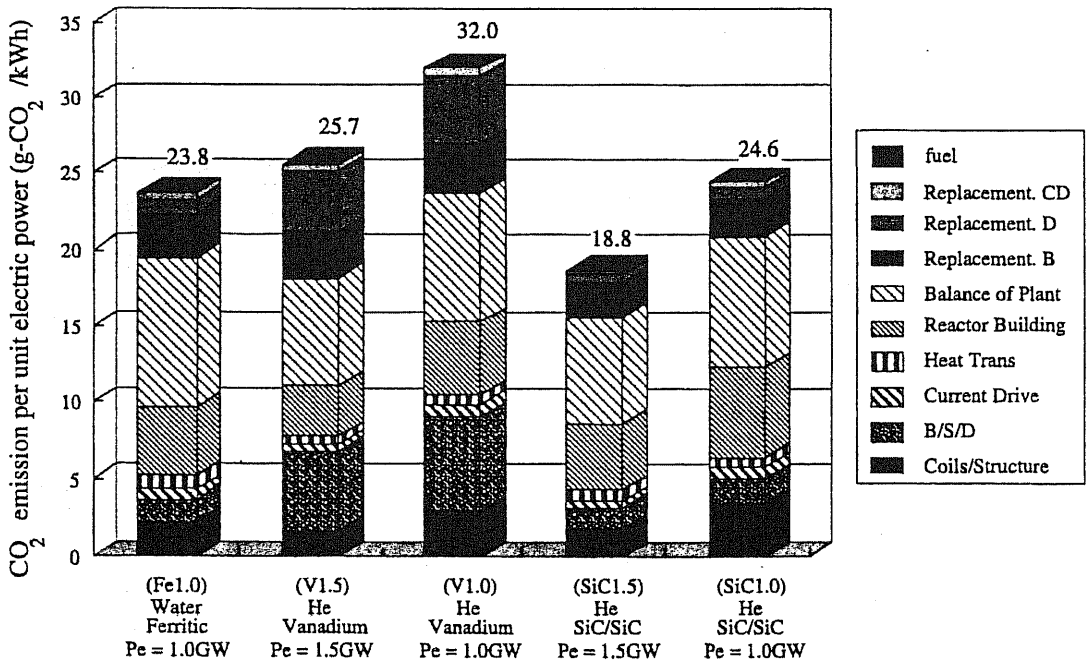

Figure IV-4(b) Comparison of the CO_2 emission for the structural material variations of Ferrite steel, Vanadium alloy, and SiC of the RS reactor. The same tendency can be seen as that observed of the ITER-like reactors. The reason why the (SiC1.0) case is larger than the (Fe1.0) case is because the CO_2 emission from the Coils/Structure is large. This (SiC1.0) case is an ARIES-RS like reactor which has a large superconductor volume than that of the (Fe1.0), which results in the enlargement of the CO_2 emission

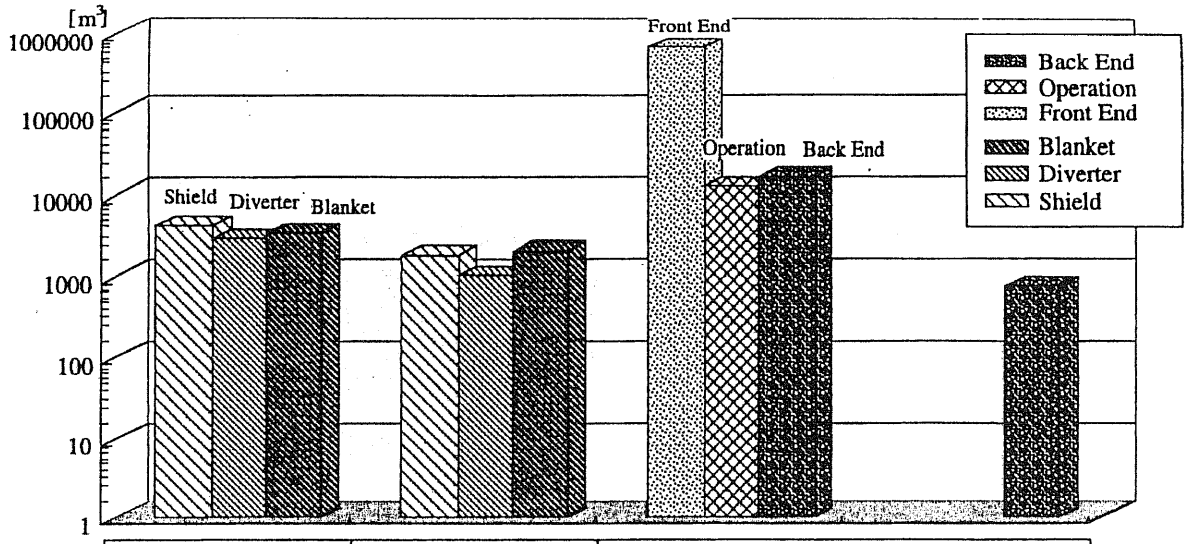

	ITER-like			RS			Fission						
Level	LLW/ILW			LLW/ILW			LLW/ILW			HLW			
	Volume	Radio activity	Dominant Nuclide	Volume	Radio activity	Dominant Nuclide	Volume	Radio activity	Dominant Nuclide	Volume	Radio activity	Dominant Nuclide	
Shield	4.0E+3	~10^{10}	Tritium	1.8E+3	~10^{10}	Tritium	6.4E+5	~10^{8}	^{238}U	0			Front End
Divertor	3.0E+3	~10^{14}		1.0E+3	~10^{14}		1.2+4	10^{10}~10^{12}	^{60}Co	0			Operation
Blanket	3.0E+3	10^{15}~10^{16}		2.0E+3	10^{15}~10^{16}		1.7+4	10^{10}~10^{13}	CP,FP, TRU	7.6E+2	10^{15}~10^{16}	CP,FP, TRU	Back End

Unit: Volume [m³], Radioactivity [Bq/m³]

Figure V Comparison of waste disposal volume among the ITER-like, the RS, and a fission reactor. Data of fission is referred from Ref. [IAEA-Tech366]. Radioactivity data of the fusion are the cases of 100 years cooling span. Data of blanket and shield are referred from Ref.[T.Tabara, AESJ], divertor is referred from Ref.[K.Maki]. Radioactive waste volume of the fusion is calculated by this study. The radioactive waste disposal from the fission reactor is characterized as "huge radioactive waste volume (not less than ~ 6E+5 m³), including long-lived nuclides (such as ^{238}U, TRU), and low radioactivity (as high as 10^{15} ~ 10^{16} even in HLW) ". In contrast, the radioactive waste from the fusion reactor is characterized as "small amount of volume (not more than ~ 1E+4 m³ which is smaller than that from the fission reactors by two orders)", including large fraction of tritium, and high radioactivity (as high as 10^{15} ~ 10^{16} even in 100 years cooling for blanket). There are possibilities, however, to reduce radioactivity by the selection of advanced low activation materials, such as low activation ferrite steel, Vanadium alloy, and SiC etc. The radioactivity can be much reduced by such structural material

5 Summary and Conclusion

The following three quantitative analysis are performed comparing (1) reactor types, (2) structural materials, and (3) other energy sources in light of (1) cost, which is based upon the ITER cost calculation, (2) energy analysis and CO_2 emission, and (3) radioactive waste.

In comparing reactor type, both the RS reactor and the ST reactor can successfully double their properties over those of the ITER-like reactor. In that, construction cost per unit of electricity, the COE, CO_2 emission per unit of electricity, and amount of radioactive waste, are reduced half, while energy gain is doubled. By further reducing the number of components over those of the RS reactor, the ST reactor can reduce costs, input energy, and CO_2 emission of reactor components. However, these properties of the ST reactor are almost identical to those of the RS. This is because the compactness of the ST reactor increases the necessity of replacement by the increse of both the neutron wall load and the necessity of installation of replacement components, which results in increasing cost, input energy, and the CO_2 emission.

In comparing structural material, Ferrite steel becomes expensive, Vanadium bears a relatively lowest radioactive level 100 years after reactor decommission, and SiC performs best in terms of energy gain and CO_2 emission intensity. The drawbacks for the above materials are high radioactive level for Ferrite steel, low energy gain and high CO_2 emission intensity for Vanadium-alloy, and the high cost of SiC. In structural material R&D, the development of low activated structural materials by element tailoring or isotopic tailoring is expected. Following this development, the cost data, energy intensity, and the CO_2 emission intensity of the materials must be obtained and the reactors that use these structural materials can be assessed.

In comparing energy sources, properties of the ITER-like reactor, such as cost, energy gain, and CO_2 emission, are inferior to those of other energy sources, and thus the ITER-like reactor is not attractive as an energy source. The present economic competitiveness of fusion reactors is difficult to be obtained, even if the RS reactor or the ST reactor attains 75 % plant availability. However, the rate of energy gain and the level of CO_2 emission of the RS reactor and the ST reactor are as acceptable as those of a fission reactor (once-through, gas diffusion type) or a hydro-electric generation which are the two most efficient present energy sources. The order of HLW of fusion reactors soon after reactor shutdown, in comparison to that of the fission reactor, is greater by one order than that of the fission reactor. However, the cooling time for the HLW is very short; namely, the duration is estimated to be as short as 100 years. Moreover, the amount of the LLW of the RS reactor and the ST reactor is smaller by two orders than that of the fission reactor.

If we regard the "present tokamak fusion reactor's certification as an energy source" as the "tokamak fusion reactors should be within the range between maximum and minimum value of the other present energy sources in terms of cost, energy gain, and CO_2 emission," the ITER-like reactor fails in these qualifications. However, the RS reactor and the ST reactor, both of which possesses high physics performance, deviates certification except in terms of cost if they can attain 75 % plant availability. Radioactive waste disposal is an inherent disadvantage of fusion reactors; however, it is the fusion reactor's

advantage that their volume and the duration of the radioactivity is smaller and shorter, respectively, than those of the fission reactor.

Therefore, tokamak fusion R&D should proceed, (1) The RS type and the ST type reactors, both of which attain high physics performance, should be developed. (2) More cost reduction should be made using any means. (3) Low activation structural materials which are both low cost and require low input energy should be focused on as the subject materials for R&D. By this R&D, expensive matters and radioactive waste disposal -- crucial drawbacks of tokamak fusion reactors in comparison with other energy sources -- should be overcome by the following two reasons. (I) Tokamak fusion rectors are easily accepted if expensive can be compensated for accepted by electric power industries which will be the tokamak fusion reactors users, or by the public who will be the consumers of electricity. (II) Public acceptance (PA) can easily be obtained if the volume and level of radioactive waste disposals are reduced.

From the viewpoint of energy development policy, it can be summarized this study in the following three points. (1) Tokamak fusion R&D has just entered the stage that high physics performance ($\beta_N \approx 6.5$, H-factor ≈ 4, $f_{bs} \approx 0.8$ at maximum) can be obtained both by experiments and by simulation study. (2) The RS and the ST reactors which attain this advanced physics performance have the possibility of fully satisfying the "present tokamak fusion reactor's certification" in energy gain and CO_2 emission. (3) Possibilities of overcoming the high expensive of the construction cost and/or the COE, and dealing with the problems of the radioactive waste disposal remain problems of physics/engineering R&D and/or material R&D. Since in this study, we did not investigate the requirement conditions for development of tokamak fusion reactors, i.e., the conditions that necessitate tokamak fusion reactors as an energy supply, we do not nor cannot assert that tokamak fusion reactors must be developed absolutely. However, we assert that tokamak fusion R&D is worth continuing their qualification for certification and the possibilities explained (2) and (3).

Part V

Summary, Discussions and conclusions of this thesis

Summary

Fusion energy, which is expected to be one of the means of resolving global environment problems and achieving sustainable development, was evaluated by this thesis in terms of tokamak type reactor that has come closest to achieving adequate confinement methods. The following issues are explained. (1) Progress of plasma physics experiments, reactor design, and evaluation studies. (2) Study of design parameters for minimizing the cost of electricity for "conventional" aspect ratio tokamaks using water as a coolant. (3) Economy, energy analysis, and environmental impacts of tokamak fusion power reactors including ST tokamak.

Part I Introduction

As was mentioned previously, fusion energy is thought to be one of the measures by which sustainable development can be achieved and global environmental problems can be avoided. Fusion energy is expected to be useful as an advanced energy technology, however, although some problems are raised for in relation to the development of fusion energy. Therefore, it is necessary to discuss potential for fusion energy. The goal of this study is to describe the possibilities for making use of fusion energy. The structure of this thesis is also described in this section. The principles and mechanisms of a tokamak fusion reactor are explained.

Part II Progress of plasma physics experiments, reactor design, and evaluation studies

Plasma physics experiments have been carried out in two basic directions. The first set of experiment has attempted to improve the energy confinement time, the other has attempted to improve the attainable beta. By improving energy confinement time regarding several operation modes, bootstrap current, and energy time confinement scaling were obtained. Recently reversed shear experiment were carried out, the results of which will allow for the development of high cost effective reactors. By beta improvement experiments, beta limit scaling was obtained. Moreover, the excellence of ST reactor has been revealed, which will result in the construction of the next ST devices or in the design of cost effective power reactors. By the DT experiments, fusion power of 10.7 MW was obtained. Reliable physics guidelines for self-ignition physics have been compiled. Energy analysis and safety studies as well as economy have been explained. Although these studies have been carried out, the results should be revised in accordance with both reactor designs and data for cost and energy gain.

Part III Study of design parameters for minimizing cost of electricity for "conventional" aspect ratio tokamaks using water as a coolant

In this study, 1 GWe conventional aspect ratio tokamak reactors using water as a coolant are evaluated for three types operations modes; i.e., FS (First Stability), SS (Second Stability), and RS (Reversed Shear). The COE is minimized by sensitivity analysis for each operating mode by using a systems code composed by the ITER physics, three arc approximation constant tension D shape TF coil, and cost calculations based upon the Generomak model. The constraints of the sensitivity analysis are, A = 3.0 ~ 4.5, $R_p \geqq 5$ m, average neutron wall load $\leqq 5$ MW/m^2, $B_{max} \leqq 20$ Tesla and so on. The MHD stability for FS and SS are defined by M.E.Mauel definition. The MHD stability of the RS case was checked for the cost-minimized design point.

The results of the minimizing the COE for each operating mode are followings. (1) In the FS case, β_N is restricted below 3.0 because of the MHD stability. Therefore, the plasma temperature as well as B_{max} have to be increased. The aspect ratio should be increased to obtain bootstrap current even if this increment leads to an increment of reactor size. (2) In the SS case, the safety factor should be raised in order to avoid MHD instability, which results in a very high bootstrap current fraction close to unity. A high bootstrap current fraction results in a low aspect ratio, possibly as low as 3. However, the plasma current as well as fusion power density is so small (by high safety factor) that B_{max} should be raised to compensate for the low fusion power density. (3) In the RS case, since high β_N as well as high f_{bs} can be obtained by a low safety factor, a small B_{max} and small aspect ratio is enough.

In reactor comparison, FS is the most expensive because of a small β_N as well as small f_{bs}, and a high aspect ratio as well as high B_{max}. The SS is more expensive than RS due to a high B_{max}, even if the SS could attain a high β_N as well as high f_{bs}. The reason that the RS is the most cost effective is that a high β_N as well as a high f_{bs} can be obtained by a low safety factor, and B_{max} and the aspect ratio can be reduced. The parameters of this cost minimized RS reactor are aspect ratio 3, elongation 2, B_{max} 13. Therefore, it can be considered that these parameters can preliminary be experimentally tested by the ITER device.

Part IV Economy, energy analysis, and environmental impacts of tokamak fusion power reactors

Economy in the Part III is evaluated by use of a past reactor cost database. The relative cost is certain, although the absolute value is uncertain. Therefore, in this study, the ITER cost calculation method as well as a cost database is applied to determine the power rector's economy. By this evaluation, the present value of fusion reactors, not the future value can be evaluated. Based upon the volume and weight of reactor components, economy, energy gain, carbon dioxide (CO_2) emission, and waste disposal of tokamak fusion power reactors are evaluated in this study. We performed the following three quantitative analysis comparing (1) reactor types, (2) structural materials, and (3) other energy sources in light of (a) cost, which is based upon the ITER cost calculation, (b) energy analysis and CO_2 emission, and (c) radioactive waste.

In comparing reactor type, both the RS reactor and the ST reactor can successfully doubles their properties over those of the ITER-like reactor. In that, construction cost per unit of electricity, the COE, CO_2 emission per unit of electricity, and amount of radioactive waste, are reduced half, while energy gain is doubled. By further reducing the number of components over those of the RS reactor, the ST reactor can reduce costs, input energy, and CO_2 emission of reactor components. However, these properties of the ST reactor are almost identical to those of the RS. This is because the compactness of the ST reactor increases the necessity of replacement by increment of both the neutron wall load and the necessity of installation of replacement components, which results in increasing cost, input energy, and CO_2 emission.

In comparing structural material, Ferrite steel becomes inexpensive, Vanadium bears the relatively lowest radioactive level 100 years after reactor decommission, and SiC performs best in terms of energy gain and CO_2 emission intensity. The drawbacks for the above materials are high radioactive level for Ferrite steel, low energy gain and high CO_2 emission intensity for Vanadium-alloy, and the high cost of SiC. In structural material R&D, the development of low activated structural materials by element tailoring or isotopic tailoring is expected. Following this development, the cost data, energy intensity, and CO_2 emission intensity of the materials must be obtained and the reactors that use these structural materials can be assessed.

In comparing energy sources, properties of the ITER-like reactor, such as cost, energy gain, and CO_2 emission, are inferior to those of other energy sources, and thus the ITER-like reactor is not attractive as an energy source. The present economic competitiveness of fusion reactors is difficult to be obtained, even if the RS or the ST reactors attains 75 % plant availability. However, the rate of energy gain and the level of CO_2 emission of the RS and the ST reactors are as desirable as those of a fission reactor (once-through, gas diffusion type) or a hydro-electric generation which are the two most efficient present energy sources. The order of HLW of fusion reactors soon after reactor shutdown, in comparison to that of the fission reactor, is greater in one order than that of the fission reactor. However, the cooling time for the HLW is very short; namely, the duration is estimated to be as short as 100 years. Moreover, the amount of the LLW of the RS and the ST reactors is smaller in two orders than that of the fission reactor.

If we regard the "present tokamak fusion reactor's certification as an energy source" as the "tokamak fusion reactors should be within the range between maximum and minimum value of the other present energy sources in terms of cost, energy gain, and CO_2 emission," the ITER-like reactor fails in these qualifications. However, the RS reactor and the ST reactor, both of which possesses high physics performance, deviates certification except in terms of cost if they can attain 75 % plant availability. Radioactive waste disposal is an inherent disadvantage of fusion reactors; however, it is the fusion reactor's advantage that their volume and the duration of the radioactivity is smaller and shorter, respectively, than those of the fission reactor.

Therefore, tokamak fusion R&D should proceed, (1) The RS type and the ST type reactors, both of which attain high physics performance, should be developed. (2) More cost reduction should be made using any means. (3) Low activation structural materials which are both low cost and require low input energy should be focused on as the subject materials for R&D. By this R&D, expensive matters and radioactive waste disposal -- crucial drawbacks of tokamak fusion reactors in comparison with other energy sources -- should be overcome the following two reasons. (I) Tokamak fusion rectors are easily accepted if expensive can be compensated for accepted by electric power industries which will be the tokamak fusion reactors users, or by the public who will be the consumers of electricity. (II) Public acceptance (PA) can easily be obtained if the volume and level of radioactive waste disposals are reduced.

The viewpoint of energy development policy, it can be summarized this study in the following three points. (1) Tokamak fusion R&D has just entered the stage that high physics performance ($\beta_N \approx 6.5$, H-factor ≈ 4, $f_{bs} \approx 0.8$ at maximum) can be obtained both by experimentally and by simulation study. (2) The RS and the ST reactors which attain this advanced physics performance have the possibility of fully satisfying the "present tokamak fusion reactor's certification" in energy gain and CO_2 emission. (3) Possibilities of overcoming the high expensive of the construction cost and/or the COE, and dealing with the problems of the radioactive waste disposal remain problems of physics/engineering R&D and/or material R&D. Since in this study, we did not investigate the requirement conditions for development of tokamak fusion reactors, i.e., the conditions that necessitate tokamak fusion reactors as an energy supply, we do not nor cannot assert that tokamak fusion reactors must be developed absolutely. However, we assert that tokamak fusion R&D is worth continuing their qualification for certification and the possibilities explained (2) and (3).

Discussions and Conclusions

As explained in Part II, tokamak fusion has reached the point of being able to predict self ignition and conceptual designs for realizable power reactors are now available after 50 years of R&D. However, the burning time as well as the fusion output power of the ITER is higher by three orders than those of present TFTR. Moreover, several uncertainties remain. For one, it is not so easy to sustain self ignition conditions for 1000 sec. And even if the ITER-level power reactor can be realized, its economy, energy gain, and CO_2 emission are not so excellent than fission reactors, but better than PV. However, the ITER is based upon conservative physics; if the RS reactor or the ST reactor using advanced physics that based upon present attainable physics data is possible, even if the economies of these rectors are not still effective, the energy gain and CO_2 emission would be excellent. Radioactive waste from fusion reactors (the ITER-like, the RS, and the ST) can be reduced by at least two orders compared to fission reactors. More reductions from fusion reactors would be possible by use of advanced low activation materials. Therefore, the RS and the ST reactor have excellent properties as an energy source. Moreover, some study have suggested that it is worthwhile to proceed with tokamak fusion R&D because (1) physics performance, engineering, and material improvement, as well as cost reduction can be expected, (2) the advanced RS reactor and the ST reactor can have excellent environmental compatible.

However, it cannot be asserted that fusion R&D must proceeded actively because this study does not analyze positive conditions for proceeding with fusion R&D. Prudent decision must be made when huge amount of money are required. This study quantitatively demonstrates that fusion energy is clean, however, it does not treat safety and resource availability as they are beyond our methodology. Hence, "Clean, safe, and eternal" can not be assured by this study except for the word "clean". It should be admitted that tokamak fusion reactors can contribute global environmental warming because of the small CO_2 emission intensity. Other papers should be referred to regarding to the safety aspects of fusion. It is uncertain as to whether fusion reactors can contribute to the "sustainable development problem" because the resource availability problem is left for future study. Fusion research should focus on the contribution of fusion energy to the "sustainable development problem".

References, Appendix, and List of Publications

References

[A-SSTR] Kikuchi, M., "An Economically competitive fusion reactor", Fusion Technology, **30**(1996)1631.

[AESJ] Atomic Energy Society of Japan," Enhancement of Reactor Technology for Fusion Demonstration Reactors", JAERI Itaku Kenkyu Report, 1995, (in Japanese).

[ARIES-I] CONN, R.W., et al., "ARIES-I, a steady-state, first-stability tokamak reactor with enhanced safety and environmental features", Plasma Physics and Controlled Nuclear Fusion Research 1990, IAEA, Vienna, **3** (1990) 659.

[ARIES-RS] F. Najmabadi and the ARIES team, "Overview of ARIES-RS Tokamak Fusion Power Plant", in the 4th International Conference on Fusion Nuclear Technology (ISFNT-4), Fusion Engineering Division of Atomic Energy Society of Japan and Nuclear Engineering Research Laboratory of The University of Tokyo, Tokyo (1997).

[ARIES-ST] R.L.Miller for the ARIES Team, "Design-Point determination for the Commercial Spherical Tokamak, ARIES-ST", 17th Symposium on Fusion Engineering (17th IEEE/NPSS SOFE), San Diego, 1997.

[ASC] Najmabadi, F., et al., "The ARIES-II and IV Second Stability Tokamak Reactors", University of California Los Angels report, UCLA-PPG-1461 (to be published).

[ASDEX] ASDEX team, "The H-mode of ASDEX", Nuclear Fusion **29**(1989)1959.

[BATHKE, C.G., 95] BATHKE, C.G., "A preliminary systems assessment of the Starlite demo candidates", 16th Symposium on Fusion Engineering 1995 (SOFE-16).

[BATHKE, C.G., 96] BATHKE, C.G., and the ARIES team, "A system assessment of the five Starlite tokamak power plants", in the 12th ANS topical meeting on the Technology of Fusion Energy, ANS, Reno (1996) 1636.

[BELL, M.G.] BELL, M.G., et al., "Overview of DT results from TFTR", Nuclear Fusion **35**(1995)1429.

[BICKERTON, R.J.] BICKERTON, R.J., CONNOR, J.W., and TAYLOR, J.B., Nat. Phys. Sci. **229**(1971)110.

[BONDERSON, A.] BONDERSON, A., and WARD, D.J., "Stabilization of external modes in Tokamaks by resistive walls and plasma rotation", Physical Review Letters **72**(1994)2709.

[BORRASS, K.] BORRASS, K., and SOLL, M., "SUPERCOIL: A model for the computational design of tokamaks", Nuclear Engineering and Design/Fusion, **4**(1986)21.

[BOUCHER, D.] BOUCHER, D., et al., "ITER scenarios including non-inductive steady state operation", 16th IAEA Fusion Energy Conference, Montreal (1996), IAEA-CN-64/FP-22.

[BUNDE, R.] BUNDE, R., "The potential net energy gain from DT fusion power plants", Nuclear Engineering and Design/Fusion **3** (1985) 1.

[BUSH, C.E] BUSH, C.E., et al., "Peaked density profiles in circular-limiter H modes on the TFTR tokamak", Physical Review Letters **65**(1990)424.

[CALLIS, C.D.] CALLIS, C.D., et al., "Non-inductively driven currents in JET", Nuclear Fusion **29**(1989)563.

[CHAPMAN, P.F.] CHAPMAN, P.F., "Energy analysis of nuclear power stations", Energy Policy **3** (1975)285.

[COHEN, B.L.] COHEN, B.L., "THE NUCLEAR ENERGY OPTION -- An Alternative for the 90s", 1994 (Japanese Version, in Japanese).

[COHN, D.R.] COHN, D.R., et al., "Characteristics of high-density tokamak ignition reactors", Nucler Fusion **16**(1976)31.

[CORDEY, J.G.] CORDEY, J.G., et al., "Bootstrap current theory and experimental evidence", Plasma Physics and Controlled Fusion, **30** (1988) 1625.

[CRIEPI-T12] CRIEPI report T12, "Prospects of tokamak fusion power reactor's utilization", 1989, (in Japanese).

[Culhum-MKII] HANCOX, R., "Reactor costs and maintenance, with reference to the Culhum Mark II conceptual tokamak reactor design", et al., IAEA-CN-35/I1-1.

[DREAM] NISHIO, S., et al., Fusion Engineering and Design **25** (1994) 289.

[ESECOM] HOLDREN, J.P., et al., "Exploring the competitive potential of magnetic fusion energy: the interaction of economics with safety and environmental characteristics", Fusion Technology **13**(1988)7.

[EnergyData97] Agency of Natural Resources and Energy, "Natural Resources and Energy Data book 1997", Denryoku shinpo-sya, 1997, (in Japanese).

[FUJITA, T.,] FUJITA, T., et al., Physical Review Letters **78**(1997)2377.

[GALAMBOS, J.D.] GALAMBOS, J.D., et al., "Commercial tokamak reactor potential with advanced tokamak operation", Nuclear Fusion **35**(1995)551.

[GENEROMAK] SHEFFIELD, J., et al., "Cost assessment of a generic magnetic fusion reactor", Fusion Technology **9**(1986)199.

[GOLDSTON, R.] GOLDSTON, R., et al., "Advanced tokamak physics – status and prospects", Plasma Physics Controlled Fusion **36**(1994)B213.

[GREENWALD, M.] GREENWALD, M., et al., Nuclear Fusion **28**(1988)2199.

[GRUBER, O.] GRUBER, O., et al., "MHD stability and transport of beam heated ASDEX discharges in the vicinity of the beta limit", Plasma Physics and Controlled Nuclear Fusion Research 1986, IAEA, Vienna, **1** (1985)357.

[HARMS, A.A.] HARMS, A.A.,/ HEINDLER, M., "Nuclear Energy Synergetics", Baifu-kan, 1986 (in Japanese).

[HATAYAMA, A.] HATAYAMA, A., et al., "Basic requirement for a 1000-MW(electric) class tokamak fusion-fission hybrid reactor and its blanket concept", Fusion Technology **26** (1994) 27.

[HAWRYLUK, R.J. 87] HAWRYLUK, R.J., et al., "TFTR plasma regimes", International Conference on Plasma Physics and Controlled Nuclear Fusion Research 1986, IAEA, Vienna, **1**(1987)51.

[HAWRYLUK, R.J. 95] HAWRYLUK, R.J., et al., "Review of Recent D-T experiments from TFTR", International Conference on Plasma Physics and Controlled Nuclear Fusion Research 1994, IAEA, Vienna, **1**(1995)11.

[HENDER, T.C.] HENDER, T.C., et al., "Tight aspect ratio tokamak reactors", 14th International

Conference on Plasma Physics and Controlled Nuclear Fusion Research 1992, IAEA-CN-56/G-2-5.

[HONDO, H.] HONDO, H., "Energy Requirements and CO_2 Emissions in the Production of Goods and Services: Application of an Input-Output Table to Life Cycle Analysis", Y95013, Socio-Economic Research Center, Central Research Institute of Electric Power Industry (1996), (in Japanese).

[HSE] BRUHNS, H., et al., "Study of the low aspect ratio limit tokamak in the Heidelberg spheromak experiment", Nuclear Fusion **27**(1987)2178.

[HUGON, M.] HUGON, M., at al., "Shear reversal and MHD activity during pellet enhanced performance pulses in JET", Nuclear Fusion **32** (1992)33.

[IAEA-Safety111] "Classification of Radioactive Waste : A Safety Guide", IAEA Safety Series No.111-G-1.1 (1994).

[IAEA-TCMII] "Conference and Symposia, fusion reactor design-II", Nuclear Fusion **18**(1978)985.

[IAEA-TCMI] "Fusion reactor design problems", Nuclear Fusion **14**(1974)281.

[IAEA-Tech101] Technical Report Series No.101,"Standardization of Radioactive Waste Categories", IAEA, Vienna, 1970.

[IAEA-Tech366] Technical Report Series No.366,"Assessment and Comparison of Waste Management System Costs for Nuclear and Other Energy Sources", IAEA, Vienna, 1994.

[IDLT-DEMO] INOUE, N., et al., "Feasibility study for an inductively operated day-long tokamak reactor", Plasma Physics and Controlled Nuclear Fusion Research 1992, IAEA, Vienna, **3**(1992) 347.

[IFT] Institute for Future Technology, "Development of Economy Assessment Method",1992, (in Japanese).

[ISHIDA, S. 91] ISHIDA, S., et al., "High poloidal beta experiments with a hot ion enhanced confinement regime in the JT-60U", International Conference on Plasma Physics and Controlled Nuclear Fusion Research 1990, IAEA, Vienna, **1**(1991)195.

[ISHIDA, S. 92a] ISHIDA, S., et al., "Observation of a fast beta collapse during high poloidal-beta discharges in JT-60", Physical Review Letters, **68**(1992)1531.

[ISHIDA, S. 92b] ISHIDA, S., et al., "Enhanced confinement of high bootstrap current discharges in JT-60U", International Conference on Plasma Physics and Controlled Nuclear Fusion Research 1992, IAEA-CN-56/A-3-5.

[ITER-16thIAEA] AYMAR, R., et al., "ITER project: a physics and technology experiment", 16th IAEA Fusion Energy Conference 1996, IAEA-CN-64/O-1-1.

[ITER-DDR] "Technical basis for ITER design detailed design report, cost review and safety analysis (DDR)", IAEA, Vienna (1997).

[ITER-EDA] ITER EDA Documentation Series , IAEA, Vienna (1992).

[ITER-IDR] "Technical Basis for the ITER Interim Design Report, Cost Review and Safety Analysis", ITER Project Cost Estimate, IAEA, Vienna (1996).

[ITER-PGL] UCKAN, N.A., and ITER Physics Group, "ITER Physics design guidelines:1989", ITER Documentation Series, No.10, IAEA, Vienna (1990).

[ITER-TAC4] "Detail of the ITER Outline Design Report, construction and operation", San Diego Joint Work Site, (1994).

[JACKSON, G.L.] JACKSON, G.L., et al., "Regime of very high confinement in the boronized DIII-D tokamak", Physical Review Letters, **67**(1991)3098.

[JAIF] Japan Atomic Industry Forum, "Nuclear Annual, 1994 version", (in Japanese).

[JASSBY, D.L.,] JASSBY, D.L., and KATSURAI, M., "Fuel provision for nonbreeding deuterium-tritium fusion reactors", Journal of Fusion Energy **2**(1982)197.

[JET89a] JET team, International Conference on Plasma Physics and Controlled Nuclear Fusion Research 1988, IAEA, Vienna, **1**(1989)41.

[JET89b] JET Team, "Heating of peaked density profiles produced by pellet injection in JET", International Conference on Plasma Physics and Controlled Nuclear Fusion Research 1988, IAEA, Vienna, **1**(1989)215.

[JET92] JET team, "Fusion energy production from a deuterium-tritium plasma in the JET tokamak", Nuclear Fusion **32**(1992)187.

[JOHNSON, D.] JOHNSON, D., et al., "High-beta experiments with neutral-beam injection on PDX", International Conference on Plasma Physics and Controlled Nuclear Fusion Research 1982, **1**(1983)9.

[JRIA] Japan Radio Isotope Association, "Isotope handbook", 1990, (in Japanese).

[JT-60U-NBI] NBI Facility Division, "Design Study of a Negative-ion Based NBI System for JT-60U", JAERI-M 94-072, 1994, (in Japanese).

[JT-60U97] FUJITA, T., et al., "Effects of negative magnetic shear in fusion plasma confinement (1) a review of experimental studies", Journal of Plasma Fusion Research, **73** (1997)549 (in Japanese).

[KAMADA, Y.] KAMADA, Y., et al., "Steady state high performance in JT-60U", International Conference on Plasma Physics and Controlled Nuclear Fusion Research 1994, IAEA, Vienna, **1**(1995) 651.

[KAYA, Y.] KAYA, Y., "Energy Analysis", Denryoku shinpo-sya, 1980, (in Japanese).

[KAYE, S.M. 85a] KAYE, S.M., "A review of energy confinement and local transport scaling results in neutral-beam-heated tokamaks", Physics of Fluids **28**(1985)2327.

[KAYE, S.M. 85b] KAYE, S.M. and GOLDSTON, R.J., "Global energy confinement scaling for neutral-beam-heated tokamaks", Nuclear Fusion **25**(1985)65.

[KAZIMI, M.S.] KAZIMI, M.S., "Safety aspects of fusion", Nuclear Fusion **24**(1984)1461.

[KESSEL, C.] KESSEL, C., et al., "Improved plasma performance in tokamaks with negative magnetic shear", Physical Revew Letters, **68**(1994)1212.

[KIKUCHI, M.] KIKUCHI, M., "Steady state tokamak reactor based on the bootstrap current", Nuclear Fusion **30**(1990)265.

[KOIDE, Y.] KOIDE, Y., et al., "Improved confinement and transport barrier in the JT-60U high β_p H mode", International Conference on Plasma Physics and Controlled Nuclear Fusion Research 1994, IAEA, Vienna, **1**(1995) 199.

[KOZAKI, Y.] KOZAKI, Y., "Analysis for realization of fusion reactors", The Institute for Future Technology, 1978, unpublished, (in Japanese).

[KRAKOWSKI, R.A.] KRAKOWSKI, R.A., and DELENE, J.G., "Connection between physics and

economics for tokamak fusion power plants", Journal of Fusion Energy **7**(1988)49.

[LAZARUS, E.A., 91] LAZARUS, E.A., et al., "Higher beta at higher elongation in the DIII-D tokamak", Physics Fluids B, **4** (1991)2220.

[LAZARUS, E.A., 96] LAZARUS, E.A., et al., 16th IAEA Fusion Energy Conference 1996, A1-2.

[LEVINTON, F.M. 89] LEVINTON, F.M., et al., "Magnetic Field pitch-angle measurements in the PBX-M tokamak using the motional Stark effect", Physical Review Letters, **63**(1989)2060.

[LEVINTON, F.M. 95] LEVINTON, F.M., et al., "Improved confinement with reversed magnetic shear in TFTR", Physical Review Letters, **75**(1995)4417.

[LUCKHARDT, S.C.] LUCKHARDT, S.C., et al, "Production and maintenance of high poloidal beta tokamak plasmas by means of rf current drive", Physical Review Letters **27**(1989)1508.

[MAIN REPORT] PEASE, R.S., et al., Main Report by the EEF-study group, Brussels, 1989.

[MAKI, K.,] MAKI, K., private communication.

[MANICKAM, J.] MANICKAM, J., et al., "The prospects for magnetohydrodynamic stability in advanced tokamak regimes", Phys. Plasmas **1**(1994)1601.

[MARCUS, F.B.] MARCUS, F.B., et al., "Neutron emission profile measurements during the first tritium experiments at JET", Nuclear Fusion, **33**(1993)1325.

[MAUEL, M.E.] MAUEL, M.E., "The use of scaling laws for the design of high beta tokamaks", Nuclear Fusion **27** (1987) 313.

[MEADOWS, D.H.] MEADOWS, D.H., et al., "Glowth to the Limit", Diamond-sya,1972 (jn Japanese).

[MILLER, R.L. 97] R.L.Miller for the ARIES Team, "Economic goals and requirements for competitive fusion energy", in 4th International Symposium on Fusion Nuclear Technology (Abstracts of the ISFNT-4), Fusion Engineering Division of Atomic Energy Society of Japan and Nuclear Engineering Research Laboratory of The University of Tokyo, Tokyo (1997).

[MITI] "Vision of global environment", Research Institute of Industrial Trade and Industry, 1997, (in Japanese).

[MIYAMOTO, K., 96] MIYAMOTO, K., "Physics researches for attaining nuclear fusion", Journal of Physical Society of Japan, **51**(1996)549 (in Japanese).

[MIYAMOTO, K.] MIYAMOTO, K., "Introduction to Plasma physics", Iwanami shoten, 1991 (in Japanese).

[MOMOTA, H.] MOMOTA, H., et al., "Research and Development of Advanced Fuel Nuclear Fusion", Journal of the Atomic Energy Society of Japan, **38**(1996)11 (in Japanese).

[MORI, M.] MORI, M., et al., "Achievement of high fusion triple product in the JT-60U high βp H mode", Nuclear Fusion, **34**(1994)1045.

[MORI, S.] Global Industrial and Social Progress Research Institute, "Status of Sustainability –2", 1996, (in Japanese).

[MORINAGA, H.] MORINAGA, H., "Stop nuclear rectors and revise solar power",Soshisya,1997, (in Japanese).

[MORITA, A.] "Expermental studies of equilibria and stabilities of low aspect ratio tokamaks", Ph.D Thesis, The University of Tokyo 1995.

[MORITA, T.,&MATSUOKA, Y.,] Society for Environmental Economics and Policy Studies, "Frontier of Society for Environmental Economics and Policy Studies", Toyo Keizai Shinpo-sya,1996, (in Japanese).

[MURAKAMI, M.] MURAKAMI, M., et al., "Neutral-beam injection experiments in the ISX-B tokamak", Plasma Physics and Controlled Nuclear Fusion Research 1980, IAEA, Vienna, **2**(1981)377.

[MUROTA, T.] MUROTA, T., "Applied Economics series 3; Energy", Kyoiku-sya,1984, (in Japanese).

[McGUIRE, K.] McGUIRE, K., et al., "Divertor and scoop limiter experiments on PDX", Plasma Physics and Controlled Nuclear Fusion Research 1984, IAEA, Vienna, **1**(1985)117.

[NISHITANI, T.,&SHIMADA, R.,] NISHITANI, T.,& SHIMADA, R., "TFTR DT experiments" Journal of Plasma and Fusion Research, **71**(1995)212 (in Japanese).

[OGAWA, Y., 94] OGAWA, Y., "The reasons why plasma experimental devices are enlargen.", Journal of Physical Society of Japan, **49**(1994)887(in Japanese).

[OGAWA, Y., 96] OGAWA, Y., "Operation Scenario and Burning Control for ITER Plasma", Journal of Plasma and Fusion Research, **72**(1996)727 (in Japanese).

[OGAWA, Y.] OGAWA, Y., et al., "Advanced design of a pulsed tokamak fusion reactor", International Conference on Plasma Physics and Controlled Nuclear Fusion Research 1994, IAEA-CN-60/F-P-8.

[OHI, K.,] OHI, K., private communication.

[OKABAYASHI, M.] OKABAYASHI, M., et al., "Studies of bean-shaped tokamaks and beta limits for reactor design", Plasma Physics and Controlled Nuclear Fusion Research 1984, IAEA, Vienna, **1**(1985)229.

[OKANO, K. 90] OKANO, K., et al, "Self-consistent analysis of steady state tokamaks sustained by beam-driven and bootstrap currents", Plasma Physics and Controlled Fusion, **32** (1990) 225.

[OKANO, K. 93] OKANO, K. and OGAWA, Y., "A necessary condition to achieve $q_0 > 1$ in a long pulse tokamak reactor", Journal of Plasma and Fusion Research, **69** (1993) 968.

[OKANO, K. 97a] OKANO, K., et al, "Study of a compact reversed shear tokamak reactor", in 4th International Symposium on Fusion Nuclear Technology (Abstracts of the ISFNT-4), Fusion Engineering Division of Atomic Energy Society of Japan and Nuclear Engineering Research Laboratory of The University of Tokyo, Tokyo (1997) 246.

[OKANO, K. 97b] OKANO, K., "Compact Reversed Shear Tokamak", AESJ **39**(1997)431 (in Japanese).

[OKANO, K. 97c] OKANO, K., et al., "A Compact Reversed Shear Tokamak Reactor Sustained by Beam Driven Currents" 17th Symposium on Fusion Engieering, SOFE-17, San Diego, Oct. 1997.

[PEARCE, D.W.] PEARCE, D., et al., "Blueprint for a green economy", Diamond-sya, 1994 (Japanese version, in Japanese).

[PEARS, W.R. 85] PEARS, W.R., et al., "Demo and FCTR Parameters", NET report No.41, 1985.

[PEARS, W.R. 86a] PEARS, W.R., et al., "Prototype Commercial-Sized Reactor PCSR-E", NET report No.67, 1986.

[PEARS, W.R. 86b] PEARS, W.R., et al., "The SCAN-2 Cost Model", NET report No.62, 1986.

[PENG, Y.K.-M. 85] PENG, Y.K.-M., et al., "Spherical torus: an approach to compact fusion at low field –

[PENG, Y.K.-M. 85] PENG, Y.K.-M., et al., "Spherical torus: an approach to compact fusion at low field – initial ignition assessments*", Fusion Technology **8**(1985)338.

[PENG, Y.K.-M. 86] PENG, Y.K.-M., and Strickler, D.J., "Features of spherical torus plasmas", Nuclear Fusion **26**(1986)769.

[PENG, Y.K.-M. 90] PENG, Y.K.-M., and Hickes, J.B., "Engineering feasibility of tight aspect ratio tokamak (spherical torus) reactors", Fusion Technology 1990, **2**(1991)1287.

[PENG, Y.K.-M. 92] PENG, Y.K.-M., et al., "Small tokamak for fusion technology testing", Fusion Technology **21**(1992)1729.

[PENG, Y.K.-M. 95] PENG, Y.K.-M., "Prospects and status of low-aspect-ratio tokamaks", Transaction of Fusion Technology **27**(1995)138.

[PENG, Y.K.-M. 96] PENG, Y.K.-M., et al., "Design assumption and basis for small D-T-fueled spherical tokamak (ST) fusion core", Fusion Technology **30**(1996)1372.

[PERKINS F.W.,] PERKINS, F.W., "Nondimensional transport scaling in the Tokamak Fusion Test Reactor: Is tokamak transport Bohm or gyro-Bohm?", Physics of Fluids **B5**(1993)477.

[PFIRSCH, D.,] PFIRSCH, D., AND SCHMITTER, K., "On the economic prospects of nuclear fusion with tokamaks", Fusion Technology **15**(1988)1471.

[PNL78] SHULTE, S.C., et al., "Fusion Reactor Design Studies-Standard Accounts for Cost Estimates", PNL-2648(1978).

[PNL79] SHULTE, S.C., et al., "Fusion Reactor Design Studies-Standard Unit Costs and Cost Scaling Rules", PNL-2648(1978).

[PULSAR] NAJMABADI, F., et al., "The PULSAR Tokamak Reactor Study", University of California San Diego Report (to be published). NAJMABADI, F., and the ARIES Team, "Overview of PULSAR Study: A Pulsed Tokamak Fusion Power Plant", US-Japan Workshop on Power Reactor Studies (Q185), March 1994, UCSD, San-Diego

[RAMOS, J.J. 91a] RAMOS, J.J., "Complete macroscopic stabilization of tokamak plasmas", Physics

[RAMOS, J.J. 91b] RAMOS, J.J., "Theory of the tokamak beta limit and implication for second stability", Phys. Fluids B **3** (1991) 2247.

[RICE, B.W.] RICE, B.W., et al., "Observations of enhanced core confinement in negative magnetic shear discharges with an L mode edge on DIII-D", Nuclear Fusion **36**(1996)1271.

[ROCCO, P.] ROCCO, P., et al., "Criteria for defining low activation materials in fusion reactor applications", Fusion Engineering and Design, **15**(1992)235.

[ROTAMAK] COLLINS, G.A., et al., "Small aspect ratio tokamak configurations generated by rotating magnetic field current drive", Nuclear Fusion **28**(1988)255.

[RTR] COOKE, P.I.H. , et al., "Parameters of a Reference Tokamak Reactor", CLM-R298, Culham Laboratory (1989).

[SAKO, K., 74] SAKO, K., et al., "Design study of a tokamak reactor", IAEA-CN-33/G1-5,1974.

[SAKO, K., 76] SAKO, K., et al., "Preliminary design of a tokamak experimental fusion reactor", IAEA-CN-35/I3-1,1976.

[SAUTHOFF, N.] SAUTHOFF, N., et al., "PBX-M research progress: approach to second stability", Plasma Physics and Controlled Nuclear Fusion Research 1990, IAEA, Vienna, Vol. 1, 709(1991).

[SEAFP] The SEAFP Project, (Safety and Environmental Assessment of Fusion Power), Report of SEAFP Project , June(1995).

[SEKIGUCHI, T.] SEKIGUCHI, T., "Plasma science and technology", Ohm sha, 1979 (in Japanese).

[SEKIMOTO, T.] YOSHINO, M., et al., "Proposal for global environment", Sankai do,1994 (in Japanese).

[SHEFFIELD, J.] SHEFFIELD, J., and GIBSON, A., "Cost scaling of tokamaks", Nuclear Fusion **15**(1975)677.

[SHIBATA, K.] SHIBATA, K., private communication.

[SHIMAZU, Y. 86] SHIMAZU, Y., "Fusion reactor SYSTEM ASSESSMENT MANUAL", energy special study (fusion), 1986, (in Japanese)

[SHIMAZU, Y. 88] The Physical Society of Japan, "Problems of Nuclear Power Generation", pp153-162,

[SHIMAZU, Y. 88] The Physical Society of Japan, "Problems of Nuclear Power Generation", pp153-162, Tokai Univ. Press, 1988, (in Japanese).

[SIMONEN, T.C.] SIMONEN, T.C., "Status and plans for DIII-D", Fusion Technology, **21**(1992)1332.

[SMEULDERS, P.] SMEULDERS, P., et al., "Survey of pellet enhanced performance in JET discharges", Nuclear Fusion **35** (1995) 225.

[SPHEX] BROWNING, P.K., et al., "Injection and sustainment of plasma in a preexisting toroidal field using a coaxial helicity source", Physical Review Letters **68**(1992)1722.

[SSTR-2] MORI, S., et al., "Preliminary design of a solid particulate cooled blanket for the steady state tokamak reactor (SSTR)", Fusion Technology, **21**(1992)1744.

[SSTR-JAERImemo] Reactor design laboratory, "Concept Study of the Steady State Tokamak Reactor (SSTR)", JAERI-memo 03-058, 1991, (in Japanese).

[SSTR] SEKI, Y., et al., "The steady state tokamak reactor", International Conference on Plasma Physics and Controlled Nuclear Fusion Research 1990, IAEA, Vienna, **3**(1991) 473.

[STACEY, W.M.] STACEY, W.M., "Tokamak demonstration reactors", Nuclear Fusion **35** (1995) 1369.

[STAMBAUGH, R.D. 85] STAMBAUGH, R.D., et al., "Tests of beta limits as a function of plasma shape in Doublet III", Plasma Physics and Controlled Nuclear Fusion Research 1984, IAEA, Vienna, **1**(1985)217.

[STAMBAUGH, R.D. 96] STAMBAUGH, R.D., et al., "The spherical torus approach to magnetic fusion development", Fusion Technology **30**(1996)1380.

[STARFIRE] BAKER, C.C., et al., "STARFIRE - A Commercial Tokamak Fusion Power Plant Study", Rep. ANL/FPP-80-1, Argonne Natl. Lab., IL (1980).

[START92] SYKES, A., et al., "First results from the START experiments", Nuclear Fusion **32**(1992)694.

[START94] SYKES, A., et al., "The START spherical tokamak", 15th International Conference on Plasma Physics and Controlled Nuclear Fusion Research 1994, IAEA-CN-60/A-5-II-5.

[START96] AKERS, R., et al., "Stability and additional heating properties of spherical tokamak plasmas on START", 16th IAEA Fusion Energy Conference 1996, IAEA-CN-64/C-2-1.

International Workshop on Spherical Torus '97, A.F.Ioffe Physico-Technical Institute, St. Petersburg, Russia, 1997.

[STRAIT, E.J. 88] STRAIT, E.J., et al., "Stability of high beta discharges in the DIII-D tokamak", Plasma Physics and Controlled Nuclear Fusion Research 1988, IAEA, Vienna, **1**(1989)83.

[STRAIT, E.J. 95] STRAIT, E.J., et al., "Enhanced confinement and stability in DIII-D discharges with reversed magnetic shear", Physical Review Letters **75**(1995)4421.

[SUPER-GM] Science and Technology Agency, "Assessment for Superconductor Technique of Resources and Energy", 1987, (in Japanese).

[SUZUKI, N.] SUZUKI, N., et al., "Recent results on the modified JFT-2 tokamak", Plasma Physics and Controlled Nuclear Fusion Research 1980, IAEA, Vienna, Vol. 2, (1981)525.

[SYKES, A. 94] SYKES, A., "Progress on spherical tokamaks", Plasma Physics Controlled Fusion **36**(1994)B93.

[TABARA, T.] TABARA, T., et al., "Radioactive Waste Management and Disposal Scenario for Fusion Power Reactors", JAERI-Tech 97-054, 1997, (in Japanese).

[TAKIZUKA, T.] 16th IAEA Fusion Energy Conference 1996, IAEA-CN-64/F-5.

[TANAKA, S.] TANAKA, S., "Non-inductive Current Drive in Toroidal System", Kakuyuugou kenkyu, **62**(1989)240 (in Japanese).

[THOMSEN, K.] THOMSEN, K., et al., "ITER H mode confinement database update", Nuclear Fusion **34**(1994)131.

[TOKIMATSU, K.] TOKIMATSU, K., OKANO, K., YOSHIDA,T., YAMAJI, K., and KATSURAI, M., "The cost minimized tokamak reactor using conservative coils/cooling technology", Forth International Symposium on Fusion Nuclear Technology(ISFNT-4), Tokyo, 1997. TOKIMATSU, K, et al., accepted to Nuclear Fusion.

[TORSAC] NISHIO, S., "Development of Tokamak Reactor Systems Analysis Code" ,JAERI-M 87-021, 1987(in Japanese).

[TRESCODE] MIZOGUCHI, T., et al, "Development of tokamak reactor conceptual design code TRESCODE", JAERI-M 87-120, JAERI (1987).

[TROYON, F.] TROYON, F., et al., "MHD-limits to plasma confinement", Plasma Physics and Controlled Fusion, **26**(1984)209.

[TSUCHIDA, A.] TSUCHIDA, A., "No future exists by oil and nuclear", Aki shobou, 1978, (in Japanese).

[TURNBULL, A.D.] TURNBULL, A.D., et al., "High beta and enhanced confinement in a second stable core VH-mode advanced tokamak", Physical Review Letters, **74**(1995)718.

[UCHIDA, T.] UCHIDA, T., and INOUE, N., "Control of Nuclear Fusion and Plasmas", The university of Tokyo press, 1980, (in Japanese).

[UCHIYAMA, Y. 95] UCHIYAMA, Y., "Life Cycle Assessment of Power Generation Systems", Y94009, Socio-Economic Research Center, Central Research Institute of Electric Power Industry (1994), (in Japanese).

[UCHIYAMA, Y. 96] UCHIYAMA, Y., and YOKOYAMA, H., "Life cycle analysis of advanced nuclear power generation technologies", Denryoku Keizai Kenkyu No. **37**, Socio-Economic Research Center, Central Research Institute of Electric Power Industry (1996), (in Japanese).

[UDA, T.] UDA, T., et al., small topics "Safety Analysis Research for Fusion Facilities", Journal of Plasma and Fusion Research, **73**(1997)767 (in Japanese).

[UWMAK-III] CONN, R.W., et al., "A high beta-performance non-circular tokamak power reactor design study – UWMAK-III", IAEA-CN-35/I-1-4.

[UWMAK-II] CONN, R.W., et al., "Major design features of the conceptual D-T tokamak power reactor, UWMAK-II", IAEA-CN-33/G-1-4.

[WAGNER, F. 82] WAGNER, F., et al., "Regime of Improved confinement and high beta in neutral-beam-heated divertor discharges of the ASDEX tokamak", Physical Review Letters **49**(1982)1408.

[WAGNER, F. 84] WAGNER, F., et al., "Development of an edge transport barrier at the H-mode transition of ASDEX", Physical Review Letters **53**(1984)1453.

of ASDEX", Physical Review Letters **53**(1984)1453.

[WOOTTON, A.J.] WOOTTON, A.J., et al., "Compact tokamak reactors", Nuclear Fusion **37**(1997)927.

[YAMAJI, K.,&FUJII, Y.] YAMAJI, K.&FUJII, Y., "Global energy strategy", Denryoku shinpo-sya, 1995, (in Japanese).

[YAMAMOTO, T.] YAMAMOTO, T., "Conceptual design of Inductively Driven Long Pulsed Tokamak Reactor", Ph.D Thesis, The University of Tokyo 1997.

[YAMAZAKI, K.] YAMAZAKI, K., "High-Beta Approach and Related MHD Instabilities in Tokamak", Kakuyu-gou Kenkyuu, **54**(1985)5 (in Japanese).

[YOSHIDA, T. 94] YOSHIDA,T., et al., "Development of Cost Assessment Code of Fusion Power Reactors", T94001, Komae Research Laboratory, Central Research Institute of Electric Power Industry (1994), (in Japanese).

[YOSHIDA, T. 96] YOSHIDA, T., "Parameter study toward economic magnetic fusion power reactors", T95069, Komae Research Laboratory, Central Research Institute of Electric Power Industry (1996), (in Japanese).

[YOSHIDA, T.] YOSHIDA,T., private communication.

Appendix – details of systems code –

Physics Models

Most calculational formulas used in this work; such as Beta limit, Safety factor, Confinement (ITER-89 power low scaling), Power balance, Fusion power density (General profiles and arbitrary temperature), Current drive (for NBI), are the same as those in the ITER Physics Guide Lines (Ref. [IAEA-PGL]). Here we explain the formulas of bootstrap current fraction which differs from that of Ref. [ITER-PGL].

Bootstrap current fraction

First Stability; Cordey's formula (Ref. [J.G.Cordey])

$$f_{bs} = C_{bs} \cdot \varepsilon^{1/2} \cdot \beta_{pa}$$

$$C_{bs} = 1.32 - 0.235 \cdot (q_{95}/q_0) + 0.0185 \cdot (q_{95}/q_0)^2, q_0 = 1.1$$

$$\beta_{pa} = \beta_{tot} \cdot \left(B_o / B_{pa}\right)^2, B_{pa} = I_P / 5a_p\kappa^{0.5}$$

Second Stability; Okano's formula (Ref. [K.Okano93])

$$f_{bs} = (\kappa\delta)^{1/2} \cdot \beta_{pa} \cdot Q_\alpha \left\{ \frac{0.0673}{\alpha_n + \alpha_T - 0.421} - \left(1 - \frac{q_0}{q_a{}^*}\right) \cdot \frac{0.0673}{\alpha_n + \alpha_T + \gamma - 0.421} \right\}$$

$$Q_\alpha = (\alpha_n + \alpha_T + 1) \cdot (9.64\alpha_n + 0.642\alpha_T)$$

$$q_a{}^* = \frac{a_p B_o}{R_p B_{pc}} \cdot \frac{1+\kappa^2}{2}, B_{pc} = \frac{\mu_0 I_p}{2\pi a_p}, q_0 = 2.0, \gamma = 0.3 \sim 0.5$$

f_{bs} = bootstrap current fraction

B_0 = toroidal magnetic field of axis

R_p = plasma major radius

a_p = plasma minor radius

κ = plasma elongation

δ = plasma triangularity

α_n = profile factor of plasma density

α_T = profile factor of plasma temperature

q_0 = safety factor at plasma center

q_{95} = safety factor on the 95% flux surfaces

I_p = plasma current

μ_0 = permeability of free space

Energy flow of a reactor system (Ref. [Generomak])

The electric power at the bas bar

$$P_e = P_{eg} - P_{CDe} - P_{os} = \eta_e\left(M \cdot f_N \cdot P_N + \eta_\alpha \cdot P_\alpha + \eta_{CDe} \cdot P_{CD}\right) - \frac{P_{CD}}{\eta_{CDe}} - P_{eg} \cdot f_r \cdot \left(\frac{P_{os}^{ref}}{P_{th}}\right)^{\gamma os}$$

where

P_{eg} = electricity at the turbine = $\eta_e \cdot P_{th}$

$P_{th} = M \cdot f_N \cdot P_N + \eta_\alpha \cdot P_\alpha + \eta_{CDe} \cdot P_{CD}$ = thermal power at the reactor

where P_N = neutron power, P_α = alpha particle power, P_{CD} = current drive power

P_{CDe} = required power for current drive components

P_{os} = electric power for other equipment (power supply for coils, B.O.P., etc.),

η_e = thermal to electricity conversion efficiency = 34.5%

M = multiplier of neutron power = 1.36

f_N = covering factor of blanket = 0.9

η_α = efficiency of collection of alpha particle power = 0.7

η_{CDe} = efficiency of current drive component = 0.5

f_r = fraction of power recirculated to the system = 0.15

P_{os}^{ref} = a standard value for scaling = 4150 [MW]

γos = a scaling power = 0.2

Engineering Models

The width of the TF coil

$$\Delta TF = R_1 - R_2 - R_3$$

where

$R_1 = R_p$-aw-$\Delta b_{in} - \Delta s_{in}$ = The major radius of the inner surface of the TF coil

$R_2 = \cos(\pi/N_{TF})\left[R_1^{\,2} - 2\cdot\Delta S_{TF}/\sin(2\pi/N_{TF})\right]^{0.5}$ = The inner radius of the TF coil

$R_3 = R_1\cdot\left[1-\cos(\pi/N_{TF})\right]$ = The gap between R_1 and the back surface of the TF coil

The volume of the TF coils

$$V_{TF} = C_{ling}\cdot S_{tot}$$

where

$S_{tot} = N_{TF}\cdot I_{TFC}/J_{TFC}$ = total cross section of TF coils; $N_{TF}\cdot I_{TFC} = (2\pi/\mu_0)\cdot R_p\cdot B_0$

C_{ling} = TF coil length which is calculated by the three-arc approximation.

aw = the plasma SOL radius = $1.1\cdot a_p$

Δb_{in} = the width of the inner blanket

Δs_{in} = the width of the inner shield

N_{TF} = the number of the TF coils

ΔS_{TF} = the space for one TF coil = S_{tot}/N_{TF}

I_{TFC} = the current of the TF coils

A method proposed by Moses and Young (Ref. [F.Moon]) is applied to calculate the constant tension D-shape TF coils. The allowable tension of TF coils is calculated by the same method of Ref. [TRESCODE].

The volume of the PF coils and the structures (Ref. [Generomak])

$$V_X = f_X\cdot V_{TF}: \quad \text{when X = PF, PF coils ; X = ST, structure}$$

where

f_X = 0.2 (X = PF), 0.75 (X = ST)

The volume of the shielding and the blanket (Ref. [Generomak])

$$V_X = 1/3 \cdot V_{Xin} + 2/3 \cdot V_{Xout}\,; \quad \text{when X = S, the shield ; X = B, the blanket}$$

where

V_{Xin} = the volume of the inner shield/blanket

V_{Xout} = the volume of the outer shield/blanket

The volume/weight of the fusion island

$$V_{FI} = \sum V_i\,, \quad W_{FI} = \sum W_i\,, \quad W_i = \rho_i \cdot V_i$$

i = TF (TF coils), PF (PF coils), ST (STructure), S (Shielding), B (Blanket)

where

V_i, ρ_i, W_i = the volume/volumetric-density/weight of each component

ρ_i = 7.9 (i = TF, PF), 6.0 (i = ST), 7.8 (i = S), 4.8 (i = B) [ton/m^3]

Cost Models

The annual cost (Ref. [Generomak])

$$C_{ac} = C_c \cdot F_{CR} = C_D \cdot f_{ind} \cdot f_{cap} \cdot F_{CR}$$

where

f_{ind} = indirect cost multiplier = 1.05

f_{cap} = capitalization factor = 1.1

F_{CR} = fixed charge rate = 0.12

$C_D = C_{FI} + C_{R.B.} + C_{B.O.P.} + C_{TR}$

The cost of fusion island

$$C_{FI} = 1.2 \cdot 1.25 \cdot (W_{TF} + W_{PF}) \cdot \$_{coil}$$ --- the cost of the coil systems

$$+ \; W_{ST} \cdot \$_{ST}$$ --- the cost of the structure

$$+ \; W_s \cdot \$_s$$ --- the cost of the shield

$$+ \; C_{FI}^{ref} \cdot \left(P_{th} / P_{th}^{ref}\right)^{\gamma^{B.O.P.}}$$ --- the cost of heat trance

$$+ \; 0.75 \cdot \$_a \cdot P_{aux}$$ --- the cost of the current drive

where

$\$_i$ = the unit cost of each component

i = coils, ST (STructure), S (Shielding), B (Blanket), a (current drive)

= 50 (i = coils), 29 (i = ST), 17 (i = S), 96.6 (i = B) [$/kg], 4.6 (i = a) [$/We]

The cost of the reactor building

$$C_{R.B.} = C_{R.B.}^{ref} \cdot \left(V_{FI} / V_{FI}^{ref}\right)^{\gamma^{R.B.}}$$

The cost of the balance of plant

$$C_{B.O.P.} = C_{B.O.P.}^{ref} \cdot \left(P_{th} / P_{th}^{ref}\right)^{\gamma^{B.O.P.}}$$

where

X_i^{ref} is the reference value for X (= C, P, V)

C_i^{ref} = 893 [M$] (i = B.O.P.), 416 [M$] (i = R.B.), 110 [M$] (i = FI)

P_{th}^{ref} = 4150 [MW]

V_{FI}^{ref} = 5100 [ton/m^3]

γ^i = the power for scaling = 0.6 (i = B.O.P.), 0.67 (i = R.B.)

The cost of the tritium

$C_{TR} = COM_{TR} \cdot \$_{TR}$ --- the initial cost of the tritium, which is treated as constant value

COM_{TR} = the initial weight of equipped tritium, which is assumed 0.4 [kg]

$\$_{TR}$ = unit cost of tritium, which is assumed 1,350,000 [$/kg]

The cost of the maintenance

C_{om} = $f_{om} \cdot$ [C_c (total capital cost) + the cost of the initial installed replacement components]

where f_{om} = factor for maintenance = 0.04

The cost of the scheduled replacement (Ref. [Generomak])

$C_{SCR} = C_{ba} + C_{da} + C_{aa}$

where

$C_{ba} = 1.1 \cdot C_b / n_{db} \cdot (1+\varepsilon)^{n_{db}/2}$ --- the cost of the scheduled replacement of the blanket

C_b = the cost of the blanket = $W_B \cdot \$_B$

$n_{db} = F_{wn} / f_{ave} \cdot P_{wn}$ = the interval year between the replacements

F_{wn} = the limit of the neutron fluence = 10 [$MW \cdot y/m^2$]

P_{wn} = the neutron wall load

f_{ave} = the plant availability = 0.75

ε = interest = 0.072

$C_{da} = 1.1 \cdot C_d \cdot (1+\varepsilon)^{1/2}$ --- the cost of the scheduled replacement of the divertor

C_d = the cost of divertor = $V_d \cdot \rho_d \cdot \$_d = (2a_p) \cdot 2\pi R_p \cdot d \cdot \rho_d \cdot \$_d$

ρ_d = volumetric density of divertor = 6.9 [ton/m^3]

$\$_d$ = unit cost of divertor = 140 [$/kg]

d = width of divertor = 0.05 [m]

$C_{aa} = C_a \cdot n_a \cdot (1+\varepsilon)^{n_a/2}$ --- the cost of the scheduled replacement of the auxiliary heating

C_a = the cost of the auxiliary heating = $0.25 \cdot P_{aux} \cdot \$_a$

$n_a = F_{wn} / f_{ave} \cdot P_{wn}$ = the interval year between the replacements

The cost of the fuel

$C_{fuel} = CON_D \cdot 365 \cdot f_{ave} \cdot \$_D$ --- the cost of fuel, which is assumed Deuterium only

Tritium is assumed as self-sufficient.

CON_D = consumption of Deuterium per day, which is assumed 0.3 [kg/day]

$\$_D$ = unit cost of Deuterium, which is assumed 2,700 [$/kg]

The cost of the disposal and the decommission

C_{dis} = 1.0 --- the cost of waste disposal

C_{dec} = 0.5 --- the cost of decommission of a reactor

List of Publications

First Author publications

[1] K.Tokimatsu, K.Okano, T. Yoshida, K.Yamaji, and M.Katsurai.
"Study of design parameters for minimizing the cost of electricity of tokamak power reactors"
Accepted in Nuclear Fusion

[2] Tokimatsu,.K., Okano, K., Yoshida, T., Yamaji, K., and Katsurai, M.
"The cost-minimized tokamak reactor using conservative coils/cooling technology"
International Symposium of Fusion Nuclear Technology-4 (ISFNT-4), Tokyo, 1997
To be appeared in Fusion Engineering and Design

[3] TOKIMATSU Koji, HONDO Hiroki, YAMAJI Kenji, and KATSURAI Makoto
"Energy Analysis and Carbon Dioxide Emission of Tokamak Fusion Power Reactors"
Journal of Plasma and Fusion Research, **74**(1998)54 (in Japanese).

[4] K.Tokimatsu, H.Hondo, Y.Ogawa, K.Okano, K.Yamaji, and M.Katsurai
"Economy, Energy Analysis, and Environmental Impacts on Tokamak Fusion Power Reactors"
In preparation to Nuclear Fusion and IAEA conference

Co-author publications

[1] Y.Ogawa, N.Inoue, Z.Yoshida, T.Yamamoto, R.Hiwatari, K.Takemura, K.Tokimatsu, K.Okano, Y.Asaoka, T.Yoshida, K.Tomabechi, T.Amano, J.F.Wang and Y.Murakami
"Design of Volumetric neutron source based on steady-state tokamak"
16th International Conference on Plasma Physics and Controlled Nuclear Fusion Research, Montreal, Canada, Oct. 1996

[2] Y.Ogawa, K.Okano, N.Inoue, T.Amano, Y.Asaoka, R.Hiwatari, Y,Murakami, K.Takemura, K.Tokimatsu, K.Tomabechi, T.Yamamoto, and T.Yoshida
"Design of a Steady-State Tokamak Device with Super-Conducting Coils for a Volumetric Neutron Source"
4th International Symposium on Fusion Nuclear Technology, Tokyo, April, 1997

[3] K.Okano, Y.Asaoka, R.Hiwatari, N.Inoue, Y.Murakami, Y.Ogawa, K.Tokimatsu, K.Tomabechi, T.Yamamoto and T.Yoshida
"Study of a Compact Reversed Shear Tokamak Reactor"
4th International Symposium on Fusion Nuclear Technology, Tokyo, April, 1997

[4] K.Okano, Y,Asaoka, A.Hatayama, R.Hiwatari, N.Inoue, Y.Murakami, Y.Ogawa, K.Tokimatsu, K.Tomabechi, T.Yamamoto, and T.Yoshida
"A Compact Reversed Shear Tokamak Reactor Sustained by Beam Driven Currents"
17th Symposium on Fusion Engieering, SOFE-17, San Diego, Oct. 1997

Conferences

[1] 時松宏治、山地憲治、桂井誠
「DT Tokamak 炉における発電原価の感度解析」
第 13 回プラズマ･核融合学会年会、京都、1996 年 3 月

[2] Tokimatsu,.K., Okano, K., Yoshida, T., Yamaji, K., and Katsurai, M.
"Sensitivity Analysis of Cost of Electricity of Fusion Power"
電気学会プラズマ･放電合同研究会、北海道、1996 年 8 月、EP-96-66

[3] 時松宏治、岡野邦彦、吉田智朗、山地憲治、桂井誠
「DT 反応 Tokamak 炉の発電原価の感度解析」
第 13 回プラズマ･核融合学会秋季講演会、東京、1996 年 10 月

[4] 時松宏治、山地憲治、桂井誠
「DT 反応 Tokamak 型核融合炉のコスト評価」
第 13 回エネルギーシステム・経済コンファレンス論文集、東京、1997 年 1 月

[5] 時松宏治、岡野邦彦、吉田智朗、山地憲治、桂井誠
「DT-Tokamak 炉の運転モードと物理／工学パラメータのコストに与える影響の評価」
第 14 回プラズマ･核融合学会年会、東京、1997 年 3 月

[6] 時松宏治、本藤祐樹、山地憲治、桂井誠
「トカマク型核融合炉の経済性、エネルギー収支及び環境負荷に関する研究」
電気学会プラズマ研究会、鳥取、1997 年 7 月

[7] 時松宏治、本藤祐樹、山地憲治、桂井誠
「核融合炉の経済性評価及びエネルギー分析」
電気学会電力・エネルギー部門大会論文Ⅱ、島根、1997 年 7 月

[8] 時松宏治、本藤祐樹、山地憲治、桂井誠
「トカマク型核融合炉のエネルギー収支と CO_2 排出に関する研究」
環境経済･政策学会、北九州、1997 年 9 月

[9]時松宏治、本藤裕樹、山地憲治、桂井誠
「トカマク型核融合動力炉の経済性、エネルギー収支、及び環境負荷に関する研究」
日本原子力学会、沖縄、1997 年 10 月

[10]時松宏治、本藤祐樹、山地憲治、桂井誠
「トカマク型核融合動力炉の経済性、エネルギー収支、及び環境負荷に関する研究」
プラズマ核融合学会、大阪、1997 年 11 月

[12]K.Tokimatsu, H.Hondo, K.Yamaji,and M.Katsurai
"Economy, Energy Analysis, and Environmental Impacts on Tokamak Fusion Power Reactors"
First Asia-Pacific International Symposium on the Basic and Application of Plasma Technology,

Taiwan, Dec. 1997

[13]時松宏治、本藤祐樹、山地憲治、桂井誠

「トカマク型核融合動力炉の経済性、ライフサイクル分析、及び放射性廃棄物量に関する研究」

エネルギーシステム・経済・環境コンファレンス、東京、1998 年 1 月

[14] K.Tokimatsu, H.Hondo, Y.Ogawa, K.Okano, K.Yamaji, and M.Katsurai

"Economy, Energy Analysis, and Environmental Impacts on Tokamak Fusion Power Reactors"

IAEA-Technical Committee Meeting, Culhum, March 1998